A STUDY OF THE ROTATIONAL SPECTRA OF HYDROGEN SELENIDE, PARTIALLY DEUTERATED AMMONIA, AND OTHER MOLECULES IN THE FAR INFRARED SPECTRAL REGION

DISSERTATION

Presented in Partial Fulfillment of the Requirements for the Degree Doctor of Philosophy in the Graduate School of The Ohio State University

By

EDWARD DANIEL PALIK, B. Sc., M. Sc.

The Ohio State University
1955

Approved by:

Robert A. Oetjen

Adviser
Department of Physics and Astronomy

ACKNOWLEDGEMENTS

I wish to express my sincere thanks to my adviser, Dr. Robert A. Oetjen, for his encouragement throughout a considerable portion of my graduate study and for his interest, comments, and criticism during this investigation.

I wish to thank Dr. Ely E. Bell for his ever present aid throughout this investigation. His lucid explanations of physical phenomena in our many discussions have been an inspiration.

I acknowledge with pleasure the help of my friends, Raymond L. Brown and Phillips B. Burnside.

I wish to acknowledge a grant-in-aid from funds allocated by The Ohio State University Research Foundation to the University for support of fundamental research in 1953-1954. Also, I wish to thank I. E. du Pont de Nemours & Company for the Dupont Fellowship received during 1954-1955.

My thanks is also expressed to the Wright Air Development Center who through a contract with The Ohio State University Research Foundation have sponsored the investigation under which the far infrared spectrograph used in my research was constructed and has been maintained in operating condition.

TABLE OF CONTENTS

LIST OF TABLES

LIST OF FIGURES

CHAPTER I

INTRODUCTION

The pure rotational absorption spectra of molecules with permanent dipole moments in the far infrared spectral region are of considerable interest because of the information about the molecules that can be obtained from analyses of the spectra. The spectra are less apt to be complicated by vibration-rotation interactions as is often the case with near infrared bands.

Transitions between the rotational levels of the vibrational ground state are those usually observed in the far infrared spectral region. From an analysis, it is possible to determine the reciprocals of inertia, effective moments of inertia for the ground state, and the dimensions of the molecule. Also, the effects of centrifugal distortion can be studied. From such a study, it is possible to determine the centrifugal distortion constants of the molecule. An important result of the analysis is the determination of the ground state rotational levels. A knowledge of these levels can, of course, be very useful in the analysis of the near infrared vibration-rotation bands.

Pure rotational spectra are studied in the microwave region also, where $\Delta J = 0,1$ transitions are observed. Because of the very high resolution, fine structure due to heavy

isotopes can be measured, along with the effects of nuclear quadrupole coupling. By application of the Stark effect, electric dipole moments can be measured. Also, it is often possible to observe the Zeeman effect. In principle, these effects could be studied in the far infrared region if the resolution were adequate.

This dissertation describes an investigation of the pure rotational spectra of several molecules, namely, deuterium bromide (DBr), hydrogen iodide (HI), deuterium iodide (DI), hydrogen selenide (H_2Se), mono-deuterated ammonia (NH_2D), and di-deuterated ammonia (NHD_2). The far infrared spectrograph described by Oetjen, et al.,[1] was used to obtain the spectra. The experimental techniques employed are described, along with the analysis carried out to obtain information about the molecules.

---

(1) R. A. Oetjen, W. H. Haynie, W. M. Ward, R. L. Hansler, H. E. Schauwecker, and E. E. Bell, J. Opt. Soc. Am., 42, 559 (1952).

CHAPTER II

PURE ROTATIONAL SPECTRA OF DBr, HI, AND DI

History:

The pure rotational spectra of the halides of hydrogen, deuterium and tritium have been measured by several investigators during the past thirty years. Between 1925 and 1927 Czerny[1] observed several of the pure rotational lines of all four hydrogen halides. More recently, measurements have been made of the rotational spectra of HCl by McCubbin and Sinton,[2] and McCubbin[3] and of HCl, DCl and HBr by Hansler and Oetjen.[4] The $J = 0 \rightarrow 1$ rotational line of DI has been observed in the microwave region at 6.5 cm^{-1} by Burrus and Gordy.[5] Actually, this line is split into a triplet because of the nuclear quadrupole coupling of I^{127} with spin 5/2 with the rotation of the molecular framework. Also, the $J = 0 \rightarrow 1$ lines of DBr^{79} and DBr^{81} have been measured by Burrus and Gordy.[6] Very recently,

---

(1) M. Czerny, Z. Physik, 34, 227 (1925); 44 235 (1927).

(2) T. K. McCubbin and W. W. Sinton, J. Opt. Soc. Am., 40, 537 (1950).

(3) T. K. McCubbin, J. Chem. Phys., 20, 668 (1952).

(4) R. L. Hansler and R. A. Oetjen, J. Chem. Phys., 21, 1340 (1953).

(5) C. A. Burrus and W. Gordy, Phys. Rev., 92, 1437 (1953).

(6) W. Gordy and C. A. Burrus, Phys. Rev., 93, 419 (1954).

the $J = 0 \rightarrow 1$ rotational lines of TBr and TI have been measured by Rosenblum and Nethercot[7] in the microwave region, while the $J = 0 \rightarrow 1$ lines of TBr and TCl have been observed by Burrus, Gordy, Livingston, and Benjamin.[8]

There has been considerable investigation of the electronic and vibration-rotation bands of several of these molecules. For a convenient summary of the many references that have appeared on the subject, the reader is referred to G. Herzberg.[9] There have been several recent studies of the vibration-rotation bands of many of the hydrogen and deuterium halides. Talley, Kayler, and Nielson[10] have measured bands of HF and DF. Mills, Thompson, and Williams[11] have examined bands of HCl^{35} and HCl^{37} while Pickworth and Thompson[12] have measured bands of DCl^{35} and DCl^{37}. Thompson, Williams, and

---

(7) B. Rosenblum and A. H. Nethercot, Jr., Phys. Rev. 97, 84 (1955).

(8) C. A. Burrus, W. Gordy, B. Benjamin, and R. Livingston, Phys. Rev. 97, 1661 (1955).

(9) G. Herzberg, "Molecular Spectra and Molecular Structure I. Spectra of Diatomic Molecules" (D. Van Nostrand Company, Inc., New York, 1950).

(10) R. M. Talley, H. M. Kaylor, and A. H. Nielsen, Phys. Rev. 77, 529 (1950).

(11) I. M. Mills, H. W. Thompson, and R. L. Williams, Proc. Roy. Soc. A, 217, 29 (1953).

(12) J. Pickworth and H. W. Thompson, Proc. Roy. Soc. A, 217, 37 (1953).

Calloman[13] have resolved the fundamental bands due to HBr^{79} and HBr^{81} while Keller and Nielsen[14] have resolved bands of DBr^{79} and DBr^{81}. Boyd and Thompson[15] have measured the fundamental band of HI.

Theory:

From a study of the electronic and vibration-rotation bands considerable information concerning the structure of these diatomic molecules has been obtained. The energy of a diatomic molecule in wave numbers can be expressed by the equation

$$W = W_{el} + G_e + \omega_e(v+\tfrac{1}{2}) - x_e\omega_e(v+\tfrac{1}{2})^2 + y_e\omega_e(v+\tfrac{1}{2})^3 + \cdots + B_v J(J+1) - D_v J^2(J+1)^2 \qquad (2.1)$$

where

$$B_v = B_e - \alpha_e(v+\tfrac{1}{2}) - \gamma_e(v+\tfrac{1}{2})^2 + \cdots$$
$$D_v = D_e + \beta_e(v+\tfrac{1}{2}) + \delta_e(v+\tfrac{1}{2})^2 + \cdots .$$

W_{el} is the electronic energy which is a function of certain electronic quantum numbers. G_e is a constant term not depending on the vibrational quantum number v or the rotational

---

(13) H. W. Thompson, R. L. Williams, and H. J. Calloman, Spectrochimica Acta 5, 313 (1952).

(14) F. L. Keller and A. H. Nielsen, J. Chem. Phys. 22, 294 (1954).

(15) D. R. J. Boyd and H. W. Thompson, Spectrochimica Acta 5, 308 (1952).

quantum number J. The constant ω_e is the normal frequency of the diatomic molecule, and $x_e\omega_e$ and $y_e\omega_e$ are constants which appear in the quadratic and cubic terms of the potential energy. B_e is the equilibrium rotational constant which equals $h/8\pi^2cI_e$ and D_e is the vibrationless contrifugal distortion constant, which is much smaller than B_e. The factors α_e, γ_e, β_e, and δ_e are very small vibration-rotation interaction constants.

The energy of a molecule in the ground electronic and vibrational state is

$$W = W_{\text{el. grd. state}} + G_e + \tfrac{1}{2}\omega_e - \tfrac{1}{4}x_e\omega_e + \tfrac{1}{8}y_e\omega_e + \cdots + B_o J(J+1) - D_o J^2(J+1)^2 \qquad (2.2)$$

where $B_o = B_e - \frac{1}{2}\alpha_e - \frac{1}{8}\gamma_e$ is the rotational constant of the ground state, and $D_o = D_e + \frac{1}{2}\beta_e + \frac{1}{8}\delta_e$ is the centrifugal distortion constant for the ground state. For pure rotational absorption spectra, transitions occur between various rotational levels of the ground electronic and vibrational states according to the selection rule $\Delta J = 1$. Rotational transitions among rotational levels in an excited vibrational state will not be considered here. The frequencies of the rotational lines are obtained from equation (2.2) using the Bohr frequency rule $\nu = W'-W''$, where W'' is the energy of the initial state and W' the energy of the final state involved in the transition. The result is

$$\nu = 2B_oJ' - 4D_oJ'^3 \qquad (2.3)$$

From this equation, it is evident that the pure rotational spectrum of a diatomic molecule with a permanent dipole moment will consist of a series of slowly converging lines, the distance between the lines being very nearly $2B_o$.

From measurement of the pure rotational spectrum of a diatomic molecule, it is possible to determine B_o and D_o. The method of least squares can be used to fit a formula of the type

$$\nu = a_o + a_1 J + a_2 J^2 + a_3 J^3 + \ldots \qquad (2.4)$$

to the data. In this case, the task is simplified, for it is known that all the coefficients are zero except $a_1 = 2B_o$ and $a_3 = 4D_o$. Using the relationship $I_o = h/8\pi^2 cB_o$, the effective moment of inertia of the molecule in the ground state can be evaluated. Then from a knowledge of the masses of the two atoms, m_1 and m_2, the effective internuclear distance r_o can be calculated from the relationship $I_o = \mu r_o^2$ where $\mu = \frac{m_1 m_2}{m_1 + m_2}$ is the reduced mass. In the ground state, the molecule executes a zero point vibration, so that the measured distance r_o is slightly larger than the equilibrium distance.

Values of most of the constants of equation (2.1) can be obtained from an analysis of electronic and vibration-rotation bands. Two of these constants are B_o and D_o. Therefore, measurement of the pure rotational spectrum can serve as a check of these data. In Table I, p. 8, are listed some

TABLE I.

MOLECULAR CONSTANTS OF THE HALIDES OF HYDROGEN AND DEUTERIUM OBTAINED FROM NEAR INFRARED AND MICROWAVE DATA

	B_o	D_o	r_o	Reference
HF	20.555 cm^{-1}	0.0022 cm^{-1}	0.92 A	10
HCl^{35}	10.442_2	0.000526_6	1.28	11
HCl^{37}	10.426_8	0.000525_6	1.28	11
HBr^{79}	8.353_3	0.000386_5	1.42	13
HBr^{81}	8.350_8	0.000386_7	1.42	13
HI	6.426^8	0.00020	1.61	15
DF	10.857	0.00067	0.92	10
DCl^{35}	5.391_8	0.000137_1	1.28	12
DCl^{37}	5.375_6	0.000136_3	1.28	12
DBr^{79}	4.2485	0.000095	1.42	14, 6
DBr^{81}	4.2459	0.000095	1.42	14, 6
DI	3.2535	0.000050	1.61	5

TABLE II.

MOLECULAR CONSTANTS OF DBr, HI, AND DI FROM FAR INFRARED DATA

	B_o	D_o
DBr	4.247_3 cm^{-1}	0.000090 cm^{-1}
HI	6.427	0.00020_4
DI	3.255_2	0.000056

of the molecular constants for the halides of hydrogen and deuterium as obtained from near infrared and microwave data. The interatomic distance r_o is given to three figures to illustrate how it varies with the various halides.

Experimental Procedure and Results:

DBr, HI, and DI are colorless gases with irritating odors. They were prepared by standard methods outlined in elementary chemistry textbooks.

DBr was prepared by the reaction

$$PBr_3 + 3D_2O \rightarrow 3DBr + P(OD)_3 .$$

The generating apparatus is shown in Figure 1, p. 10. The D_2O used was obtained from the Stuart Oxygen Company and was $>$ 99.5% pure. The rate of this reaction was easily controlled by immersing the generating flask in liquid nitrogen. The gas was dried by passing it through a U-shaped drying tube containing phosphorus pentoxide. This served to remove D_2O vapor which has a strong pure rotational spectrum in the far infrared region of the spectrum. The gas was admitted directly into a cell which was located in the optical path of the spectrograph just in front of the entrance slit. Two cells were used in this investigation. One cell was made of glass with a length of 13 cm. The other was a stainless steel cell 19 cm. in length designed by Stroup.[16] Both cells were equipped

---

(16) R. E. Stroup, "A Study of the Rotational Spectra of Some of the Tri-hydrides of the Fifth Group of Elements of the Periodic Table." (Ph. D. Dissertation, The Ohio State University, 1953).

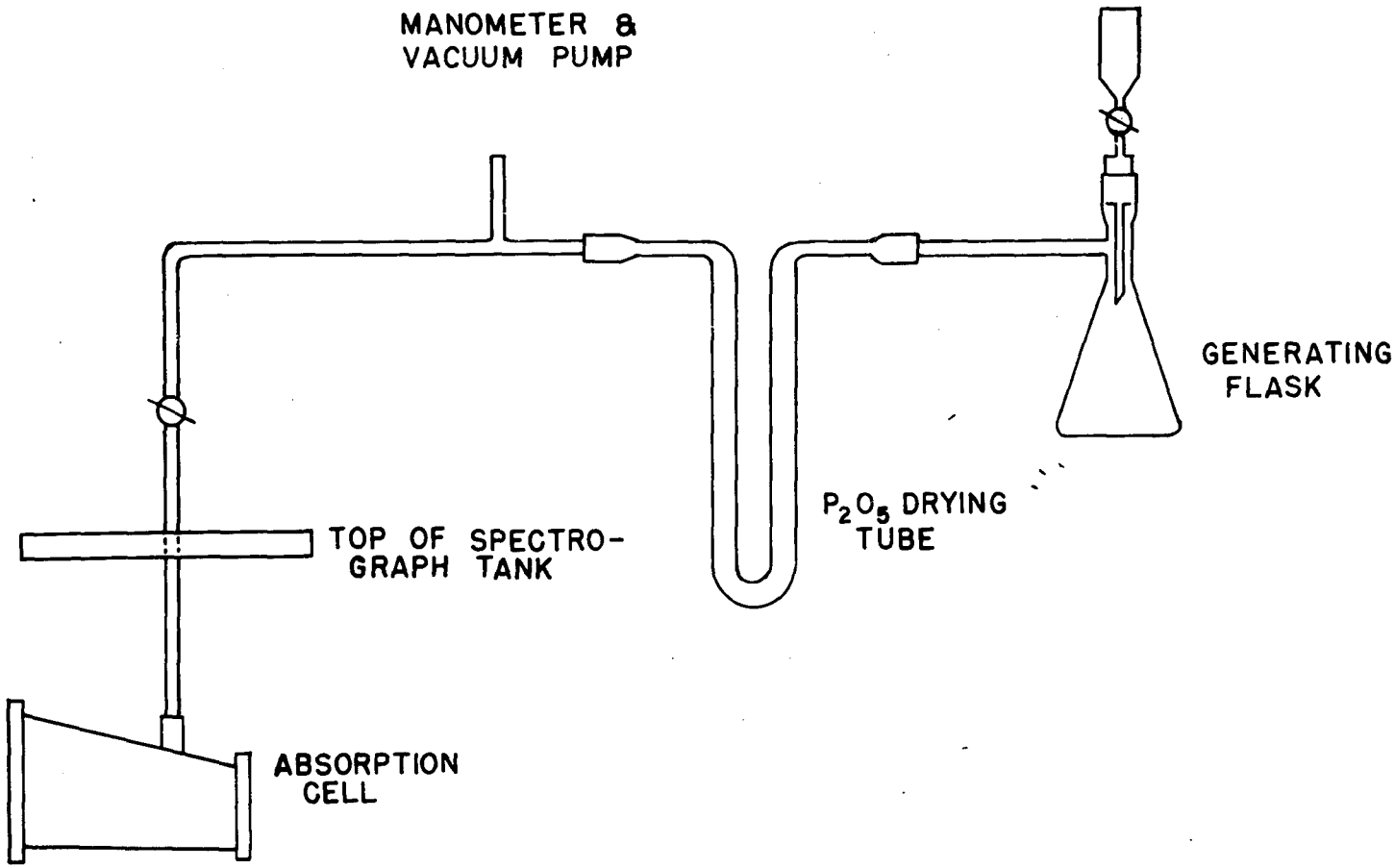

FIG. 1. Gas generating system for DBr, HI, and DI.

with polyethylene windows 0.01 in. thick. Spectrograms were obtained using several gas pressures from 10 to 40 cm Hg and using various spectral slit widths ranging from 0.4 to 0.7 cm^{-1}. Each spectrum line was recorded two or three times, and the frequencies measured for each line were averaged.

As many investigators can testify, it is difficult to prepare a pure deuterated compound. Invariably, there is enough hydrogen, in the form of water or other impurity in the chemicals and apparatus to produce some of the hydrogen-containing compound. For the spectroscopist this can mean the appearance of spectral lines due to the hydrogen-containing molecules, which interfere with the spectrum of direct interest.

In the first attempt to produce DBr, the pure rotational lines of HBr appeared as strongly as the DBr lines. In a second attempt, the gas-generating equipment and the cell were flushed with D_2O liquid and vapor several times over a period of twenty-four hours. The glass was also heated to drive off any water vapor adsorbed on the walls of the apparatus. In this manner perhaps most of the H_2O could be removed from the system and replaced by D_2O primarily and some HDO. However, these precautions proved of little value, for the spectrograms still showed strong HBr lines. There were two other sources of possible contamination, the PBr_3 and P_2O_5. While transferring the PBr_3 to the generating flask, it was exposed to the atmosphere (and consequently to the atmospheric water vapor) for a short time. Since PBr_3 reacts rapidly with water,

perhaps enough $P(OH)_3$ was produced to cause considerable contamination of the sample with hydrogen. Also, the P_2O_5 was exposed to atmospheric water vapor for a short time while a part of the apparatus was assembled. However, despite the large amount of HBr in the sample, the HBr lines usually did not interfere with accurate determination of the positions of the DBr lines.

HI and DI were made by similar reactions of H_2O and D_2O with PI_3. However, PI_3 is not available commercially. The preparation of PI_3, and from this HI, was carried out in the same container. Red phosphorus and iodine crystals were placed together in a flask. When H_2O was dropped on this mixture, a reaction was initiated which produced PI_3, and then HI, as follows

$$2P + 3I_2 \rightarrow 2PI_3$$

$$PI_3 + 3H_2O \rightarrow 3HI + P(OH)_3 \ .$$

The HI was then passed over P_2O_5 to remove any water vapor and then put directly into the stainless steel absorption cell. Pressures were measured with a mercury manometer, but HI reacted with the mercury to form a greenish-yellow compound Hg_2I_2 and a red compound $Hg\ I_2$. These compounds are soluble in a potassium iodide solution. The manometer was closed off from the rest of the system usually. Only occasionally was it used to obtain a rough value for the pressure which varied from 20 to 60 cm Hg.

In the preparation of DI, the same problems with hydrogen contamination as were encountered with DBr were again met. A portion of a typical spectrogram is shown in Figure 2, p. 14. The HI and DI lines are indicated by their J' values. The contour of the background is due to various factors such as the blaze of the 180 lines/inch grating used, the filtering, and water vapor absorption. The total pressure is approximately 30 cm Hg, the partial pressures of HI and DI are not known. In this spectrogram the HI lines are very strong while the DI lines with quantum numbers about twice as large are, because of the Boltzmann factor, quite weak.

Fifteen rotational lines of DBr, fourteen of HI and thirteen of DI were observed in the spectral region between 60 and 175 cm^{-1}. A curve of the form $\nu = a_1 J + a_3 J^3$ was fitted to the data for each molecule to obtain values for $a_1 = 2B_o$ and $a_3 = 4D_o$. The molecular constants B_o and D_o so obtained are listed in Table II, p. 8. The calculated and observed values for the frequencies in wave numbers are listed in Table III, p. 15. The available data for these molecules is quite good. Lines of some of these molecules could be used for calibration of far infrared spectrographs. It is planned to calibrate from 60 cm^{-1} to lower frequencies using CO lines since B_o and D_o are known very well for this molecule from near infrared data.

An attempt was made to plot carefully the per cent absorption of these lines to determine where the Boltzmann

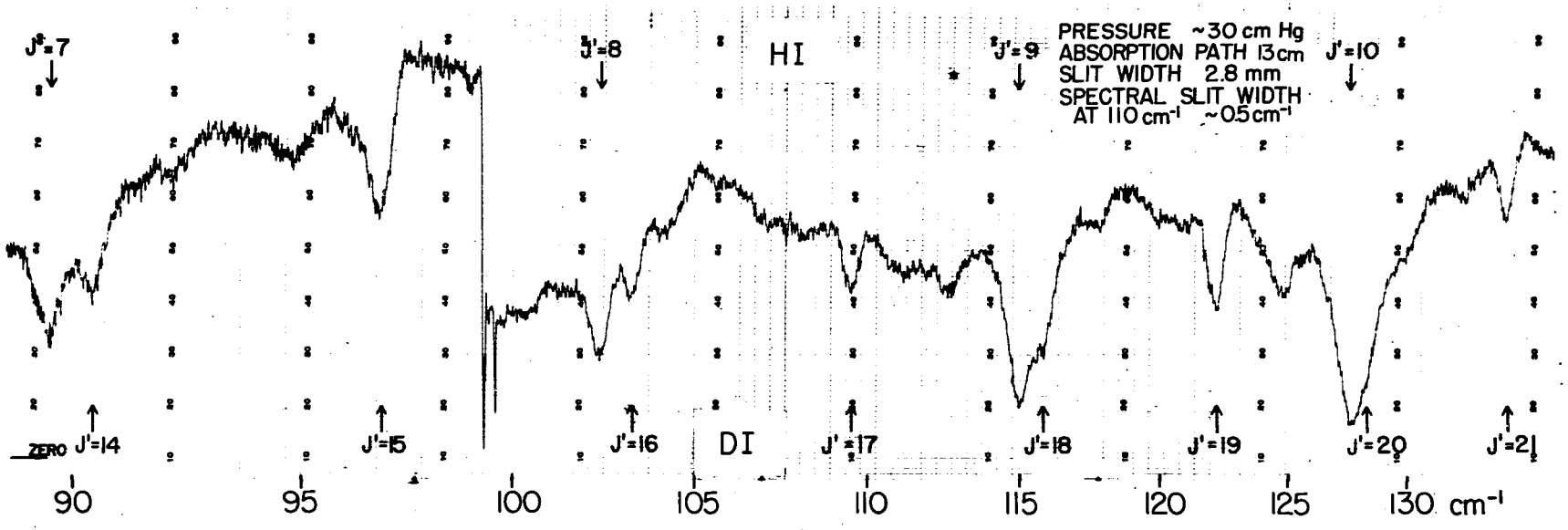

FIG. 2. Typical spectrogram of DI and HI.

TABLE III

PURE ROTATIONAL LINES OF DB_r, HI, AND DI

	DB_r		HI		DI	
	Frequency		Frequency		Frequency	
J'	Observed	Calculated	Observed	Calculated	Observed	Calculated
5			64.19K	64.17 cm^{-1}		
6			76.98	76.95		
7	59.32K	59.34 cm^{-1}	89.66	89.70		
8	67.83	67.77	102.37	102.42		
9	76.19	76.19	115.10	115.09	58.45K	58.43 cm^{-1}
10	84.62	84.58	127.76	127.73	64.89	64.88
11	92.93	92.97	140.32	140.31	71.33	71.32
12	101.29	101.31	152.90	152.83	77.70	77.74
13	109.64	109.63	165.32	165.31	84.17	84.14
14	117.91	117.94	177.65	177.72	90.53	90.53
15	126.21	126.20	189.99	190.00	96.85	96.90
16	134.40	134.44	202.52[b]	202.32	103.24	103.25
17	142.63	142.64	214.49	214.51	109.60	109.57
18	150.84	150.81	226.59	226.62	115.92	115.88
19	158.98	158.93			122.18	122.16
20	166.93[a]	167.01			128.42	128.41
21	175.05	175.05			134.62	134.64

a. Falls beside HBr line corresponding to J' = 8.

b. Distorted by strong H_2O line.

distribution of intensities was a maximum. The envelope for the DB_r spectrum was calculated using the expression

$$I \propto \nu g e^{-\frac{W'' hc}{kT}} \left(1 - e^{\frac{hc\nu}{kT}}\right) \left| \mu_{J'',M'';J',M'} \right|^2 \qquad (2.5)$$

where g is the weight factor of the initial level, $\left|\mu_{J'',M'';J',M'}\right|^2$ is the square of the electric dipole matrix element, k is the Boltzmann constant, T is the absolute temperature, h is Planck's constant, and c is the speed of light. Neglecting the dipole moment term, the envelope was calculated to be a maximum at J = 8. However, a dip appeared in the envelope of the lines in the 100 cm^{-1} region making it difficult to determine exactly where the experimental maximum of intensity is. This was attributed to the presence of higher orders of radiation than the first in the spectral region from 120 to 80 cm^{-1}. This stray radiation would lead to a false percentage absorption measurement. Another difficulty in making accurate absorption measurements was the fact that the spectral slits were not the same throughout the entire spectral region examined.

There are two isotopes of bromine, Br^{79} (50.5%) and Br^{81} (49.5%). Consequently, there are two kinds of DBr molecules, DBr^{79} and DBr^{81} with slightly different moments of inertia. Therefore, there is a pure rotational spectrum for each molecule. However, the difference in rotational constants is not large enough to produce spectra which could be resolved with the spectrograph. The molecular constants obtained here are averages of the constants of the two isotopic molecules.

These results have been published recently by the author[17].

---

[17] E. D. Palik, J. Chem. Phys. 23, 217 (1955).

CHAPTER III

PURE ROTATIONAL SPECTRUM OF HYDROGEN SELENIDE

History:

Hydrogen selenide is the third member of the series of triatomic, non-linear molecules which includes H_2O, H_2S, H_2Se, and H_2Te. While the vibration-rotation and pure rotational bands of H_2O and H_2S have been studied in considerable detail by many investigators, very little work has been done with H_2Se and H_2Te. In 1931 Mischke[1] measured several near infrared bands of H_2Se. In 1935 Dadieu and Engler[2] observed Raman bands of H_2Se, HDSe, and D_2Se. Cameron, Sears, and Nielsen[3] have measured the fundamental bands of H_2Se, HDSe, and D_2Se with high resolution. From the fairly simple structure of the rotational lines of the H_2Se bands, they concluded that the molecule was an almost accidently symmetric top with $a \approx b \approx 2c$. The values they obtained are $a = 7.7\ cm^{-1}$, $b = 7.7\ cm^{-1}$, and $c = 3.8\ cm^{-1}$.

---

(1) W. Mischke, Z. Physik 106, 67 (1931).

(2) A. Dadieu and W. Engler, Wiener Anzeiger 128, 13 (1935).

(3) D. M. Cameron, W. C. Sears and H. H. Nielsen, J. Chem. Phys. 7, 994 (1939).

Recently, King, Hainer, and Cross[4] have analyzed the ν_2 band of H_2Se using the data of Cameron, Sears, and Nielsen. For the reciprocals of inertia, they obtained the values $a = 8.91\ cm^{-1}$, $b = 7.19\ cm^{-1}$, and $c = 3.89\ cm^{-1}$ which give the asymmetry parameter κ a value of 0.315. This would indicate that the molecule is quite asymmetric. During this investigation the rigid rotator spectrum was calculated using these values of a, b, and c. However these values do not fit the pure rotational spectrum observed. The present work indicates that the molecule is only slightly asymmetric with $a = 8.16_5\ cm^{-1}$, $b = 7.71_2\ cm^{-1}$, and $c = 3.91_5\ cm^{-1}$ with $\kappa = 0.787$.

This chapter of the dissertation describes an investigation of the pure rotational spectrum of H_2Se leading to the determination of the reciprocals of inertia for the ground state and the dimensions of the molecule. Also, the effect of centrifugal distortion on the energy levels is discussed.

Experimental Procedure:

Much information about selenium and hydrogen selenide which proved useful has been given by Mellor.[5]

---

(4) G. W. King, R. M. Hainer and P. C. Cross, Phys. Rev. 71, 433 (1947).

(5) J. W. Mellor, "A Comprehensive Treatise on Inorganic and Theoretical Chemistry," Vol. 10 (Longmans, Green and Co., New York, 1928).

H_2Se is poisonous and has an offensive odor similar to H_2S. It has a melting point of $-64^{\circ}C$ and a boiling point of $-42^{\circ}C$. Because of its poisonous property, the gas was prepared in a hood.

The gas was made by the chemical reaction

$$Al_2Se_3 + 6H_2O \rightarrow 2Al(OH)_3 + 3H_2Se$$

A schematic diagram of the gas generating apparatus is shown in Figure 3, p. 21.

The Al_2Se_3 was prepared by mixing combining weights of finely ground aluminum and selenium in a pyrex test tube six inches long, the end of which was closed with a one-holed rubber stopper. The mixture was spread in a line along three-quarters of the length of the test tube. This part of the tube was heated uniformly with a Meker burner for a minute or two. Then the flame was concentrated on the closed end of the tube where shortly there occurred an endothermic reaction in which the Al_2Se_3 was formed. The reaction is vigorous with the emission of light. The hole in the rubber stopper permitted the hot gases formed in the reaction to escape. When the reaction was completed, the Al_2Se_3 adhered to the walls of the tube. Immediately, the Al_2Se_3 would react with atmospheric water vapor to form H_2Se, which was detected by its odor.

The test tube and contents were quickly dropped into another larger test tube which acted as a generator. Distilled water had previously been frozen in this generator.

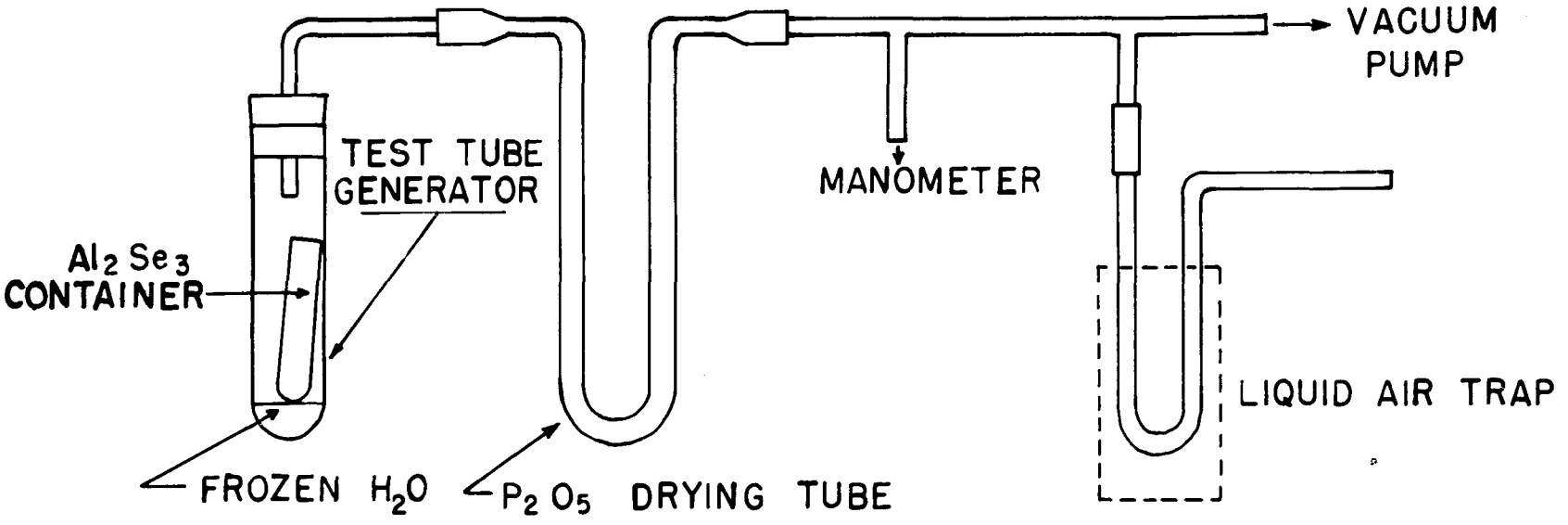

FIG. 3. Gas generating system for H_2Se.

This system was sealed with a rubber stopper and evacuated. As the ice melted, the water vapor reacted with the Al_2Se_3. To speed this reaction, the generator was sometimes tipped into a horizontal position, so that the water made direct contact with the Al_2Se_3. The gas passed through a U-shaped drying tube held in a horizontal position which contained phosphorous pentoxide to remove any water vapor. Pressures were measured with a mercury manometer.

The gas was collected in a trap which consisted of a U-shaped tube immersed in liquid nitrogen. As the gas was produced and passed through the drying tube, it was frozen out in the trap. The solid H_2Se was white in appearance. The gas is somewhat unstable, being sensitive to light. Parts of the generating apparatus consisted of Tygon tubing, and as the generating continued, these parts slowly turned pink and then dark red in color. The red substance is one of the allotropic forms of selenium. This variety is crystalline, monoclinic, melts at 175°C and is soluble in carbon disulfide. Only a small amount of selenium deposited on the glass parts of the apparatus or on the stainless steel walls of the absorption cell or on the polyethylene windows. This would seem to indicate that H_2Se could be kept in a glass container for a long period of time.

When the generating was complete, usually in two or three hours, the trap containing the solid H_2Se was removed from the rest of the system and taken to the spectrograph

where it was connected to another system containing the 19 cm stainless steel absorption cell with a small tray of phosphorus pentoxide in it, another drying tube, a manometer, and a vacuum pump. The pressure in the cell was adjusted to any desired value by removing the trap from the liquid nitrogen for a short time to allow a portion of the frozen H_2Se to melt and vaporize. Spectrograms at several different gas pressures between 2 and 7 cm Hg were obtained during the course of this investigation.

To determine whether the gas was dry, points in the spectrum where strong water lines appear were carefully checked. Usually, even the strongest water lines did not appear.

Since the selenium used was claimed to be 99.95% pure by its supplier* there was little possibility of any impurities giving rise to an undesirable spectrum. However, sulfur could possibly be an impurity, so that H_2S might be present. A close comparison of the H_2Se spectrum and the H_2S spectrum obtained by Hansler[6] revealed no H_2S lines as impurities.

The spectrum obtained extends from 50 cm^{-1} to 250 cm^{-1}. To study this frequency range with the spectrograph, it is necessary to divide the spectrum into several regions

---

*A. D. Mackay, Inc., New York, N. Y.

(6) R. L. Hansler, "Recent Studies in the Spectral Region from 40 to 140 Microns" (Ph. D. Dissertation, The Ohio State University, 1952).

depending on the kind of grating and types of filtering. This problem is discussed by Oetjen, et al.[7] Davis[8] discusses the problems from 250 to 600 cm^{-1}. Parameters such as slit widths, filtering, amplifier gain, etc. vary from region to region. Two echelette gratings were used to obtain the spectrum, a 180 lines/inch grating in the region from 60 to 250 cm^{-1} in both the first and second orders and a 90 lines/inch grating in the region from 40 to 60 cm^{-1} in first order. This latter grating has recently been obtained from the University of Michigan. It is blazed at 200 μ (50 cm^{-1}) and will enable the range of the spectrograph to be extended to about 30 cm^{-1}.

To obtain the H_2Se data from 40 to 60 cm^{-1}, fused quartz 1 mm thick and mica sheets ~ 0.001 inch thick were used as filters to eliminate second and higher orders of undesirable radiation along with one KRS-5 resthrahlen crystal, a 360 line/inch filter grating, one roughened sheet of polyethylene to scatter the short wave length radiation, and one sheet of polyethylene coated with turpentine soot. However, despite these precautions there are still doubts as to the purity of the radiation from 40 to 50 cm^{-1}.

---

(7) R. A. Oetjen, W. H. Haynie, W. M. Ward, R. L. Hansler, H. E. Schauwecker and E. E. Bell. J. Opt. Soc. Am. 42, 559 (1952).

(8) P. W. Davis, "The Far Infrared Spectra of Several Pyramidal Trihalides," (Ph. D. Dissertation, The Ohio State University, 1954).

The composite spectrum, shown at the top of Figures 4, p. 26, 5, p. 27, 6, p. 28, 7, p. 29, 8, p. 30 and 9 p. 31, is composed of several spectra obtained under slightly different conditions. Therefore, factors like per cent absorption and line widths are only approximate. The dotted portions of the spectrum indicate regions of doubtful purity or regions where there may be water vapor absorption or weak H_2Se absorption. The two calculated spectra in these figures will be discussed in the latter part of this chapter.

Spectra of H_2Se were obtained with two different Golay detectors, one with a crystal quartz window and the other with a diamond window,* both approximately 0.5 mm thick. The quartz windowed detector is limited to use in the spectral region of wave lengths longer than 40 μ, since crystal quartz is opaque to radiation of shorter wavelengths. The diamond-windowed detector has been used in the spectral region from 15 to 200 μ, since diamond is quite transparent here. However, when the diamond detector is used with the standard filtering techniques in the 40 - 200 μ region, the radiation is not as pure as that obtained when the quartz detector is used in this region. This is because the quartz window acts as an additional filter to remove unwanted radiation of wavelength shorter than 40 μ while the diamond window does not.

---

*The author wishes to express thanks to Elia Burstein of the Naval Research Laboratories, Washington D. C., for making available the Golay detector with a diamond window.

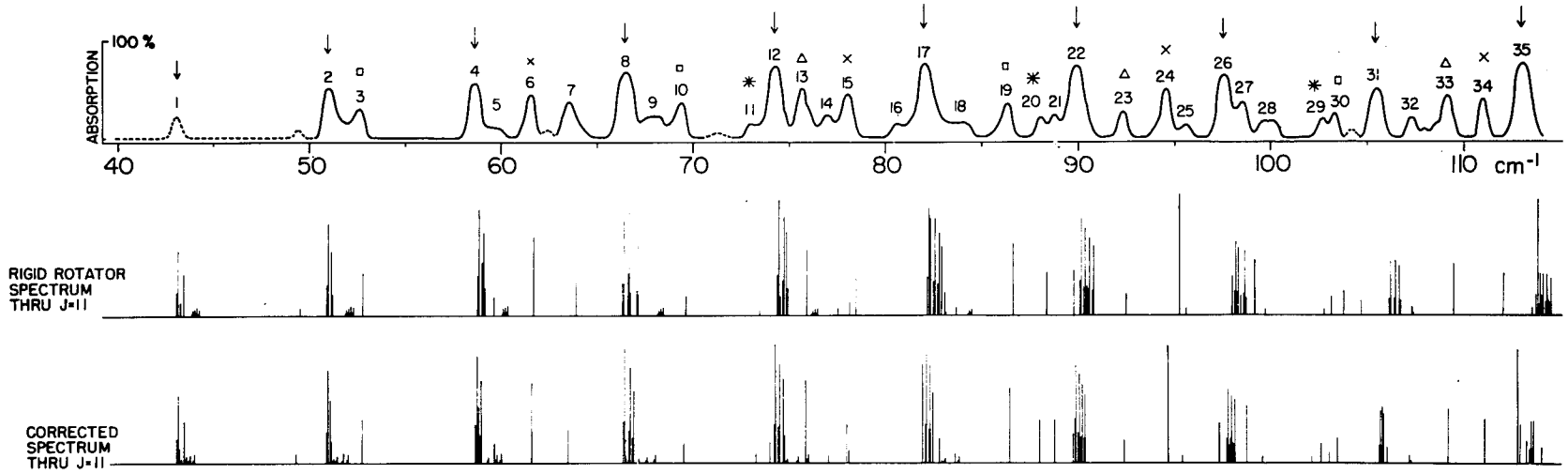

FIG. 4. Observed spectrum, rigid rotator spectrum, and spectrum corrected for centrifugal distortion with Lawrance and Strandberg formula – H_2Se.

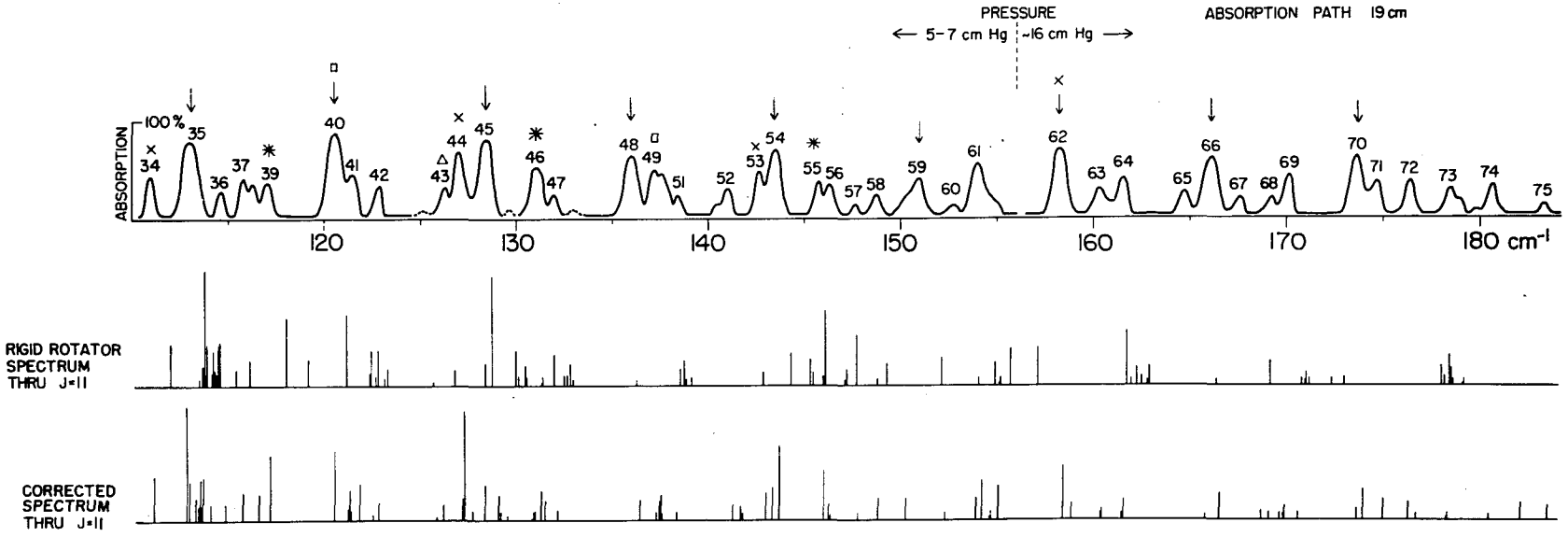

FIG. **5**. Observed spectrum, rigid rotator spectrum, and spectrum corrected for centrifugal distortion with Lawrance and Strandberg formula - H_2Se.

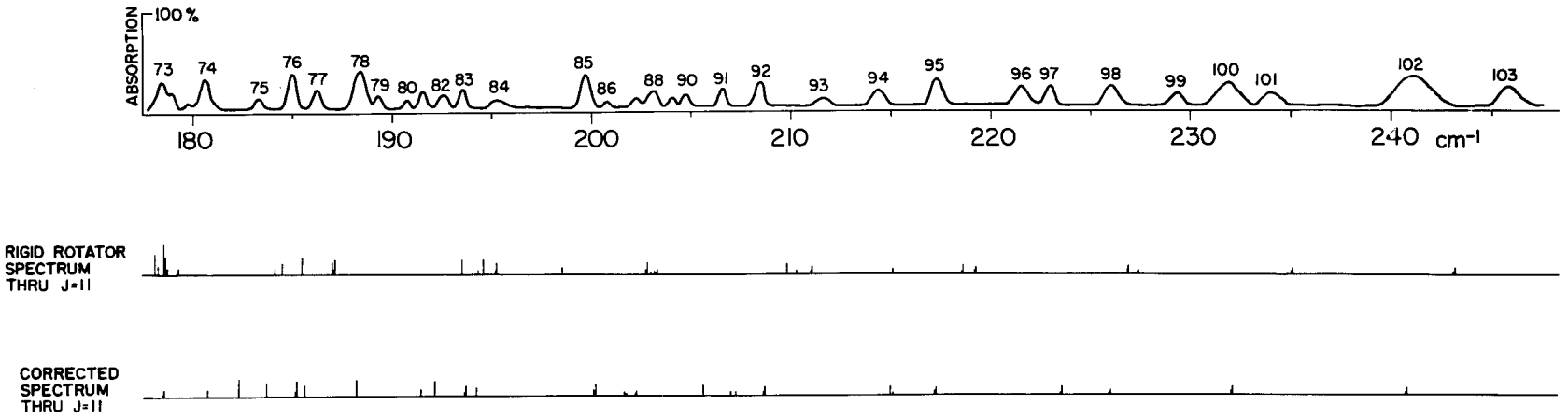

FIG. **6.** Observed spectrum, rigid rotator spectrum, and spectrum corrected for centrifugal distortion with Lawrance and Strandberg formula - H_2Se.

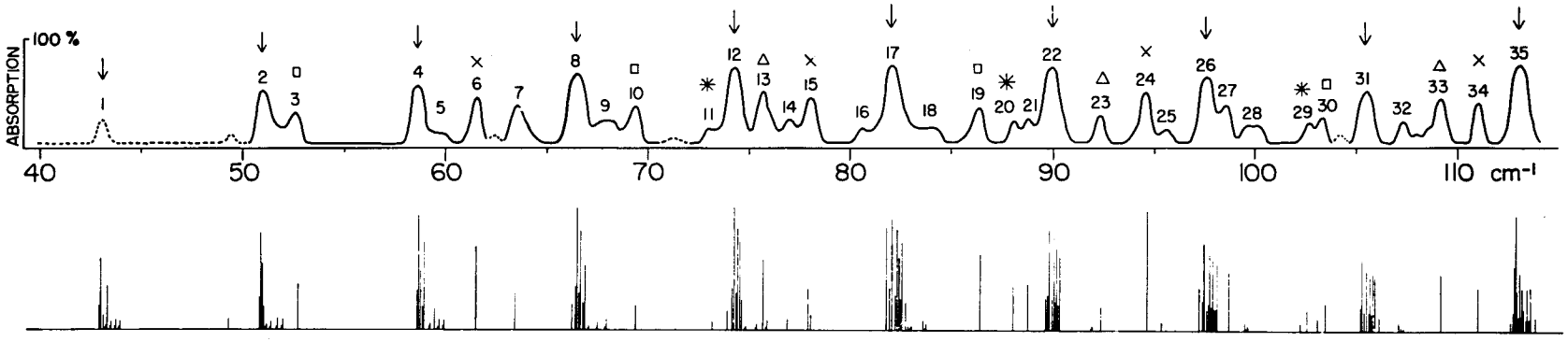

FIG. **7.** Observed spectrum and best fit spectrum of H_2Se.

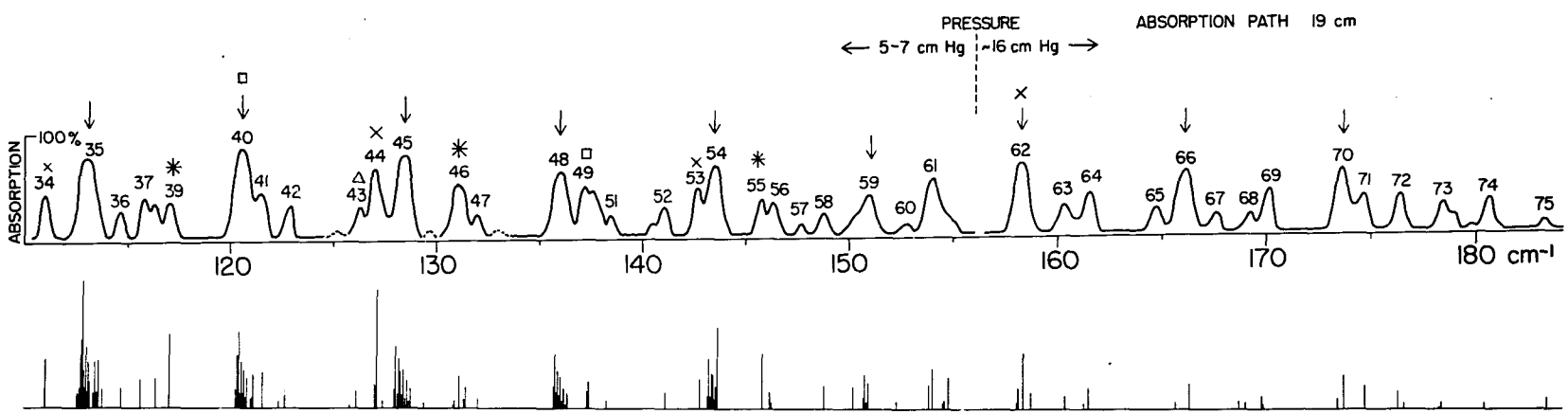

FIG. **8.** Observed spectrum and best fit spectrum of H_2Se.

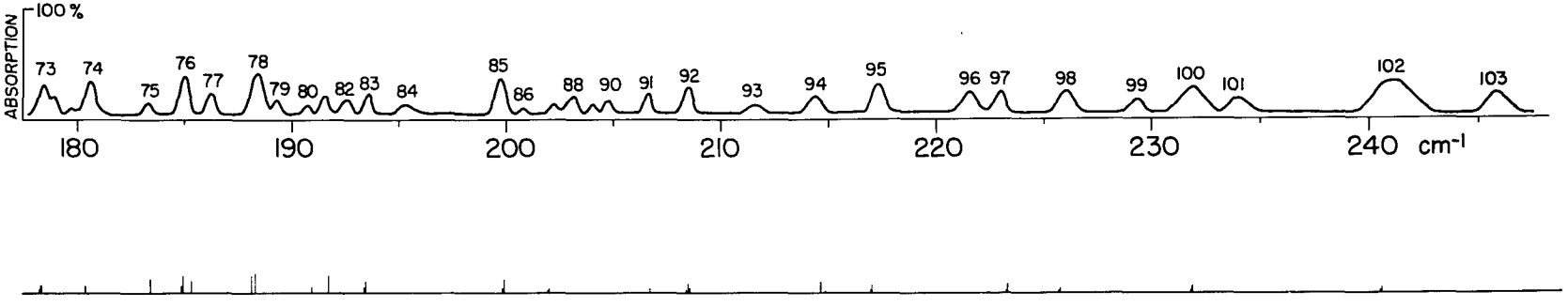

FIG. 9. Observed spectrum and best fit spectrum of H_2Se.

However, the diamond detector is more sensitive than the quartz detector, and there is considerable improvement in resolution using the diamond detector in the region from 40 to 200 μ.

The spectrum of H_2Se was recorded with both detectors. The spectrum obtained with the diamond-windowed detector was compared with the spectrum obtained with the quartz-windowed detector for spurious lines which could be higher order impurities. Figure 10, p. 33, a photograph of typical spectrograms obtained, will give the reader an idea of the noise level and resolution. Several spurious deflections evident are due to instrumental difficulties. The top two spectrograms were obtained with the quartz-windowed detector, while a diamond-windowed detector was used to obtain the bottom spectrogram. In this bottom spectrogram, slit widths were changed in the 135 cm^{-1} region. The improved resolution is evident. For the spectrograms shown, the spectral slit width at 115 cm^{-1} is $\sim$ 0.45 cm^{-1} with the quartz-windowed detector and $\sim$ 0.30 cm^{-1} with the diamond-windowed detector. Generally, spectral slit widths varied from 0.25 to 0.7 cm^{-1}.

The obvious feature of the spectrum is the series of strong, almost evenly spaced lines typical of a symmetric rotator. These lines are marked by arrows in Figures 4, p. 26, 5, p. 27, 7, p. 29, and 8, p. 30. There are a few weaker lines between these main lines, some of which can also be grouped into series. The most prominent of these weaker

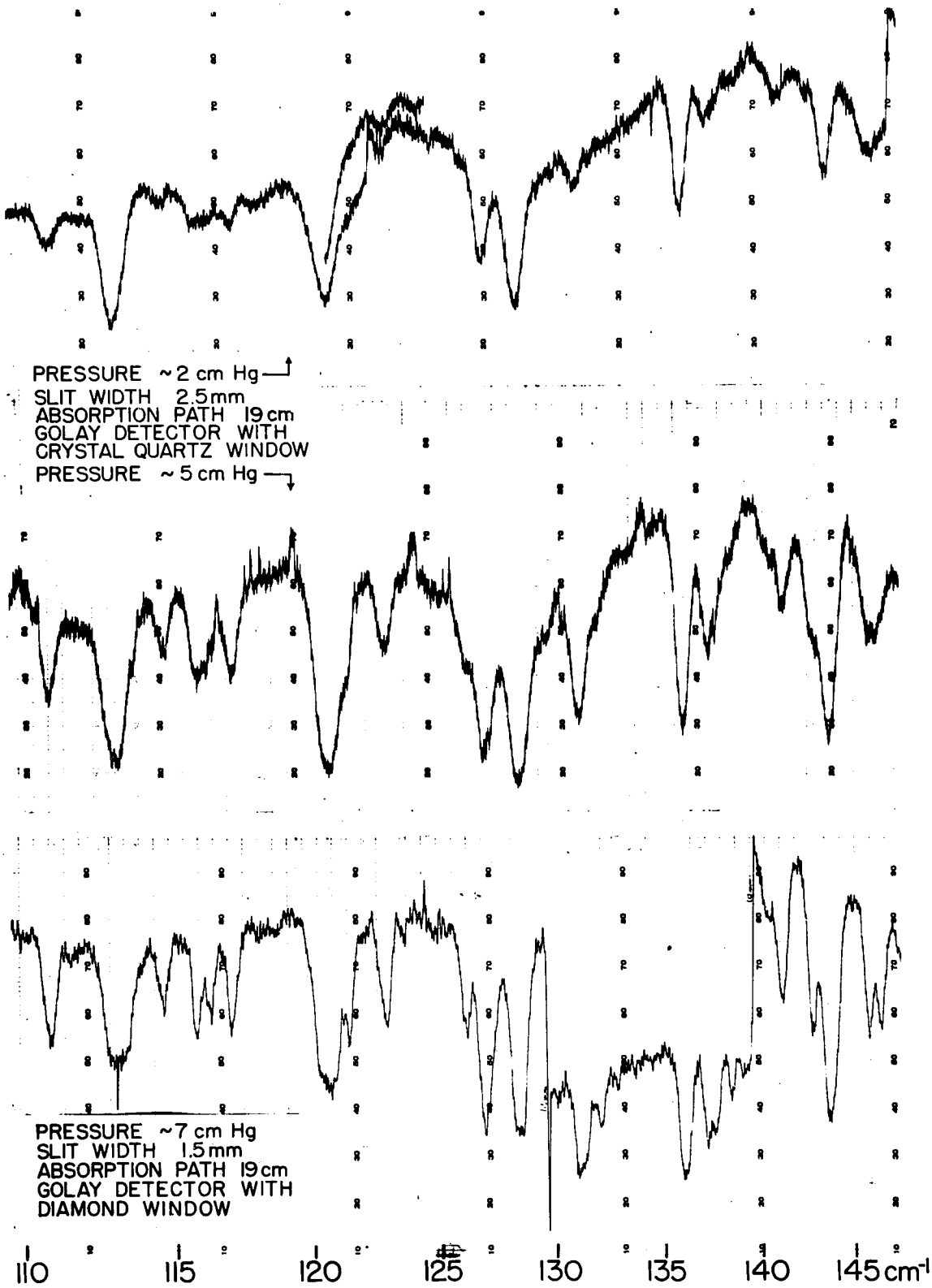

Fig. 10. Typical spectrograms of H_2Se.

series is indicated by crosses. Other series, not as evident, are also marked with the symbols △ , □ , and * .

Line positions were measured from three or four records independently and averaged. Many measurements by several different investigators using this spectrograph indicate that in the range from 50 to 250 cm^{-1}, frequencies of sharp absorption lines can be measured with an accuracy of $\pm$ 0.1 cm^{-1} or better.

It should be remembered that there are several isotopes of selenium, Se^{74} (0.87%), Se^{76} (9.02%), Se^{77} (7.58%), Se^{78} (23.52%), Se^{80} (49.82%), and Se^{82} (9.19%). Therefore, a gas sample contains several different H_2Se molecules, each with slightly different moments of inertia. However, the spectra of the various molecules could not be resolved.

Theory and Analysis:

Review of Asymmetric Rotator Theory.

Considerable information about the H_2Se molecule can be obtained from work reported in the literature. Cameron, Sears, and Nielsen give values for the reciprocals of inertia, moments of inertia, and the H-Se distance r, assuming the molecule to be an exactly accidently symmetric, oblate rotator with the apex angle $2\alpha = 90^{\circ}$.

Pauling[9] has given values for the ionic radii of

---

(9) L. S. Pauling, "The Nature of the Chemical Bond and the Structure of Molecules and Crystals" (Cornell University Press, Ithaca, N. Y., 1939).

hydrogen and selenium which indicate that in the H_2Se molecule r(H-Se) = 1.46 A.

For the planar rigid model shown in Figure 11, p. 36, the moments of inertia I_a, I_b, and I_c of H_2Se are given by the expressions

$$\begin{aligned} I_a &= \frac{2M_H M_{Se}}{2M_H+M_{Se}} r^2 \cos^2\alpha \\ I_b &= 2M_H r^2 \sin^2\alpha \\ I_c &= 2M_H r^2 \left[1 - \cos^2\alpha \left(1 - \frac{M_{Se}}{2M_H+M_{Se}}\right) \right] \end{aligned} \qquad (3.1)$$

where M_H and M_{Se} are the masses of the hydrogen and selenium atoms. From the structure of the three fundamental vibration-rotation bands, Cameron, Sears and Nielsen concluded that the geometric symmetry axis is the axis of intermediate moment of inertia. From equations (3.1) it can easily be shown that

$$\begin{aligned} \tan\alpha &= \left[\frac{M_{Se}\, I_b}{(2M_H+M_{Se})\, I_a} \right]^{\frac{1}{2}} \\ r &= \left[\frac{(M_{Se}+2M_H)\, I_c}{2M_H(M_{Se}+2M_H \sin^2\alpha)} \right]^{\frac{1}{2}} \end{aligned} \qquad (3.2)$$

Since the dipole moment lies along the b axis of intermediate moment of inertia, the selection rules $\begin{matrix} ++ \leftrightarrow -- \\ +- \leftrightarrow -+ \end{matrix}$ and $\Delta J = 0, \pm 1$ apply here.

The energy of an asymmetric rotator have been discussed by many authors. Two of the most frequently used descriptions

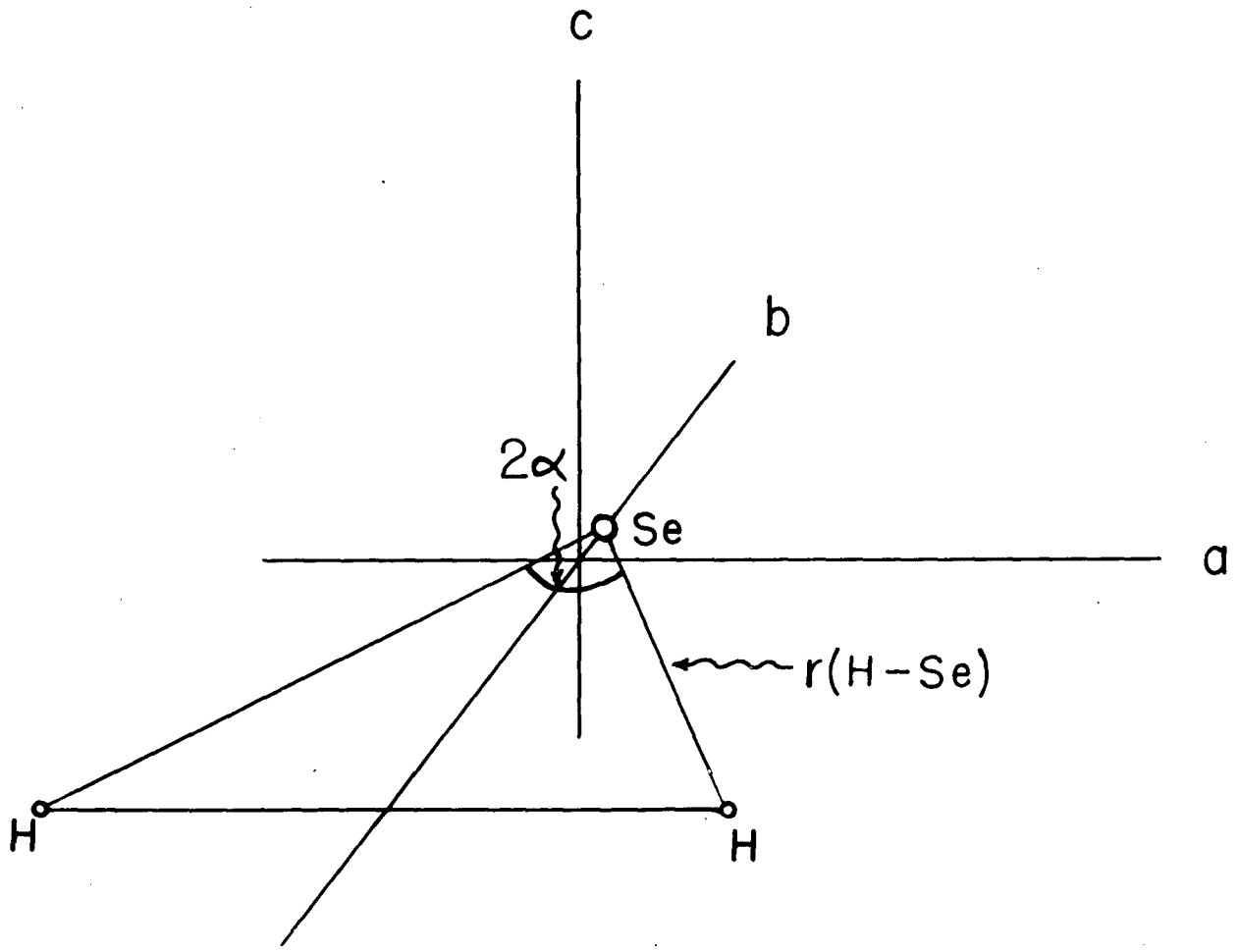

FIG. 11. Molecular model for H_2Se.

are due to Wang[10] and Ray[11]. The formulation of Ray was further developed by King, Hainer and Cross[12]. The energy formula due to Wang can be written as

$$W(J_\tau) = \frac{1}{2}(B_x+B_y)J(J+1)+[B_z - \frac{1}{2}(B_x+B_y)]\, W_\tau \qquad (3.3)$$

where B_x, B_y and B_z are the reciprocals of inertia, B_x being the smallest or largest, B_y the intermediate and B_z the closest to unique. W_τ is a quantity which depends on B_x, B_y, B_z and J in a complicated manner. For a given J, there are 2J + 1 levels which are labled by the index τ which ranges from J to -J.

The other expression for the energy is

$$W(J_\tau) = \frac{1}{2}(a + c)J(J + 1) + \frac{1}{2}(a-c)E^J_\tau(\varkappa) \qquad (3.4)$$

where $E^J_\tau(\varkappa)$ is the so-called reduced energy, values of which have been tabulated by King, Hainer and Cross through J = 12 for various values of the asymmetry parameter $\varkappa = \frac{2b-(a+c)}{a-c}$. Turner, Hicks and Reitwiesner[13] have given a more detailed

---

(10) S. C. Wang, Phys. Rev. 34, 243 (1929).

(11) B. S. Ray, Z. Physik 78, 74 (1932).

(12) G. W. King, R. M. Hainer and P. C. Cross, J. Chem. Phys. 11, 27 (1943).

(13) T. E. Turner, B. L. Hicks and G. Reitwiesner, "Asymmetric Rotor Eigenvalue Table" (Ballistic Research Laboratories, Report 878, Aberdeen Proving Ground, Maryland, 1953).

tabulation of $E_{\tau}^{J}(\varkappa)$ with $\varkappa = 0.00(0.01)1.00$ through $J = 12$. As usual, $a > b > c$.

Levels are also classified by the behavior of the rotational wave functions for rotation by 180° about the a, b and c axes, that is + if the wave function does not change sign and - if it does change sign. Dennison[14] has shown that for C_c^2, the highest level for a given J is + . The next two highest are -, the next two +, etc., while for C_a^2, the lowest level is +, the next higher two are -, etc. This classification is shown in Figure 12, p. 39. The behavior of the rotational wave function for C_b^2 is just the product of the behavior for C_a^2 and C_c^2 .

The energy levels of H_2Se also have a nuclear statistical weight factor because of the presence of the two identical hydrogen particles which obey Fermi-Dirac statistics. From an investigation of the behavior of the total wave function of the molecule which is a product of the translational, electronic, vibrational, rotational, nuclear, etc. wave functions when the identical particles are exchanged, it can be shown that levels with + for C_b^2 will have weight factor 1 while levels with - will have weight factor 3. This weight factor is important in the calculation of relative intensities. The weight factors for some of the low J levels are shown in Figure 12, p. 39.

---

[14] D. M. Dennison, Rev. Mod. Phys. 3, 280 (1931).

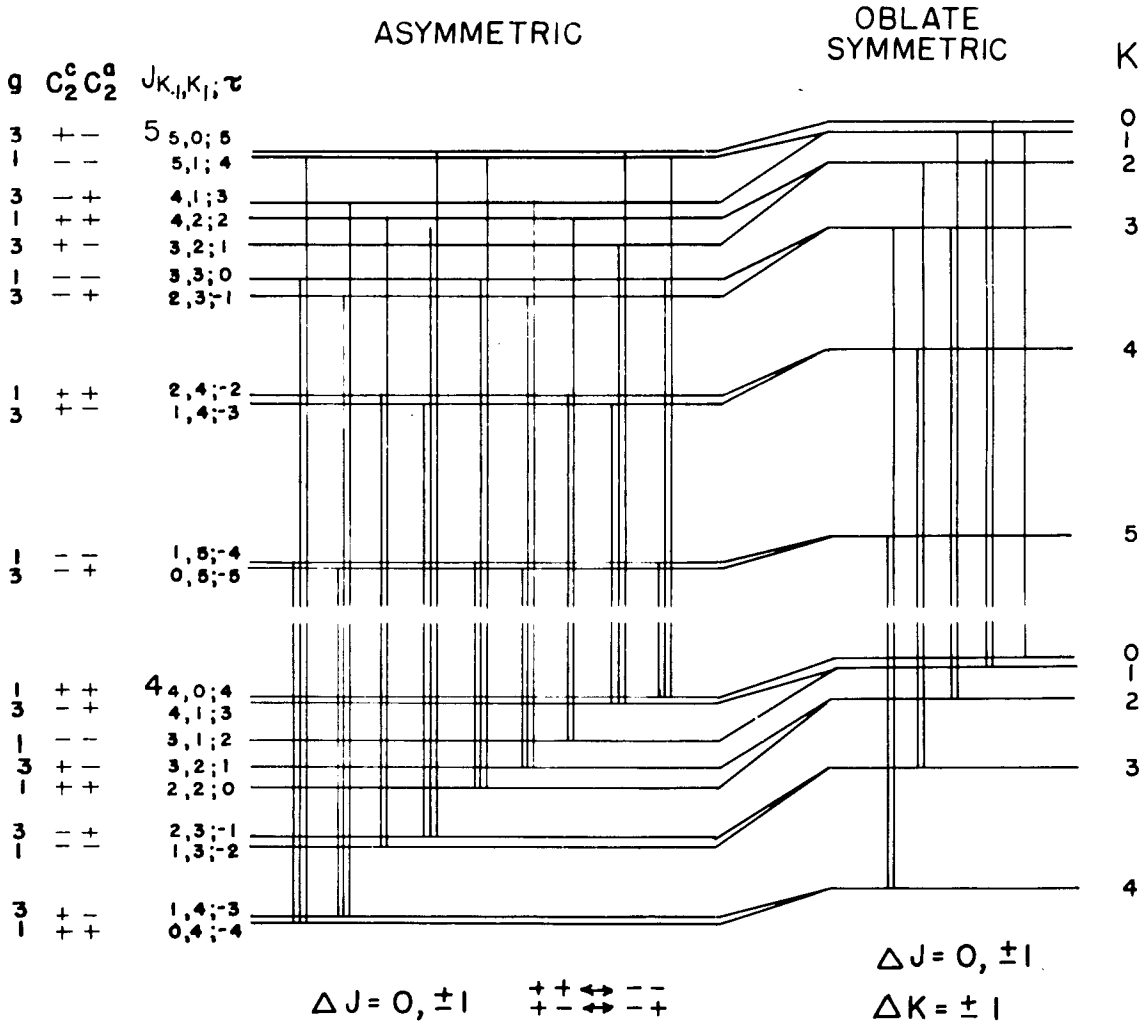

FIG. 12. Comparison of the energy levels of an asymmetric rotator with those of an oblate symmetric rotator.

Relative intensities for H_2Se lines were calculated using the table of line strengths for the asymmetric rotator as given by Cross, Hainer and King.[15] The intensity of an absorption line is given by the expression

$$I_{n'', n'} = \frac{8\pi^3 \nu N g_{n''} (1-e^{-\frac{h\nu}{kT}}) e^{-W_{n''}/kT}}{3hc \sum g_n e^{-W_n/kT}} \left|\mu_{n'', n'}\right|^2 \qquad (3.5)$$

where n'' represents all the quantum numbers associated with the initial state, n' represents all the quantum numbers associated with the final state, ν is the frequency of the absorption line, h is Planck's constant and c is the speed of light. N is the number of molecules per cm^3, and $g_{n''}$ is the nuclear weight factor of the initial state. The quantity $(1-e^{-h\nu/kT})$ is the induced emission factor, and $e^{-W_{n''}/kT}$ is the Boltzmann factor for the initial level. The last term is the square of the n'', n' element of the dipole moment matrix. Cross, Hainer and King have tabulated a quantity proportional to this term called the line strength, which is a function of χ. The term $\sum g_n e^{-W_n/kT}$ is just the partition function which is a constant for the molecule. Therefore, the relative intensity can be computed by the formula

$$I_{n'',n'} \propto \nu g_{n''} (1-e^{-h\nu/kT}) e^{-W_{n''}/kT} \quad \text{(line strength)}. \qquad (3.6)$$

---

(15) P. C. Cross, R. M. Hainer and G. W. King, J. Chem. Phys. 12, 210 (1944).

Application of Symmetric Rotator Theory:

The theory that has been reviewed for the asymmetric rotator has been used in the analysis described in this chapter. However, since it is evident that the molecule is only slightly asymmetric, it is possible to start the analysis by an application of oblate symmetric rotator theory.

First, consider that the molecule is an accidently oblate symmetric rotator with a = b = 2c since the model is non-linear. The inertial defect will be neglected in this discussion. For this model, the figure or unique axis is the c axis. The permanent dipole moment lies along the b axis. Therefore, for this symmetric rotator $\Delta K = \pm 1$ and $\Delta J = 0, \pm 1$. The energy of this rotator is expressed as

$$W(J,K) = bJ(J+1) + (c-b)K^2 . \qquad (3.7)$$

Some of the levels are shown in Figure 12, p. 39.

Letting $\Delta J = +1$ and $\Delta K = \pm 1$ in the expression for the frequencies

$$\nu = W(J',K') - W(J'',K'') \qquad (3.8)$$

gives

$$\nu = 2bJ' + (c-b)\,[\pm 2K'-1] . \qquad (3.9)$$

Now if $K' = J'$ and $\Delta K = +1$ corresponding to high K transitions, equation (3.9) becomes, using the upper sign

$$\nu = 2cJ' - (c-b) = 2cJ' + c . \qquad (3.10)$$

Thus, there will be a series of lines separated by 2c for the rigid model. If this series is graphed by plotting J along the absiccsa and ν along the ordinate, the resulting

straight line has a slope 2c and intercepts the ν axis at c.

If the set of transitions with K' = 1 and $\Delta K = +1$ is considered, another series is obtained,

$$\nu = 2bJ' + (c-b) = 4cJ' - c \ . \qquad (3.11)$$

The lines of this series fall on every other line of the series of equation (3.10).

Other series can also be calculated, for example for K' = 0, $\Delta K = -1$

$$\nu = 2bJ' - (c-b) = 4cJ' + c \ . \qquad (3.12)$$

All these series will coincide to form a spectrum consisting of a series of evenly spaced lines 2c apart. The interesting feature is that the spectrum lines, while evenly spaced, are spaced by 2c instead of 2b which is the usual case for pure rotational spectra of geometrically symmetric rotators. This is because the dipole moment is perpendicular to the figure axis in H_2Se, but would not be perpendicular to the figure axis in a geometrically symmetric rotator. Also, the first line is at 3c, the next at 5c, the next at 7c, etc., while for the usual case, the first line is at 2b, the next at 4b, the next at 6b, etc.

If now, the molecule becomes asymmetric, the low K levels will shift from their symmetric rotator positions much more than the high K levels. This effect is illustrated in Figure 13, p. 43. Here, $E_\tau^J(K)/J(J+1)$ is plotted against κ. It is evident that the high K levels are not very sensitive to the asymmetry while the low K levels are quite sensitive.

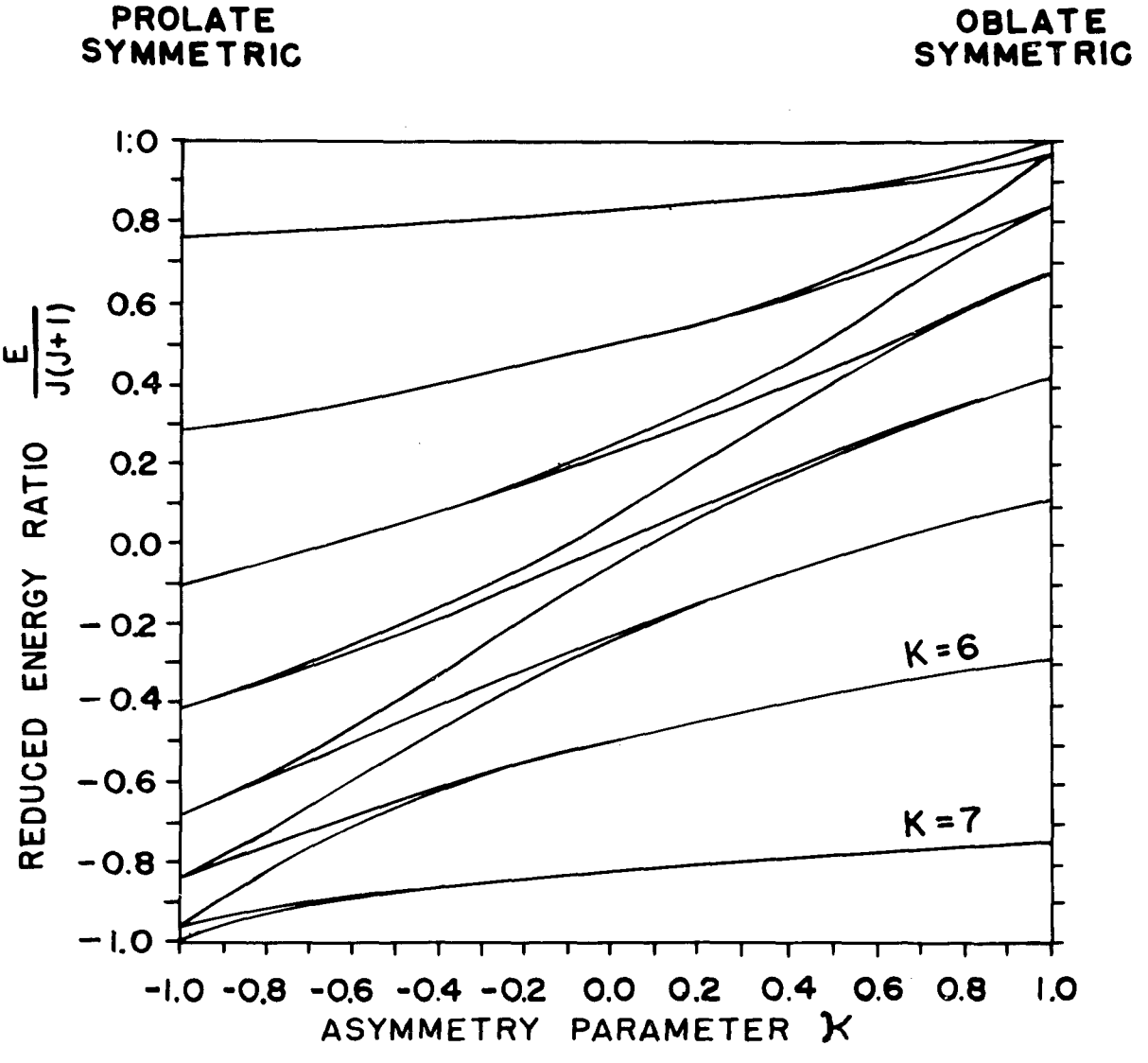

FIG. 13. Reduced energy levels of an asymmetric rotator for J=7 versus the asymmetry parameter κ.

As the molecule becomes slightly asymmetric, the series represented by equation (3.10) remains essentially unchanged. However, the series which correspond to equations (3.11) and (3.12) will move from the main series for the oblate rotator into the regions between the main lines. These series will have the approximate spacing $4c \approx 2b \approx 2a$. Other series may also move out from the main series. If H_2Se is only slightly asymmetric, its spectrum should exhibit these gross features. There will be a strong series of lines spaced by 2c corresponding to high K transitions (low τ transitions), indicated by arrows in Figures 4, p. 26, 5, p. 27, 6, p. 28, 7, p. 29, 8, p. 30 and 9, p. 31, and perhaps two or more series spaced by $2b \approx 2a$ corresponding to low K transitions (high τ transitions). One of these is marked by crosses in Figures 4, p. 26, 5, p. 27, 7, p. 29 and 8, p. 30.

Application of Approximate Oblate Rotator Theory:

This method of approach can be refined by making use of an approximate expression for a slightly asymmetric oblate-limiting case given by Herzberg.[16] According to the Wang formulation, the energy of an asymmetric rotator near the oblate-limiting case $a \approx b$ will be

$$W(J_\tau) = \frac{1}{2}(a+b)J(J+1) + [c - \frac{1}{2}(a+b)]\, W_\tau \,. \qquad (3.13)$$

---

(16) G. Herzberg, "Molecular Spectra and Molecular Structure II. Infrared and Raman Spectra of Polyatomic Molecules" (D. Van Nostrand Company, Inc., New York 1951).

In the oblate-limiting case, W_τ becomes K^2. For a nearly oblate rotator, the approximation $K^2 \approx W_\tau$ can be made in equation (3.13) to obtain

$$W(J_\tau) = \frac{1}{2}(a+b)J(J+1) + [c - \frac{1}{2}(a+b)]\ K^2 \qquad (3.14)$$

remembering that a does not exactly equal b. This formula does not indicate the splitting of the low K levels, but gives an average value between any two levels formed by an originally two-fold degenerate K level.

Manipulating equation (3.14) in the same manner as equation (3.7), the following series of lines should occur for the slightly asymmetric oblate rotator. For $\Delta J = +1$, $\Delta K = \pm 1$

$$\nu = (a+b)J' + [c - \frac{1}{2}(a+b)][\pm 2K' - 1] \ . \qquad (3.15)$$

For $K' = J'$ and $\Delta K = +1$

$$\nu = 2cJ' + [-c + \frac{1}{2}(a+b)] \ . \qquad (3.16)$$

Therefore, there will occur a series spaced by 2c. For $K' = 1$ and $\Delta K = +1$

$$\nu = (a+b)J' + [c - \frac{1}{2}(a+b)] \ . \qquad (3.17)$$

For $K' = 0$ and $\Delta K = -1$

$$\nu = (a+b)J' - [c - \frac{1}{2}(a+b)] \ . \qquad (3.18)$$

These are only a few of the possible series which will occur. Equation (3.16) corresponds to the high K transitions or for the asymmetric rotator, low τ transitions. Equations (3.17)

and (3.18) are low K transitions for the oblate rotator or high τ transitions for the asymmetric rotator. To indicate from which limiting prolate and oblate levels the asymmetric levels originate, the notation of King, Hainer and Cross is adopted. The level is designated by $J_{K_{-1}, K_1, \tau}$ where K_{-1} is the K value for the prolate-limiting energy level from which the asymmetric level is derived, K_1 is the K value for the oblate-limiting level, and τ is the index identifying the asymmetric level. Then $(K_{-1})-(K_1) = \tau$.

The various series will not coincide as in the case of the exactly symmetric oblate rotator since account is being taken of the fact that a = b. When these series are plotted, the slopes will give approximate values of 2c and a + b, while the intercepts will give $[c-\frac{1}{2}(a+b)]$. Assuming that $I_c = I_a + I_b$, it is possible to express a in terms of b, thus

$$a = c(a+b)\left(\frac{1}{b}\right) . \qquad (3.19)$$

The series given by equation (3.16) is easily found, since it is the very strongest series in the spectrum. Actually, each line of this series is a cluster of several low τ transitions. Another series spaced by approximately a+b was found. It is indicated by crosses in Figures 4, p. 26, 5, p. 27, 7, p. 29 and 8, p. 30. This series is given by equation (3.17). It was finally found that equation (3.15) becomes

$$\nu = 16.4\ J' - 4.2(\pm\ 2K'-1) . \qquad (3.20)$$

This equation predicts several of the series fairly well, for example, the series for which $K'=J'$, $\Delta K = +1$ (↓); $K'=1$, $\Delta K = +1$ (x); $K' = 3$, $\Delta K = +1$ (△); and $K' = 2$, $\Delta K = +1$ (□). Several of the experimentally observed series are plotted in Figure 14, p. 48. They do not quite form straight lines because of the effect of centrifugal distortion on the energy levels. It was from slopes and intercepts of such plots that the constants of equations (3.16) and (3.17) were determined.

This simple theory, then, definitely indicates that the low K transitions move into the regions between the lines of the main series when the oblate rotator becomes slightly asymmetric.

To check the validity of using equation (3.14), the following tests were made. Regular series in the pure rotational spectra of H_2O, D_2O, H_2S, NH_2D, and NHD_2 were plotted against J'. The slopes and intercepts of the resulting lines were measured to obtain values for the various combinations of a, b and c. These values, obtained using the approximate formula for the energy levels of a slightly asymmetric rotator were checked with the best values that have been obtained from analyses of the bands. In general, it was noticed that the errors in determining the various combinations of a, b and c increased as the molecules became more asymmetric, that is, as κ went from +1 or -1 to 0. This, of course, is to be expected. Table IV, p. 49, summarizes these results.

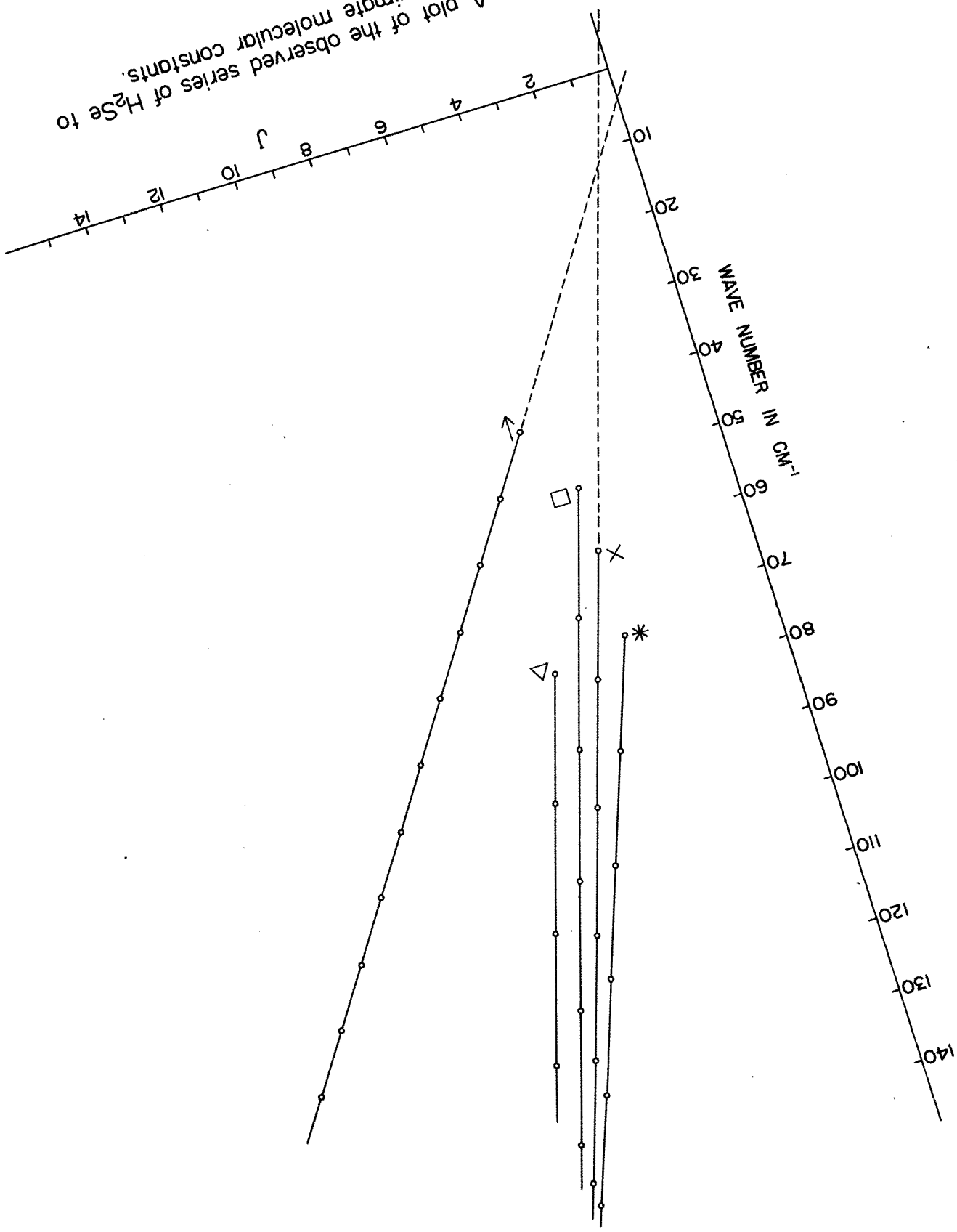

Fig. **14**. A plot of the observed series of H_2Se to determine approximate molecular constants.

TABLE IV.

SOME MOLECULAR CONSTANTS OF H_2Se, H_2S, NHD_2, NH_2D, H_2O, and D_2O. THE COLUMN MARKED C_{approx}, A_{approx}, $(a + b)_{approx}$, and $(b + c)_{approx}$, GIVE VALUES DETERMINED FROM APPROXIMATE FORMULAE FOR SLIGHTLY ASYMMETRIC ROTATORS.
THE COLUMNS MARKED C, A, (a+b), and (b+c) GIVE VALUES OBTAINED FROM ANALYSES OF FAR INFRARED ROTATIONAL SPECTRA.

Molecule	κ	C_{approx}	C	$(a+b)_{approx}$	(a+b)
H_2Se	+0.78	3.9	3.91	16.2	15.87
H_2S	+0.52	4.6	4.72	20.0	19.43

	κ	A_{approx}	A	$(b+c)_{approx}$	(b+c)
NHD_2	-0.13	7.3	7.44	12.4	9.11
NH_2D	-0.31	9.5	9.68	15.5	11.13
H_2O	-0.40	28.0	27.80	20.0	23.76
D_2O	-0.54	15.5	15.38	9.7	12.08

But even for H_2S with $\kappa = 0.5$, the approximation is fairly good giving a 5% error in determining a-b and a 2% error in determining c. It was reasonable to expect that the constants for H_2Se would be quite good using this approximation.

The analysis discussed so far does not indicate how much a and b differ, that is, how asymmetric the molecule is. However, a reasonable guess as to the values of a and b can be made from consideration of the geometry of the molecule. For H_2S, the bond angle is approximately 92.2° and the H-S distance is 1.33 A. Replacing the sulfur atom by the heavier selenium atom will cause the center of mass to move closer to the selenium atom. Assuming that 2α is approximately 90°, and that the H-Se distance is only slightly larger than the H-S distance, the molecule is even more symmetric than H_2S which has an asymmetry parameter $\kappa = 0.53$. A comparison of the experimental spectra of H_2S and H_2Se also indicates that H_2Se is more symmetric than H_2S. The main series of lines spaced by 2c is much more evident for H_2Se than H_2S. Therefore, it was assumed that κ for H_2Se has a value between 0.6 and 0.9. With c and a+b known approximately, values for a and b were calculated for various values of κ using equation (3.19) and $\kappa = \frac{2b-(a+c)}{a-c}$. As is discussed later, these values were used with the more accurate representation for the energy of an asymmetric rotator to obtain the best fit for the low J lines which were already assigned tentatively.

The centrifugal distortion effects were first treated as follows. With approximate values for c and a+b determined, the positions of the rigid rotator lines corresponding to the two main series were calculated. The experimental values for the line positions were subtracted from the corresponding rigid rotator values, and this difference was plotted against J'^3. The results proved to be straight lines. This general type of result was shown to be reasonable for H_2O by Randall et al,[17] and for D_2O by Fuson, Randall and Dennison.[18] An attempt was made to account for the centrifugal distortion by symmetric rotator theory. For an oblate, symmetric rotator, taking into consideration centrifugal distortion, the energy can be represented by the formula

$$W(J,K) = bJ(J+1) + (c-b)K^2 - D_J J^2(J+1)^2 - D_{JK}J(J+1)K^2 - D_K K^4 \quad . \tag{3.21}$$

For $\Delta J = +1$ and $\Delta K = \pm 1$ and neglecting D_K since usually $D_K \ll D_J$

$$\nu = 2J' + (c-b)[\mp 2K' - 1] - 4D_J J'^3 - D_{JK}[J'^2(\pm 2K' - 1) + J'(2K'^2 \mp 2K' + 1)] \quad . \tag{3.22}$$

For the series of equation (3.17) where $K' = 1$ and $\Delta K = +1$,

---

(17) H. M. Randall, D. M. Dennison, N. Ginsburg and L. R. Weber, Phys. Rev. 52, 160 (1937).

(18) N. Fuson, H. M. Randall and D. M. Dennison, Phys. Rev. 56, 982 (1939).

the difference in frequency $\Delta\nu$ between the rigid rotator and experimental lines can be shown to be

$$\Delta\nu = 4D_J J'^3 + D_{JK} J'(J' + 1) \qquad (3.23)$$

If $D_J \approx D_{JK}$, as is usually the case for the regular oblate symmetric rotator, the $4D_J J'^3$ term is the dominant one, the second term being only a few per cent of the first then, $\Delta\nu \approx 4D_J J'^3$. For the series of equation (3.16)

$$\Delta\nu = 4D_J J'^3 + D_{JK}[4J'^3 - 3J'^2 + J'] \; . \qquad (3.24)$$

For oblate molecules like NH_3, PH_3, and AsH_3, D_J is positive and D_{JK} is negative. If this case obtains for H_2Se along with $D_J \approx D_{JK}$ the term $-3J'^2 - J'$ cannot be neglected. Evidently, then, the symmetric rotator centrifugal distortion formula does not predict the simple J'^3 relationship for the lines of the two series. It is observed that for the series of equation (3.17) indicated by x in Figures 4, p. 26, 5, p. 27, 7, p. 29 and 8, p. 30, $\Delta\nu = 0.00328\ J'^3$. For the series of equation (3.16), indicated by $\downarrow$, $\Delta\nu = 0.000254\ J'^3$. In a latter part of this chapter, a more satisfactory centrifugal distortion correction is discussed.

Application of Asymmetric Rotator Theory:

Considerable information about the H_2Se molecule has been obtained by application of simple oblate symmetric rotator theory. The two main series have been identified, and

some of the other lines have been tentatively assigned. The effect of centrifugal distortion on the highest and lowest levels is known. Now, recourse will be made to the more exact formulation of the energy of an asymmetric rotator as given by King, Hainer and Cross.

Using the several sets of values for a, b and c obtained from the above analysis for κ = 0.6, 0.7, 0.8 and 0.9, the lower J levels for the rigid, asymmetric rotator were computed, the allowed transitions determined, and the intensities calculated for κ = 0.8. The four spectra obtained were compared with the experimental spectrum. The best fit was obtained for the low J lines for κ = 0.8.

A more accurate method of determining the constants of H_2Se was attempted. From the expression for the energy levels $W(J_\tau) = \frac{1}{2}(a+c)J(J+1) + \frac{1}{2}(a-c)\,E^J_\tau(\kappa)$, the frequency of any transition can be obtained by application of the proper selection rules. The result is

$$\nu = W(J'_\tau) - W(J''_\tau) = (a+c)J' + \frac{1}{2}(a-c)[E^{J'}_{\tau'}(\kappa) - E^{J''}_{\tau''}(\kappa)] \qquad (3.25)$$

Neglecting centrifugal distortion which was assumed small for several low J transitions, several equations of the form of equation (3.25) were set up. The quantities a+c, a-c and κ were considered as unknowns, although approximate values were known for them. It was assumed that κ had a value between 0.7 and 0.9. These equations were combined to eliminate (a+c) as a variable. The resulting set of equations were in terms

of (a-c) and $\varkappa$. Values of $\varkappa$ were chosen and the corresponding values for (a-c) were computed. The results were plotted as shown in Figure 15, p. 55. The curves intersect at almost one point. The coordinates of this point give a value of $\varkappa$ and (a-c) which satisfy all the equations. Then, a value for (a+c) is easily determined from equation (3.25) and the line frequencies. A value for b is obtained from the relation $\varkappa = \frac{2b-(a+c)}{(a-c)}$. Several such plots were made, using various combinations of lines as a check on other assignments. If one of the assignments were wrong, this would usually show up in the plot as a curve not intersecting at the common point. The very steep curve obtained from the transitions 5_1-4_3 / 5_2-4_2 indicates that one or both of the two lines used is very sensitive to the asymmetry of the molecule. The line is the $5_1 - 4_3$ transition. This line along with several other sensitive lines proved very helpful in the determination of a reasonable $\varkappa$ and a-c. These values are not quite correct because the experimental frequencies were used and not the rigid rotator frequencies. Using the simple centrifugal distortion correction obtained above, the experimental frequencies can be corrected to the rigid rotator frequencies somewhat. The final results for the best rigid rotator fit are $a = 8.16_5$, $b = 7.71_2$, $c = 3.91_5$ cm^{-1}.

Using these new values, the rigid rotator spectrum was recomputed with a resulting better fit to the experimental

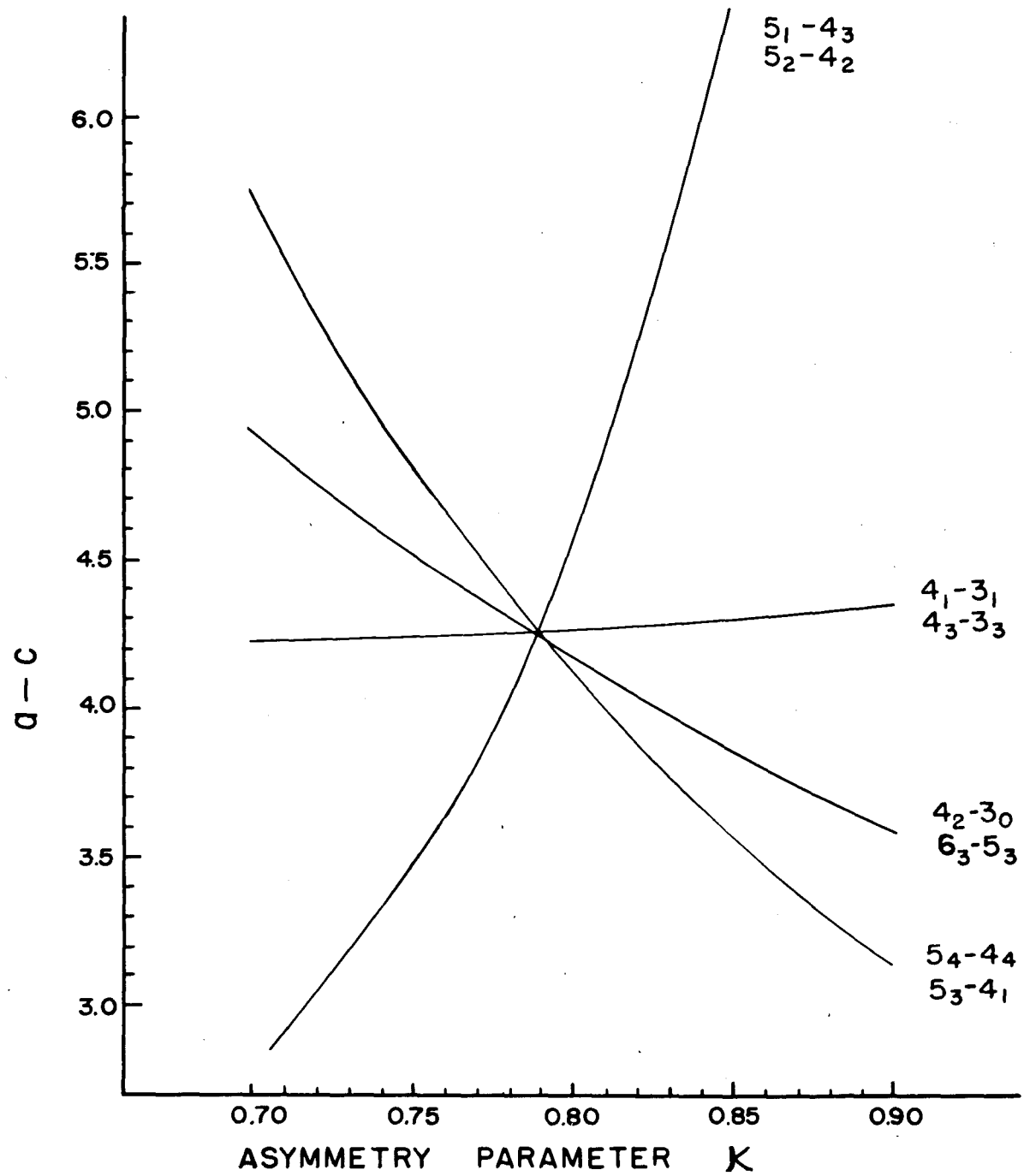

FIG. 15. Determination of a−c and κ.

spectrum and the consequent tentative assignment of more of the higher J transitions. The rigid energy levels are listed in the second column of Table V, p. 57.

The rigid rotator spectrum through J = 11 is shown in Figures 4, p. 26, 5, p. 27 and 6, p. 28. The agreement is fair for low frequencies but becomes bad as J increases. The calculated frequencies of several pairs of lines, especially low τ transitions, coincide. These pairs usually have an intensity ratio of 3 to 1. For clarity of identification these calculated lines are drawn slightly separated. Also any calculated lines accidently falling on each other are separated slightly.

When there are available the lowest J transitions, it is often easy to determine the rotational constants. The energy levels of a rigid asymmetric rotator can be expressed as combinations of the various rotational constants as given by Gordy, Smith and Trambarulo[19]. These results are obtained from the Mecke sum rules. For example, neglecting centrifugal distortion, the 1_0-0_0 transition directly gives a+c, the 2_{-1}-1_{-1} transition gives a+3c, the 2_1-1_1 transition gives 3a+3c. Higher J transitions can be expressed as more complicated functions of a, b and c. During the course of this investigation, it was attempted to determine the rotational

---

(19) W. Gordy, W. V. Smith and R. F. Trambarulo, "Microwave Spectroscopy" (John Wiley & Sons, Inc., New York, 1953).

TABLE V.

RIGID ROTATOR ENERGY LEVELS FOR H_2Se, BEST FIT ENERGY LEVELS, AND CENTRIFUGAL DISTORTION ENERGY ΔW.

$J_{K_{-1},K_1;\tau}$	Rigid rotator energy levels (cm^{-1})	Best fit energy levels (cm^{-1})	$-\Delta W$ (cm^{-1})
$0_{0,0;0}$	0.00	0.00	0.00
$1_{1,0;1}$	15.87	15.87	0.00
$1_{1,1;0}$	12.08	12.08	0.00
$1_{0,1;-1}$	11.62	11.62	0.00
$2_{2,0;2}$	47.67	47.65	0.02
$2_{2,1;1}$	44.28	44.28	0.00
$2_{1,1;0}$	42.92	42.89	0.03
$2_{1,2;-1}$	31.54	31.54	0.00
$2_{0,2;-2}$	31.50	31.50	0.00
$3_{3,0;3}$	95.45	95.38	0.07
$3_{3,1;2}$	92.62	92.59	0.03
$3_{2,1;1}$	89.90	89.81	0.09
$3_{2,2;0}$	79.16	79.15	0.01
$3_{1,2;-1}$	78.98	78.90	0.08
$3_{1,3;-2}$	59.03	59.03	0.00
$3_{0,3;-3}$	59.03	59.03	0.00
$4_{4,0;4}$	159.32	159.09	0.23
$4_{4,1;3}$	157.10	156.93	0.17
$4_{3,1;2}$	152.59	152.43	0.21
$4_{3,2;1}$	142.70	142.62	0.08
$4_{2,2;0}$	142.15	141.91	0.24
$4_{2,3;-1}$	122.46	122.38	0.08
$4_{1,3;-2}$	122.45	122.36	0.09
$4_{1,4;-3}$	94.37	94.34	0.03
$4_{0,4;-4}$	94.37	94.34	0.03

TABLE V. (Cont'd.)

$5_{5,0;5}$	239.40	238.86	0.54
$5_{5,1;4}$	237.77	237.30	0.47
$5_{4,1;3}$	231.03	236.65	0.43
$5_{4,2;2}$	222.17	221.97	0.25
$5_{3,2;1}$	220.93	220.41	0.57
$5_{3,3;0}$	201.74	201.47	0.27
$5_{2,3;-1}$	201.68	201.40	0.28
$5_{2,4;-2}$	173.67	173.51	0.16
$5_{1,4;-3}$	173.67	173.51	0.16
$5_{1,5;-4}$	137.54	137.47	0.07
$5_{0,5;-5}$	137.54	137.47	0.07
$6_{6,0;6}$	335.78	334.64	1.14
$6_{6,1;5}$	334.64	333.52	1.07
$6_{5,1;4}$	325.30	324.50	0.80
$6_{5,2;3}$	317.61	317.04	0.57
$6_{4,2;2}$	315.26	314.19	1.07
$6_{4,3;1}$	296.84	296.22	0.62
$6_{3,3;0}$	296.68	295.89	0.79
$6_{3,4;-1}$	268.80	268.37	0.43
$6_{2,4;-2}$	268.78	268.34	0.44
$6_{2,5;-3}$	232.71	232.45	0.26
$6_{1,5;-4}$	232.71	232.45	0.26
$6_{1,6;-5}$	188.54	188.42	0.12
$6_{0,6;-6}$	188.54	188.42	0.12
$7_{7,0;7}$	448.51	446.35	2.16
$7_{7,1;6}$	447.76	445.63	2.08
$7_{6,1;5}$	435.49	434.11	1.38
$7_{6,2;4}$	429.04	427.93	1.11
$7_{5,2;3}$	425.11	423.33	1.78
$7_{5,3;2}$	407.78	406.59	1.19
$7_{4,3;1}$	407.38	405.78	1.60
$7_{4,4;0}$	379.75	378.71	1.04

TABLE V. (Cont'd.)

$^{7}_{3,4;-1}$	379.74	378.66	1.08
$^{7}_{3,5;-2}$	343.70	343.01	0.69
$^{7}_{2,5;-3}$	343.70	343.01	0.69
$^{7}_{2,6;-4}$	299.57	299.20	0.37
$^{7}_{1,6;-5}$	299.57	299.20	0.37
$^{7}_{1,7;-6}$	247.36	247.17	0.19
$^{7}_{0,7;-7}$	247.36	247.17	0.19
$^{8}_{8,0;8}$	577.61	573.93	3.68
$^{8}_{8,1;7}$	577.13	573.48	3.65
$^{8}_{7,1;6}$	561.70	559.41	2.29
$^{8}_{7,2;5}$	556.52	554.56	2.01
$^{8}_{6,2;4}$	550.53	547.78	2.75
$^{8}_{6,3;3}$	534.56	532.49	2.07
$^{8}_{5,3;2}$	533.70	530.96	2.79
$^{8}_{5,4;1}$	506.52	504.56	1.96
$^{8}_{4,4;0}$	506.47	504.31	2.06
$^{8}_{4,5;-1}$	470.53	469.03	1.50
$^{8}_{3,5;-2}$	470.53	469.03	1.49
$^{8}_{3,6;-3}$	426.44	425.47	0.97
$^{8}_{2,6;-4}$	426.44	425.47	0.97
$^{8}_{2,7;-5}$	374.26	373.70	0.56
$^{8}_{1,7;-6}$	374.26	373.70	0.56
$^{8}_{1,8;-7}$	314.02	313.73	0.29
$^{8}_{0,8;-8}$	314.02	313.73	0.29
$^{9}_{9,0;9}$	723.09	717.08	6.01
$^{9}_{9,1;8}$	722.79	716.81	5.98
$^{9}_{8,1;7}$	704.06	700.44	3.62
$^{9}_{8,2;6}$	700.08	696.76	3.32
$^{9}_{7,2;5}$	691.57	687.33	4.04
$^{9}_{7,3;4}$	677.19	673.90	3.29
$^{9}_{6,3;3}$	675.57	670.96	4.51

TABLE V. (Cont'd.)

$^{9}_{6,4;2}$	649.07	645.76	3.31
$^{9}_{5,4;1}$	648.96	645.38	3.58
$^{9}_{5,5;0}$	613.18	610.42	2.76
$^{9}_{4,5;-1}$	613.18	610.40	2.78
$^{9}_{4,6;-2}$	569.14	567.11	2.03
$^{9}_{3,6;-3}$	569.14	567.11	2.03
$^{9}_{3,7;-4}$	517.00	515.71	1.34
$^{9}_{2,7;-5}$	517.00	515.71	1.34
$^{9}_{2,8;-6}$	456.79	456.01	0.78
$^{9}_{1,8;-7}$	456.79	456.01	0.78
$^{9}_{1,9;-8}$	388.51	388.06	0.45
$^{9}_{0,9;-9}$	388.51	388.06	0.45
$^{10}_{10,0;10}$	884.93	875.63	9.30
$^{10}_{10,1;9}$	884.75	875.46	9.29
$^{10}_{9,1;8}$	862.68	857.24	5.54
$^{10}_{9,2;7}$	859.76	854.52	5.24
$^{10}_{8,2;6}$	848.32	842.66	5.76
$^{10}_{8,3;5}$	835.71	830.74	4.97
$^{10}_{7,3;4}$	832.90	826.19	6.71
$^{10}_{7,4;3}$	807.42	802.11	5.16
$^{10}_{6,4;2}$	807.17	801.36	5.71
$^{10}_{6,5;1}$	771.63	766.96	4.57
$^{10}_{5,5;0}$	771.62	766.89	4.63
$^{10}_{5,6;-1}$	727.67	724.02	3.65
$^{10}_{4,6;-2}$	727.67	724.02	3.65
$^{10}_{4,7;-3}$	675.57	672.90	2.67
$^{10}_{3,7;-4}$	675.57	672.90	2.67
$^{10}_{3,8;-5}$	615.39	613.63	1.76
$^{10}_{2,8;-6}$	615.39	613.63	1.76
$^{10}_{2,9;-7}$	547.14	546.08	1.06

TABLE V. (Cont'd.)

$^{10}_{1,9;-8}$	547.14	546.08	1.06
$^{10}_{1,10;-9}$	470.82	470.17	0.65
$^{10}_{0,10;-10}$	470.82	470.17	0.65
$^{11}_{11,0;11}$	1063.13	1049.24	13.79
$^{11}_{11,1;10}$	1063.02	1049.13	13.79
$^{11}_{10,1;9}$	1037.66	1029.27	8.19
$^{11}_{10,2;8}$	1035.60		7.91
$^{11}_{9,2;7}$	1020.90		8.00
$^{11}_{9,3;6}$	1010.15		7.21
$^{11}_{8,3;5}$	1005.66		9.44
$^{11}_{8,4;4}$	981.54		7.63
$^{11}_{7,4;3}$	981.03		8.69
$^{11}_{7,5;2}$	945.86		7.09
$^{11}_{6,5;1}$	945.83		7.23
$^{11}_{6,6;0}$	902.01	896.04	5.97
$^{11}_{5,6;-1}$	902.01	896.04	5.97
$^{11}_{5,7;-2}$	849.98	845.29	4.69
$^{11}_{4,7;-3}$	849.98	845.29	4.69
$^{11}_{4,8;-4}$	789.84	786.42	3.42
$^{11}_{3,8;-5}$	789.84	786.42	3.42
$^{11}_{3,9;-6}$	721.61	719.31	2.30
$^{11}_{2,9;-7}$	721.61	719.31	2.30
$^{11}_{2,10;-8}$	645.32	643.90	1.42
$^{11}_{1,10;-9}$	645.32	643.90	1.42
$^{11}_{1,11;-10}$	560.97	560.02	0.95
$^{11}_{0,11;-11}$	560.97	560.02	0.95
$^{12}_{12,0;12}$	1257.67	1237.7	
$^{12}_{12,1;11}$	1257.61	1237.6	

TABLE V. (Cont'd.)

$^{12}_{11,1;10}$	1229.05	
$^{12}_{11,2;9}$	1227.66	
$^{12}_{10,2;8}$	1209.41	
$^{12}_{10,3;7}$	1200.55	
$^{12}_{9,3;6}$	1193.86	
$^{12}_{9,4;5}$	1171.46	
$^{12}_{8,4;4}$	1170.47	
$^{12}_{8,5;3}$	1135.86	
$^{12}_{7,5;2}$	1135.80	
$^{12}_{7,6;1}$	1092.14	
$^{12}_{6,6;0}$	1092.14	
$^{12}_{6,7;-1}$	1040.20	1032.3
$^{12}_{5,7;-2}$	1040.20	1032.3
$^{12}_{5,8;-3}$	980.11	974.0
$^{12}_{4,8;-4}$	980.11	974.0
$^{12}_{4,9;-5}$	911.93	907.2
$^{12}_{3,9;-6}$	911.93	907.2
$^{12}_{3,10;-7}$	835.66	832.4
$^{12}_{2,10;-8}$	835.66	832.4
$^{12}_{2,11;-9}$	751.33	749.4
$^{12}_{1,11;-10}$	751.33	749.4
$^{12}_{1,12;-11}$	658.95	657.5
$^{12}_{0,12;-12}$	658.95	657.5
$^{13}_{5,9;-4}$		1110.2
$^{13}_{4,9;-5}$		1110.2
$^{13}_{4,10;-6}$		1035.8
$^{13}_{3,10;-7}$		1035.8
$^{13}_{3,11;-8}$		953.0
$^{13}_{2,11;-9}$		953.0
$^{13}_{2,12;-10}$		862.4

TABLE V. (Cont'd.)

$^{13}_{1,12;-11}$	862.4
$^{13}_{1,13;-12}$	762.8
$^{13}_{0,13;-13}$	762.8
$^{14}_{4,11;-7}$	1171.9
$^{14}_{3,11;-8}$	1171.9
$^{14}_{3,12;-9}$	1081.4
$^{14}_{2,12;-10}$	1081.4
$^{14}_{2,13;-11}$	982.9
$^{14}_{1,13;-12}$	982.9
$^{14}_{1,14;-13}$	875.6
$^{14}_{0,14;-14}$	875.6
$^{15}_{3,13;-10}$	1217.4
$^{15}_{2,13;-11}$	1217.4
$^{15}_{2,14;-12}$	1111.2
$^{15}_{1,14;-13}$	1111.2
$^{15}_{1,15;-14}$	996.0
$^{15}_{0,15;-15}$	996.0
$^{16}_{3,14;-11}$	1360.9
$^{16}_{2,14;-12}$	1360.9
$^{16}_{2,15;-13}$	1247.1
$^{16}_{1,15;-14}$	1247.1
$^{16}_{1,16;-15}$	1124.2
$^{16}_{0,16;-16}$	1124.2

TABLE V. (Cont'd.)

$^{17}_{2,16;-14}$	1390.5
$^{17}_{1,16;-15}$	1390.5
$^{17}_{1,17;-16}$	1260.0
$^{17}_{0,17;-17}$	1260.0
$^{18}_{2,17;-15}$	1541.4
$^{18}_{1,17;-16}$	1541.4
$^{18}_{1,18;-17}$	1403.3
$^{18}_{0,18;-18}$	1403.3
$^{19}_{1,19;-18}$	1554.1
$^{19}_{0,19;-19}$	1554.1
$^{20}_{1,20;-19}$	1712.2
$^{20}_{0,20;-20}$	1712.2

constants by solving some of these complicated expressions assuming that c was well known from the spacing of the lines of the main series. This approach was not very fruitful. Of course, the final values chosen for a, b and c do satisfy these relationships.

The reciprocals of inertia a, b and c are constants of the molecule in the lowest J level of the ground vibration state. In this state the molecule still executes zero point vibrations. The expression for the vibrational energy in the ground state suggests that the zero point vibration is a superposition of the three fundamental modes of vibration, since all of these modes contribute to the zero point energy.

At any instant, the three moments of inertia should obey the relationship $I_c = I_a + I_b$. The average moments $I_{a\ ave.}$, $I_{b\ ave.}$, and $I_{c\ ave.}$ should also follow this relationship. The equilibrium moments $I_{a\ e}$, $I_{b\ e}$ and $I_{c\ e}$ also obey this relationship. However, from the experimental spectrum only average values of a, b and c, denoted $a_{ave.}$, $b_{ave.}$ and $c_{ave.}$ are determined. From the value for $a_{ave.}$, the quantity $\left(\frac{1}{I_a}\right)_{ave.}$ is determined using the expression $a_{ave.} = \frac{h}{8\pi^2 c} \left(\frac{1}{I_a}\right)_{ave.}$ The c in this relation is the speed of light. Reciprocating $\left(\frac{1}{I_a}\right)_{ave.}$ gives the effective moment of inertia $I_{a\ eff.}$. The effective moments of inertia do not follow the relationship $I_c = I_a + I_b$.

Darling and Dennison[20] have shown that

$$\Delta = I_c - (I_a + I_b) \neq 0 \tag{3.26}$$

for the non-linear XY_2 type molecule. The exact expression for Δ is

$$\Delta = \left[\frac{h K_1^2 \omega_3^2}{\pi^2 c \omega_1 (\omega_3^2 - \omega_1^2)}\right](v_1 + \tfrac{1}{2}) + \left[\frac{h K_2^2 \omega_3^2}{\pi^2 c \omega_2 (\omega_3^2 - \omega_2^2)}\right](v_2 + \tfrac{1}{2}) - \left[\frac{h K_1^2 \omega_1^2}{\pi^2 c \omega_3 (\omega_3^2 - \omega_1^2)} + \frac{h K_2^2 \omega_2^2}{\pi^2 c \omega_3 (\omega_3^2 - \omega_2^2)}\right](v_3 + \tfrac{1}{2}) \tag{3.27}$$

where $K_1 = \mu \ell \delta_{33} (\delta_{21} - \frac{b \delta_{11}}{2a})$ and

$$K_2 = \mu \ell \delta_{33} (\delta_{22} - \frac{b \delta_{11}}{2a})$$

and $K_1^2 + K_2^2 = 1$. Here, $\mu = \frac{2mM}{2m+M}$, M is the mass of the X atom and m is the mass of the Y atom. Also, $\ell = \frac{1}{(1 + \frac{\mu b^2}{2ma^2})}$ where 2a is the Y-Y distance and b is the altitude of the triangle. Also,

$$\delta_{33} = \left[\frac{1}{\mu} + \frac{b^2}{2ma^2}\right]^{\frac{1}{2}} \qquad \delta_{1i} = \frac{D}{\left[(\tfrac{1}{2} m \lambda_i - C)^2 \mu + \tfrac{1}{2} m D^2\right]^{\frac{1}{2}}}$$

$$\delta_{2i} = (\tfrac{1}{2} m \lambda_i - C) \Big/ \left[(\tfrac{1}{2} m \lambda_i - C)^2 \mu + \tfrac{1}{2} m D^2\right]^{\frac{1}{2}}.$$

The factors C and D are certain constants in the expression for the potential energy.

Darling and Dennison showed that $K_1 \approx 0$ and $K_2 \approx 1$ for H_2O, so that Δ can be simplified to the form

$$\Delta = \frac{h}{\pi^2 C} \left\{ \frac{\omega_3^2}{\omega_2 (\omega_3^2 - \omega_2^2)} (v_2 + \tfrac{1}{2}) - \frac{\omega_2^2}{\omega_3^2 (\omega_3^2 - \omega_2^2)} (v_3 + \tfrac{1}{2}) \right\} \tag{3.28}$$

---

(20) B. T. Darling and D. M. Dennison, Phys. Rev. 57, 128 (1940).

so that only a knowledge of the normal frequencies is necessary to approximate Δ . This approximation has also been shown to be valid for D_2O by King[21] and H_2S by Hainer and King.[22] Consequently, it was used to estimate Δ for H_2Se. However, the frequencies of the band centers and not the normal frequencies were used, since the latter are not known. However, for H_2O, D_2O and H_2S, using the band centers instead of the normal frequencies introduces an error not larger than about 16% in the values of Δ . Δ was computed to be 0.119×10^{-40} gm cm^2. The experimental value for is $0.09_0 \times 10^{-40}$ gm cm^2. Actually, extrapolation to the normal frequencies on the basis of the results for H_2O and H_2S indicates that Δ should be 0.113×10^{-40} gm cm^2.

Centrifugal Distortion Corrections and Results:

As yet, no quantitative centrifugal distortion corrections have been made. To determine the actual energy levels of the non-rigid rotator, the following approach was used. The lowest transitions that were observed were $J = 3 \rightarrow 4$ transitions. The highest and lowest τ levels for $J = 3$ were determined using the simple centrifugal distortion correction described above. The other $J = 3$ levels were adjusted

---

(21) G. W. King, J. Chem. Phys. 15, 85 (1947).

(22) R. M. Hainer and G. W. King, J. Chem. Phys. 15, 89 (1947).

to what seemed reasonable values. Then the frequencies for the various $J = 3 \rightarrow 4$ transitions were added to the appropriate $J = 3$ level to obtain values for the $J = 4$ levels. Then the tentatively assigned $J = 4 \rightarrow 5$ transitions were added to the proper $J = 4$ levels to obtain values for the $J = 5$ levels. The levels obtained in this manner are the actual distorted levels. There are certain combination relations between various lines which can be used as checks. This method does not allow too much liberty in adjusting the levels since usually each level has associated with it four lines of considerable intensity, two transitions terminating at the level and two more originating there. Therefore, when a level is adjusted to give a better fit for one line, the other three lines will also become adjusted, not always in the proper direction. This may necessitate adjustment of other levels. The succeeding adjustment becomes tedious. However, this method is not very accurate, since so many of the lines fall into the main series and cannot be assigned a definite frequency. For example, of the transitions $5_1 - 4_3$, $5_5 - 4_3$, $6_5 - 5_1$, and $6_5 - 5_5$, only $5_1 - 4_3$ at 63.59 cm^{-1} and $6_5 - 5_5$ at 94.55 cm^{-1} appear to be single. The other two are strong but fall into the main series. In spite of these difficulties, this approach was fairly successful, since many of the lines had been assigned from the rigid rotator levels. Also, because of the near symmetry of the molecule, many of the lines gathered into the main

series, so that there were only a few lines between the very strong lines of the main series. This made the task of assigning some of the high J transitions on the basis of intensity fairly easy, since there were not many lines to choose from.

Levels were adjusted so that the single sharp lines were predicted to within $\pm$ 0.2 cm^{-1}. Since so many of the low τ transitions fall into the main series, there is some doubt as to the accuracy of most of these low τ levels.

The levels were chosen to predict most of the lines in the spectrum from 50 to 150 cm^{-1} and do not predict any lines of appreciable intensity in the open regions of the observed spectrum. Because the lines of the main series are actually groups of lines, they can be traced to transitions as high as $^{18}_{-17} - ^{17}_{-17}$. It was possible to extrapolate some of the levels to J = 13 and higher to get a rough idea of what the energy levels should be and then adjust these values slightly to predict some of the lines.

During the course of making this empirical determination, there was occasion to plot the difference between the rigid levels and the distorted levels ΔW against the various τ values for each J. It was noticed that this difference oscillates for high τ values within a given J. The low levels follow a fairly smooth pattern. Such a plot is shown in Figure 16, p. 70. This oscillation indicates that at least for positive τ's, centrifugal forces have a considerably different effect on adjacent levels. To determine

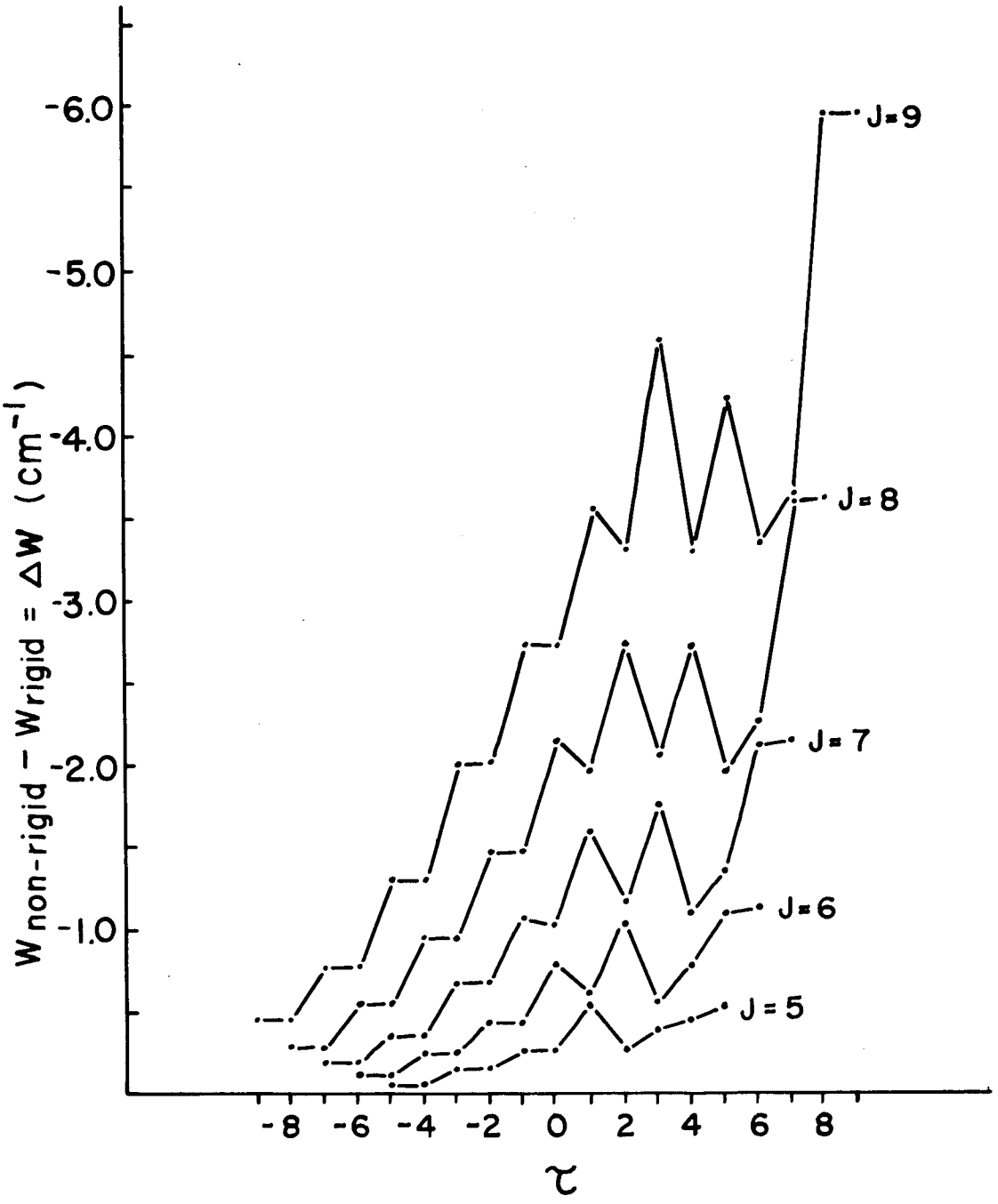

FIG. 16. Centrifugal distortion energy of the rotational levels of H_2Se.

whether this is reasonable, similar plots were made for H_2O and H_2S data, since these data are known. The same type of oscillation was found for both cases. For both H_2S and H_2Se, for the same J level, the corresponding τ levels were similarly effected. This oscillation was used to advantage in the determination of several of the levels.

To account for this result from theoretical aspects, recourse was made to the first order centrifugal distortion theory as developed by Lawrance and Strandberg.[23] Actually, their results can be obtained by making simplifications in the more complete first order theory developed by Kivelson and Wilson.[24] The simplifications are such that the approximation is good in the region where $\frac{E}{J(J+1)}$ is very different from K, K_1 is large, and the asymmetry slight. The results of Lawrance and Strandberg give the shift ΔW of the actual level from the rigid rotator level because of centrifugal distortion of the molecule. Thus

$$W = L\left(\frac{dE}{dX}\right)^2 + M\left(\frac{dE}{dX}\right)E + N\left(\frac{dE}{dX}\right)J(J+1) + QE^2 + R\,EJ\,(J+1) + S\,J^2(J+1)^2 . \qquad (3.29)$$

---

(23) R. B. Lawrance and M. W. P. Strandberg, Phys. Rev. 83, 363 (1951).

(24) D. Kivelson and E. B. Wilson, J. Chem. Phys. 20, 1575 (1952).

The quantities L, M, N, Q, R and S depend on parameters of the molecule such as normal frequencies, force constants, and reciprocals of inertia, but they are independent of the quantum numbers. The quantity E is the reduced energy. This formulation has been used with considerable success to correct $\Delta J = 0$ transitions for centrifugal distortion in microwave spectra. The constants are determined from the data to best predict the lines.

If the oscillation of ΔW is real, this expression for the centrifugal distortion should indicate it. It appears that the first three terms of ΔW can account for the oscillation. The quantity $\frac{dE}{d\tau}$ oscillates for positive τ values similarly to ΔW. It seems reasonable to expect that the six constants can be chosen to predict the distortion ΔW which is observed.

The alternative is to compute the centrifugal distortion constants using the results of the analysis of the near infrared vibration-rotation bands. This has been attempted by Burnside[25] for the pure rotational spectrum of H_2S using the distortion formula of Kivelson and Wilson. However, such an approach cannot be followed for H_2Se, since the near infrared bands have not been analyzed in detail.

---

(25) P. B. Burnside, "An Analysis of the Far Infrared Absorption Spectrum of Hydrogen Sulfide," (M. Sc. Thesis, The Ohio State University (1954).

Six ΔW's for $J = 7$ and $J = 8$ were used to determine the six constants. Since $\frac{dE}{dX}$ and E are known with some accuracy, it was possible to form six equations in the six unknowns L, M, N. Q, R, S. These equations were solved by a method of Doolittle which is discussed by Taussky[26]. The six constants satisfied the six equations, but did not give a good fit for other J values. After several attempts, only values of ΔW for $J = 8$ were used. These gave constants which predicted the experimentally observed distortion fairly well, at least to $J = 7$, with, however, several exceptions. It proved possible to reassign several lines, thereby changing some of the ΔW's, and then recompute the six constants. This resulted in an improved fit for the distortion. The final fit obtained with the six constants is shown in Figures 4, p. 26, 5, p. 27 and 6, p. 28, as the bottom calculated spectrum. Most of the lines from 50 to 150 cm^{-1} are predicted to within 0.2 cm^{-1}. Above 150 cm^{-1} the fit becomes poorer.

Many of the sets of six constants determined predicted the low J transitions, $J = 3 \rightarrow 4$, $4 \rightarrow 5$ and $5 \rightarrow 6$ quite well. But for higher J transitions, each set gave different results which did not predict the spectrum satisfactorily. The present fit with six constants is encouraging. It seems

---

(26) Taussky, "Contributions to the Solutions of Systems of Linear Equations the Determination of Eigenvalues," (National Bureau of Standards, Applied Mathematics Series, U. S. Government Printing Office, Washington 25, D.C., 1954).

reasonable to expect that continued refining of the constants would lead to a better fit.

The six constants used to make the centrifugal distortion corrections are complicated functions of the six constants A_1, A_2, A_3, A_4, A_5, A_6 in the more exact formulation of Kivelson and Wilson. These, in turn, are functions of certain distortion constants D_J, D_{JK}, D_K, R_5, R_6, δ_J defined for the general nonrigid asymmetric rotator by Nielsen[27]. These constants are functions of certain quantities $\tau_{\mu\nu\xi\varsigma}$ which appear in the Hamiltonian in the term $\sum \tau_{\mu\nu\xi\varsigma} P_\mu P_\nu P_\xi P_\varsigma$.

Benedict[28] has found that sometimes P^6 terms in the Hamiltonian must be used to satisfactorily account for the centrifugal distortion. This consideration, of course, would introduce more distortion constants to be determined.

If the six constants L, M, ··· are determined, it is, in principle, possible to calculate A_1, A_2 ··· and from these D_J, D_{JK}, ··· . Since the Lawrance and Strandberg formula is an approximation which can be obtained from the Kivelson and Wilson formula, it may be more expedient to fit the distortion to the Kivelson and Wilson formula directly.

---

(27) H. H. Nielsen, Rev. Mod. Phys. 23, 90 (1951).

(28) W. S. Benedict, Phys. Rev. 75, 1317 A (1949).

In the present case, the constants L, M, ··· are not known well yet. To work back to D_J, D_{JK}, ··· is somewhat complicated, so there is some doubt as to whether the results would approach the actual physical constants of the molecule.

To obtain the final best-fit energy levels, several of the ΔW's predicted by the six constant formula were adjusted slightly, usually < 0.2 cm^{-1} to obtain the best possible fit. This fit to the spectrum is shown in Figures 7, p. 29, 8, p. 30 and 9, p. 31. Most of the transitions through $J = 9 \rightarrow 10$ are accounted for. Several low τ transitions through $J = 20$ are also assigned. Since the low τ transitions fall together in clusters, these frequencies are not known well. However, guesses were made at their frequencies, and these were used to determine the low τ energy levels through $J = 20$. It is possible that these levels become progressively in error. Intensities for the low τ transitions above $J = 12$ were obtained by extrapolating the rough Boltzmann envelope of the lines.

The best-fit energy levels are listed in the third column of Table V, p. 57. The distortion corrections ΔW as computed from the six constants listed in the fourth column of Table V, p. 57. To determine the energy levels which are used to obtain the corrected spectrum in Figures 4, p. 26, 5, p. 27 and 6, p. 28, it is only necessary to subtract each ΔW from the corresponding rigid level.

In Table VI, p. 77, are listed the observed and best-fit calculated frequencies, the assigned transitions, and relative intensities.

The predicted relative intensities do not always agree with the per cent absorption observed, as for example at 116 cm^{-1}. This may be due to some higher J lines of considerable intensity, which were not considered, falling in this frequency range. However, in most cases, the intensities are reasonable.

Although $\Delta J = 0$ transitions are weak for this molecule, some are evident at $\sim$ 60, 68, 76 and 84 cm^{-1} because several fall together at approximately the same frequency.

In Table VII, p. 87, are listed the molecular constants obtained from this analysis. Using the effective moments of inertia in equations (3.2), the dimensions r and 2α were computed. The present results confirm, at least to the third member, the assumption that the bond distance should increase with each succeeding heavier member of the H_2O, H_2S, H_2Se and H_2Te family, while the apex angle decreases.

The energy levels determined here should be helpful in the analysis of the fundamental vibration-rotation bands of H_2Se. It is rather surprising that no thorough study of H_2Se and H_2Te has appeared to date in view of the great interest in H_2O and H_2S.

TABLE VI.

OBSERVED AND BEST-FIT CALCULATED TRANSITIONS FOR H_2Se.

Line No.	ν_{obs} (cm^{-1})	$\nu_{calc.\ best\ fit}$ (cm^{-1})	Transition $J'_\tau - J''_\tau$	Relative Intensity
1	43.11	43.13	$5_{-4} - 4_{-4}$	229
		43.13	$5_{-5} - 4_{-3}$	688
		43.22	$4_{-2} - 3_{0}$	137
		43.29	$9_{0} - 9_{-2}$	19
		43.29	$9_{-1} - 9_{-3}$	57
		43.48	$4_{-1} - 3_{-1}$	423
		43.56	$8_{-2} - 8_{-4}$	30
		43.56	$8_{-1} - 8_{-3}$	88
		43.81	$7_{-2} - 7_{-4}$	37
		43.81	$7_{-3} - 7_{-5}$	102
		44.03	$6_{-4} - 6_{-6}$	34
		44.03	$6_{-3} - 6_{-5}$	72
		49.32	$4_{0} - 3_{2}$	91
2	50.89	50.85	$6_{-5} - 5_{-5}$	940
		50.85	$6_{-6} - 5_{-4}$	314
		51.13	$5_{-3} - 4_{-1}$	650
		51.15	$5_{-2} - 4_{-2}$	217
		51.12	$10_{-2} - 10_{-4}$	16
		51.12	$10_{-1} - 10_{-3}$	47
		51.40	$9_{-2} - 9_{-4}$	26
		51.40	$9_{-3} - 9_{-5}$	79
		51.77	$8_{-4} - 8_{-6}$	36
		51.77	$8_{-3} - 8_{-5}$	109
		52.03	$7_{-4} - 7_{-6}$	39
		52.03	$7_{-5} - 7_{-7}$	106
a 3	52.54	52.81	$4_{-1} - 3_{-1}$	440

TABLE VI. (Cont'd.)

	4	58.70	58.75	$7_{-6} - 6_{-6}$	378
			58.75	$7_{-7} - 6_{-5}$	1130
			58.78	$5_{-1} - 4_{1}$	546
			58.94	$6_{-4} - 5_{-2}$	282
			58.94	$6_{-3} - 5_{-3}$	848
			59.27	$10_{-4} - 10_{-6}$	21
			59.27	$10_{-3} - 10_{-5}$	65
	5	59.50	59.60	$5_{0} - 4_{0}$	197
			59.70	$9_{-4} - 9_{-6}$	32
			59.70	$9_{-5} - 9_{-7}$	97
			59.97	$8_{-6} - 8_{-8}$	33
			59.97	$8_{-5} - 8_{-7}$	100
×	6	61.49	61.55	$4_{3} - 3_{3}$	804
	7	63.59	63.48	$5_{1} - 4_{3}$	359
	8	66.61	66.50	$4_{4} - 3_{2}$	234
			66.56	$8_{-8} - 7_{-6}$	415
			66.56	$8_{-7} - 7_{-7}$	1250
			66.75	$7_{-4} - 6_{-4}$	325
			66.75	$7_{-5} - 6_{-3}$	975
			66.88	$6_{-2} - 5_{0}$	247
			66.97	$6_{-1} - 5_{-1}$	740
			67.11	$11_{-5} - 11_{-7}$	17
			67.11	$11_{-4} - 11_{-6}$	51
			67.55	$10_{-6} - 10_{-8}$	27
			67.55	$10_{-5} - 10_{-7}$	80
			67.95	$9_{-6} - 9_{-8}$	30
			67.95	$9_{-7} - 9_{-9}$	89
	9	68.02			
□	10	69.35	69.44	$5_{2} - 4_{2}$	209
*	11	73.33	73.28	$4_{2} - 3_{0}$	79
			74.02	$6_{0} - 5_{2}$	188
	12	74.23	74.33	$9_{-8} - 8_{-8}$	400
			74.33	$9_{-9} - 8_{-7}$	1200

TABLE VI. (Cont'd.)

			74.50	$8_{-6} - 7_{-4}$	344
			74.50	$8_{-5} - 7_{-5}$	1030
			74.64	$7_{-3} - 6_{-1}$	850
			74.67	$7_{-2} - 6_{-2}$	284
			74.8	$12_{-6} - 12_{-8}$	12
			74.8	$12_{-7} - 12_{-5}$	36
			75.41	$11_{-7} - 11_{-9}$	20
			75.41	$11_{-6} - 11_{-8}$	61
△	13	75.69	75.81	$6_{1} - 5_{1}$	668
			75.91	$10_{-8} - 10_{-10}$	23
			75.91	$10_{-7} - 10_{-9}$	69
	14	77.06	76.89	$6_{2} - 5_{4}$	91
×	15	78.07	77.96	$5_{4} - 4_{4}$	384
			78.03	$4_{3} - 3_{-1}$	143
	16	81.05			
	17	82.08	81.93	$5_{5} - 4_{3}$	1030
			82.11	$10_{-10} - 9_{-8}$	390
			82.11	$10_{-9} - 9_{-9}$	1160
			82.31	$9_{-6} - 8_{-6}$	332
			82.31	$9_{-7} - 8_{-5}$	995
			82.44	$7_{-1} - 6_{1}$	690
			82.46	$8_{-4} - 7_{-2}$	285
			82.46	$8_{-3} - 7_{-3}$	850
			82.82	$7_{0} - 6_{0}$	235
	18		83.00	$12_{-8} - 12_{-10}$	15
			83.00	$12_{-7} - 12_{-9}$	45
			83.58	$4_{1} - 3_{-3}$	80
			83.88	$11_{-9} - 11_{-11}$	19
			83.88	$11_{-8} - 11_{-10}$	57
□	19	86.36	86.39	$6_{3} - 5_{3}$	750
*	20	88.12	88.03	$5_{3} - 4_{1}$	440
	21	88.77	88.74	$7_{1} - 6_{3}$	445

TABLE VI. (Cont'd.)

	22	89.95	89.81	$7_3 - 6_5$	307
			89.85	$11_{-10} - 10_{-10}$	345
			89.85	$11_{-11} - 10_{-9}$	1030
			90.07	$10_{-8} - 9_{-6}$	298
			90.07	$10_{-7} - 9_{-7}$	890
			90.24	$9_{-4} - 8_{-4}$	266
			90.24	$9_{-5} - 8_{-3}$	795
			90.33	$8_{-2} - 7_0$	246
			90.37	$8_{-1} - 7_{-1}$	705
			91.9	$12_{-10} - 12_{-12}$	14
			91.9	$12_{-9} - 12_{-11}$	42
Δ	23	92.31	92.40	$7_2 - 6_2$	220
×	24	94.55	94.71	$6_5 - 5_5$	1250
	25	95.37	95.39	$5_4 - 4_0$	72
	26	97.58	97.34	$6_6 - 5_4$	405
			97.5	$12_{-11} - 11_{-10}$	285
			97.5	$11_{-11} - 11_{-11}$	855
			97.72	$8_0 - 7_2$	185
			97.82	$11_{-8} - 10_{-8}$	250
			97.82	$11_{-9} - 10_{-7}$	750
			97.97	$10_{-6} - 9_{-4}$	230
			97.97	$10_{-5} - 9_{-5}$	690
			98.03	$5_1 - 4_{-1}$	211
			98.07	$9_{-2} - 8_{-2}$	216
			98.09	$9_{-3} - 8_{-1}$	640
	27	98.57	98.73	$8_1 - 7_1$	586
	28	99.75	99.51	$5_2 - 4_{-2}$	66
			99.6	$13_{-11} - 13_{-13}$	12
			99.6	$13_{-10} - 13_{-12}$	36
*	29	102.70	102.15	$8_4 - 7_6$	75
			102.63	$6_4 - 5_2$	204
□	30	103.29	103.03	$8_2 - 7_4$	127
			103.43	$7_4 - 6_4$	257

TABLE VI. (Cont'd.)

31	105.41	105.3	$13_{-12} - 12_{-12}$	200
		105.3	$13_{-13} - 12_{-11}$	600
		105.5	$12_{-10} - 11_{-8}$	200
		105.5	$12_{-9} - 11_{-9}$	600
		105.68	$11_{-6} - 10_{-6}$	185
		105.68	$11_{-7} - 10_{-5}$	555
		105.80	$10_{-4} - 9_{-2}$	178
		105.80	$10_{-3} - 9_{-3}$	580
		105.84	$9_{-1} - 8_{1}$	520
		106.10	$9_{0} - 8_{0}^{1}$	174
32	107.34	107.06	$5_{-1} - 4_{-3}$	80
		107.13	$5_{0} - 4_{-4}$	27
		107.3	$14_{-12} - 14_{-14}$	10
		107.3	$14_{-11} - 14_{-13}$	30
Δ 33	109.06	109.16	$8_{3} - 7_{3}$	565
× 34	110.92	111.04	$7_{6} - 6_{6}$	440
35	113.02	112.72	$6_{2} - 5_{0}$	110
		112.8	$14_{-14} - 13_{-12}$	166
		112.8	$14_{-13} - 13_{-13}$	500
		112.83	$7_{7} - 6_{5}$	1190
		112.89	$9_{1} - 8_{3}$	424
		113.0	$13_{-10} - 12_{-10}$	157
		113.0	$13_{-11} - 12_{-9}$	470
		113.1	$12_{-8} - 11_{-6}$	143
		113.1	$12_{-7} - 11_{-7}$	430
		113.11	$6_{5} - 5_{1}$	226
		113.52	$11_{-4} - 10_{-4}$	142
		113.52	$11_{-5} - 10_{-3}$	425
		113.60	$10_{-2} - 9_{0}$	145
		113.62	$10_{-1} - 9_{1}$	444
		113.85	$9_{5} - 8_{7}$	169
36	114.60	114.76	$9_{2} - 8_{2}$	148
37	115.77	115.64	$6_{3} - 5_{-1}$	248

TABLE VI. (Cont'd.)

	38	116.26	116.40	$9_3 - 8_5$	264
*	39	117.04	117.07	$7_5 - 6_3$	684
□	40	120.61	120.4	$15_{-14} - 14_{-14}$	133
			120.4	$15_{-15} - 14_{-13}$	400
			120.45	$8_5 - 7_3$	705
			120.5	$14_{-12} - 13_{-10}$	125
			120.5	$14_{-11} - 13_{-11}$	375
			120.6	$13_{-8} - 12_{-8}$	116
			120.6	$13_{-11} - 12_{-7}$	350
			120.8	$12_{-6} - 11_{-4}$	102
			120.8	$12_{-5} - 11_{-5}$	306
			121.13	$10_0 - 9_2$	86
			121.27	$11_{-2} - 10_{-2}$	110
			121.27	$11_{-3} - 10_{-1}$	328
	41	121.43	121.58	$10_1 - 9_1$	340
	42	122.83	122.38	$6_0 - 5_{-2}$	61
			122.71	$6_1 - 5_{-3}$	184
			125.85	$10_6 - 9_8$	30
△	43	126.18	126.12	$9_4 - 8_4$	152
×	44	126.97	127.04	$7_3 - 6_1$	220
			127.13	$8_7 - 7_7$	1120
			127.46	$10_2 - 9_4$	79
			128.2	$16_{-16} - 15_{-14}$	100
			128.2	$16_{-15} - 15_{-15}$	300
			128.3	$15_{-12} - 14_{-12}$	93
			128.3	$15_{-13} - 14_{-11}$	280
	45	128.41	128.30	$8_8 - 7_6$	340
			128.4	$14_{-10} - 13_{-8}$	87
			128.4	$14_{-9} - 13_{-9}$	260
			128.6	$13_{-6} - 12_{-6}$	80
			128.6	$13_{-7} - 12_{-5}$	240
			128.7	$12_{-4} - 11_{-2}$	77
			128.7	$12_{-3} - 11_{-3}$	232
			129.43	$10_4 - 9_6$	55

TABLE VI. (Cont'd.)

✳	46	131.09	130.90	$6_{-2} - 5_{-4}$	29
			130.90	$6_{-1} - 5_{-5}$	86
			131.15	$10_{3} - 9_{3}$	295
			131.44	$7_{6} - 6_{2}$	100
			131.48	$8_{6} - 7_{4}$	212
	47	132.03	132.04	$7_{4} - 6_{0}$	100
	48	135.99	135.8	$17_{-16} - 16_{-16}$	93
			135.8	$17_{-17} - 16_{-15}$	280
			135.9	$16_{-14} - 15_{-12}$	83
			135.9	$16_{-13} - 15_{-13}$	250
			136.0	$15_{-10} - 14_{-10}$	73
			136.0	$15_{-11} - 14_{-9}$	220
			136.1	$14_{-8} - 13_{-6}$	66
			136.1	$14_{-7} - 13_{-7}$	200
			136.2	$13_{-4} - 12_{-4}$	60
			136.2	$13_{-5} - 12_{-3}$	180
			136.3	$12_{-2} - 11_{0}$	50
			136.3	$12_{-1} - 11_{-1}$	174
□	49	137.16	137.35	$9_{6} - 8_{6}$	186
	50	137.52	137.60	$7_{1} - 6_{-1}$	257
	51	138.38	138.25	$7_{2} - 6_{-2}$	80
	52	140.98	141.19	$8_{4} - 7_{2}$	140
x	53	142.69	142.88	$9_{8} - 8_{8}$	278
	54	143.52	143.3	$18_{-18} - 17_{-16}$	66
			143.3	$18_{-17} - 17_{-17}$	200
			143.4	$17_{-14} - 16_{-14}$	60
			143.4	$17_{-15} - 16_{-13}$	180
			143.41	$10_{5} - 9_{5}$	320
			143.5	$16_{12} - 15_{-10}$	50
			143.5	$16_{-11} - 15_{-11}$	150
			143.60	$9_{9} - 8_{7}$	765

TABLE VI. (Cont'd.)

*	55	145.79	145.88	$9_7 - 8_5$	507
	56	146.45	146.21	$7_{-1} - 6_{-3}$	165
			146.26	$7_0 - 6_{-4}$	54
	57	147.72			
	58	148.64	148.78	$8_5 - 7_1$	219
	59	151.05	150.15	$8_7 - 7_3$	224
			150.8	$19_{-18} - 18_{-18}$	50
			150.8	$19_{-19} - 18_{-17}$	150
			150.9	$18_{-16} - 17_{-14}$	40
			150.9	$18_{-15} - 17_{-15}$	120
	60	152.77	152.25	$8_2 - 7_0$	90
	61	154.02	153.83	$8_3 - 7_{-1}$	230
			154.08	$10_7 - 9_7$	394
			154.59	$7_{-2} - 6_{-6}$	25
			154.59	$7_{-3} - 6_{-5}$	77
			154.84	$9_5 - 8_3$	370
x	62	158.35	158.1	$20_{-20} - 19_{-18}$	33
			158.1	$20_{-19} - 19_{-19}$	100
			158.38	$10_9 - 9_9$	565
			158.82	$10_{10} - 9_8$	174
	63	160.27	160.48	$10_8 - 9_6$	117
	64	161.51	161.30	$8_0 - 7_{-2}$	66
			161.55	$8_1 - 7_{-3}$	200
	65	164.80			
	66	166.16	165.71	$9_6 - 8_2$	57
			166.40	$9_3 - 8_1$	244
	67	167.50			
	68	169.20	168.76	$10_6 - 9_4$	86
			169.03	$9_8 - 8_4$	67

TABLE VI. (Cont'd.)

69	170.12	169.83	$8_{-1} - 7_{-5}$	123
		169.84	$8_{-2} - 7_{-4}$	41
70	173.60	173.50	$11_{10} - 10_{10}$	110
		173.78	$11_{11} - 10_{9}$	310
71	174.65	174.75	$11_{9} - 10_{7}$	215
72	176.46	176.35	$9_{1} - 8_{-1}$	188
		176.68	$9_{2} - 8_{-2}$	61
73	178.41	178.30	$8_{-4} - 7_{-6}$	22
		178.30	$8_{-3} - 7_{-7}$	65
74	180.64	180.43	$8_{4} - 9_{2}$	64
75	183.33	183.46	$10_{7} - 9_{3}$	126
76	184.98	184.93	$9_{0} - 8_{-4}$	50
		184.93	$9_{-1} - 8_{-3}$	148
		185.36	$10_{5} - 9_{1}$	116
77	186.30			
78	188.39	188.13	$10_{9} - 9_{5}$	148
		188.4	$12_{11} - 11_{11}$	175
79	189.34			
80	190.69	190.94	$10_{2} - 9_{0}$	50
81	191.58	191.71	$10_{3} - 9_{-1}$	149
82	192.63			
83	193.51	193.41	$9_{-2} - 8_{-6}$	33
		193.41	$9_{-3} - 8_{-5}$	106
84	195.22			
85	199.74	199.88	$10_{0} - 9_{-2}$	43
		199.95	$10_{1} - 9_{-3}$	125
86	200.82			

TABLE VI. (Cont'd.)

87	202.29	201.98	$9_{-4} - 8_{-8}$	16
		201.98	$9_{-5} - 8_{-7}$	47
88	203.20			
89	204.04			
90	204.75			
91	206.55	206.67	$11_{10} - 10_{6}$	34
92	208.38	208.36	$10_{-2} - 9_{-4}$	30
		208.36	$10_{-1} - 9_{-5}$	91
		208.4	$12_{12} - 11_{10}$	54
93	211.65			
94	214.37	214.58	$11_{2} - 10_{-2}$	92
		214.75	$11_{1} - 10_{-1}$	29
95	217.29	216.89	$10_{-4} - 9_{-6}$	25
		216.89	$10_{-3} - 9_{-7}$	74
96	221.57			
97	222.96	223.14	$11_{0} - 10_{-4}$	28
		223.14	$11_{-1} - 10_{-3}$	83
98	226.04	225.57	$10_{-5} - 9_{-9}$	13
		225.57	$10_{-6} - 9_{-8}$	40
99	226.04			
100	231.95	231.66	$11_{-2} - 10_{-6}$	24
		231.66	$11_{-3} - 10_{-5}$	71
101	234.02			
102	241.10	240.34	$11_{-4} - 10_{-8}$	16
		240.34	$11_{-5} - 10_{-7}$	50
103	245.90			

TABLE VII.

MOLECULAR CONSTANTS OF H_2Se.

$a = 8.16_5$ cm^{-1}	$I_a = 3.43_0 \times 10^{-40}$ gm cm^2
$b = 7.71_2$	$I_b = 3.62_8$
$c = 3.91_5$	$I_c = 7.14_8$
$\chi = 0.787$	$\Delta = 0.09_0 \times 10^{-40}$ gm cm^2
$r(H\text{-}Se) = 1.47_0$ A	$2\alpha = 91.0^\circ$
$L = 0.001139$	$Q = -0.002891$
$M = 0.009570$	$R = -0.0005379$
$N = -0.009134$	$S = 0.002303$

CHAPTER IV

PURE ROTATIONAL SPECTRA OF THE PARTIALLY DEUTERATED AMMONIAS

History:

Stroup, Oetjen and Bell[1] have observed pure rotational lines of phosphine (PH_3) in an excited vibrational state. E. E. Bell suggested that this same effect might be observed for regular ammonia (NH_3), if a long path cell and high gas pressures were used. A search of the spectrum between the widely spaced lines of NH_3 was made using commercial NH_3 at a pressure of approximately one atmosphere in the stainless steel absorption cell 43 cm long designed by Stroup.[2] Between the pure rotational lines due to transitions among the ground state levels, there were other weak absorption lines not due to any water impurity.

E. E. Bell attempted to account for these lines as transitions between rotational levels of the ν_2 excited vibrational state with no success. He then suggested that these absorption lines were due to the small amount of NH_2D

---

(1) R. E. Stroup, R. A. Oetjen and E. E. Bell, J. Opt. Soc. Am. 43, 1096 (1953).

(2) R. E. Stroup, "A Study of the Rotational Spectra of Some of the Tri-hydrides of the Fifth Group of Elements of the Periodic Table." (Ph. D. Dissertation, The Ohio State University, 1953).

which would occur naturally in ammonia. This suggestion initiated the investigation which comprises this chapter of the dissertation. As deuterium occurs naturally to 1 part in 5000 of hydrogen, the amount of NH_2D in natural ammonia should be about 0.05%. The analysis of the NH_2D spectrum confirmed the suggestion, since the strong absorptions of NH_2D correspond to the weak absorptions seen in the spectrum of commercial ammonia.

Regular ammonia has been the object of a great deal of spectroscopic work. However, the other ammonias, NH_2D, NHD_2, and ND_3 have not been studied nearly as thoroughly. Migeotte and Barker[3] have examined several of the vibration-rotation bands of all four molecules. The unraveling of the bands of the partially deuterated ammonias is difficult since bands of all four molecules overlap to some extent. Berlad[4] has measured several bands of ND_3 with high resolution and carried out a partial analysis, while Burgess[5] has examined several bands of NH_2D, NHD_2 and ND_3.

---

(3) M. V. Migeotte and E. F. Barker, Phys. Rev. 50, 418 (1936).

(4) A. L. Berlad, "Infrared Spectrum of Trideutero-Ammonia." (Ph. D. Dissertation, The Ohio State University, 1950).

(5) J. S. Burgess, "Infrared Spectra of Methane and Deutero-Ammonia." (Ph. D. Dissertation, The Ohio State University, 1949).

The pure rotational spectrum of NH_3 has been studied in the far infrared region by Badger and Cartwright,[6] Wright and Randall,[7] who observed the inversion splitting, and Foley and Randall,[8] who observed the K splitting due to the effects of centrifugal distortion. More recently, McCubbin,[9] Hansler and Oetjen,[10] and Hadni[11] have made further measurements.

Several pure rotational lines of ND_3 were observed by Barnes[12] to have no detectable inversion splitting. Stroup, Oetjen and Bell[13] have more completely measured the spectrum of ND_3.

---

(6) R. M. Badger and C. H. Cartwright, Phys. Rev. 33, 692 (1929).

(7) N. Wright and H. M. Randall, Phys. Rev. 44, 391 (1933).

(8) H. M. Foley and H. M. Randall, Phys. Rev. 59, 171 (1941).

(9) T. K. McCubbin, J. Chem. Phys. 20, 668 (1932).

(10) R. L. Hansler and R. A. Oetjen, J. Chem. Phys. 21, 1340 (1953).

(11) A. Hadni, Comp. Rend. 237, 317 (1953).

(12) R. B. Barnes, Phys. Rev. 39, 562 (1932).

(13) R. E. Stroup, R. A. Oetjen and E. E. Bell, J. Chem. Phys. 21, 2072 (1953).

There has been considerable study of the ammonias in the microwave region where $\Delta J = 0$ transitions have been observed. Here, the primary interest has been in the inversion effect. Kyhl[14] was the first to investigate the microwave spectrum of the partially deuterated ammonias. He observed one line of NHD_2 at 9515 Mc/sec (0.317 cm^{-1}). Lyons, et al.[15] have observed a number of $\Delta J = 0$ transitions of the deuterated ammonias. Weiss and Strandberg[16] have measured fifty $\Delta J = 0$ lines of NH_2D and NHD_2. Their work has provided considerable information about these molecules, some of which proved very useful in the present investigation.

The microwave work has established values for a-c and the asymmetry parameter κ. It has also produced information about the effects of centrifugal distortion on the molecules. In this investigation it has been possible to determine values for a+c and consequently a, b and c which agree with the microwave data and predict the spectra quite well. The rotational energy levels of the ground states of NH_2D and NHD_2 have been determined. These should prove useful in any

---

(14) R. L. Kyhl, M. I. T. Physics Department Thesis (1947).

(15) H. Lyons, M. Kessler, L. J. Reuger and R. G. Nuckolls, Phys. Rev. 81, 297, 630 (1951).

(16) M. T. Weiss and M. W. P. Strandberg, Phys. Rev. 83, 567 (1951).

subsequent attempt to analyse the fundamental vibration-rotation bands. Centrifugal distortion has not been treated analytically.

Experimental Procedure:

Since the pure rotational spectra of NH_3 and ND_3 have been studied in some detail in the far infrared region, the frequencies of the spectrum lines are well known. The spectra are quite simple, consisting of series of approximately evenly spaced lines. In any attempt to prepare the partially deuterated ammonias, all four molecules will be present in the sample. Consequently, in observing the rotational spectrum of either partially deuterated ammonia, there will also be present absorption due to the other ammonias acting as "impurities." However, in preparing the gas sample, it is possible to obtain mixtures in which only two of the four molecules are present in large enough concentrations to produce appreciable absorption.

The gases were prepared by dropping mixtures of H_2O and D_2O on magnesium nitride (Mg_3N_2), since NH_3 is readily produced according to the equation

$$6H_2O + Mg_3N_2 \rightarrow 2NH_3 + 3Mg(OH)_2$$

In the usual case, very strong absorption by NH_3 moderately strong absorption by NH_2D, weak absorption by NHD_2 and no observable absorption by ND_3 can be obtained by proper variation of the concentration of the initial H_2O-D_2O mixture.

It is more difficult to reverse these results, however, i.e., to produce a spectrum with very strong ND_3 absorption, moderately strong NHD_2 absorption, weak NH_2D absorption, and no observable NH_3 absorption. Only when extreme care is taken to eliminate hydrogen in the form of H_2O or otherwise, from the gas generating system and Mg_3N_2, and pure D_2O is used, is it possible to obtain a spectrum relatively free from NH_2D and NH_3 lines.

Assuming that the only source of hydrogen and deuterium is the mixture of H_2O and D_2O dropped on the Mg_3N_2, the final concentrations of the four ammonias can be calculated using the formula

$$1 = p^3 + 3p^2q + 3pq^2 + q^3 \qquad (4.1)$$

where p is the fraction of H atoms available to form the ammonia, and q is the fraction of the D atoms available. The term p^3 is the fraction of NH_3 molecules produced, $3p^2q$ is the fraction of NH_2D molecules, $3pq^2$ is the fraction of NHD_2 molecules, and q^3 is the fraction of ND_3 molecules. This formula is discussed in Appendix I. For example, using a mixture of 9 parts of H_2O to 1 part of D_2O, so that the H fraction is $p = 0.9$ and the D fraction is $q = 0.1$, the final concentration of NH_3 is 0.729, of NH_2D-0.243, of NHD_2-0.027, and of ND_3-0.001. However, since the amount of hydrogen in the Mg_3N_2 and on the walls of the glass generating system is unknown, equation (4.1) can be used only to get a rough idea

of the relative concentrations.

Another method of preparing NH_2D and NHD_2 suggested by Kirshenbaum[17] is by dissolving commercial NH_3 in D_2O. The ions NH_4^+, NH_3D^+, $NH_2D_2^+$, etc. are formed by the exchange reaction of hydrogen and deuterium in solution. The relative concentrations of the final equilibrium mixture can be regulated by controlling the initial numbers of D_2O and NH_3 molecules. Heating the aqua ammonia drives off the ammonia.

Stedman[18] has mixed samples of NH_3 and ND_3 in various concentrations and observed the growth of the ν_2 band of each of the four ammonias over a period of minutes. Evidently, the exchange of H and D atoms is a wall effect which reaches equilibrium in a matter of a few minutes.

Two different samples of Mg_3N_2 were used during this investigation. One sample was prepared by Berlad several years ago. The second sample was prepared in the following manner. Fine magnesium powder in a cylindrical stainless steel tube 1 in. in diameter was heated in an electric oven. The oven temperature was controlled at $\sim 700^{\circ}C$. The temperature was measured by observing the heated cylinder with an optical pyrometer. A stream of dry nitrogen was passed through the tube. The ends of the tube were closed with

---

(17) I. Kirshenbaum, "Physical Properties and Analysis of Heavy Water," (McGraw-Hill, New York, 1951), p. 55.

(18) D. F. Stedman, J. Chem. Phys. 20, 718 (1952).

asbestos plugs except for the entrance and exit holes for the nitrogen. The magnesium reacted with the nitrogen to form a yellow-orange compound Mg_3N_2. It was very important to keep air away from the hot magnesium during the reaction since oxygen in the air would react with the magnesium vigorously forming MgO. After several hours the reaction was complete. The Mg_3N_2 was removed from the tube as quickly as possible and put into bottles which were placed into a desicator. Since Mg_3N_2 reacts so quickly with water, there was some NH_3 produced, leaving $Mg(OH)_2$ in the Mg_3N_2. This could be one of the undesirable sources of hydrogen.

The gas generating system was similar to that used for preparing the diatomic molecules discussed in Chapter II, except that no P_2O_5 was used as a drying agent since it reacts with ammonia. Instead, Mg_3N_2 was placed in the U-shaped drying tube and in the absorption cell and since it reacts readily with water vapor, it serves as an ideal drying agent producing more ammonia. Pressures were regulated by immersing the bottom of the generating flask into a Dewar of liquid nitrogen. The same glass and stainless steel gas cells used in the investigation of the spectra of the diatomic molecules were used. Spectrograms were obtained using several gas pressures between 2 and 6 cm Hg. Also, several different initial mixtures of H_2O and D_2O were used. Spectral slit widths of from 0.3 to 0.7 cm^{-1} were used depending on the

spectral region measured.

From an examination of the various records, it can be seen how the relative intensities of various lines change as the concentrations of the ammonias are changed. If drying is not thorough, lines due to H_2O, D_2O and HDO could also appear. However, careful checks of the records revealed no absorption due to strong water lines. In the worst possible case, there could be significant absorption by the four ammonias and three types of water molecules. Considerable care reduced this to detectable absorption by only two or three of these seven types of molecules.

As in the case of H_2Se, both the diamond-windowed and the quartz-windowed Golay detectors were employed. The same precautions were taken to insure the purity of the spectra observed as were taken with H_2Se.

Composite pictures of the spectra of NH_2D and NHD_2 in the spectral region from 50 to 200 cm^{-1} are shown in Figures 17, p. 97, 18, p. 98, 19, p. 99 and 20, p. 100. The spectra are divided into several sections with different gas pressures ranging from 2 or 3 to 6 cm Hg. The absorption path length is 19 cm. Per cent absorption is only approximate. The theoretical spectra shown below the observed spectra will be discussed in the latter part of this chapter. The spectrum of NH_2D contains strong NH_3 absorption which masks some of the NH_2D lines. The NH_3 lines are marked by brackets. Similarly, strong ND_3 lines appear in the NHD_2 spectrum.

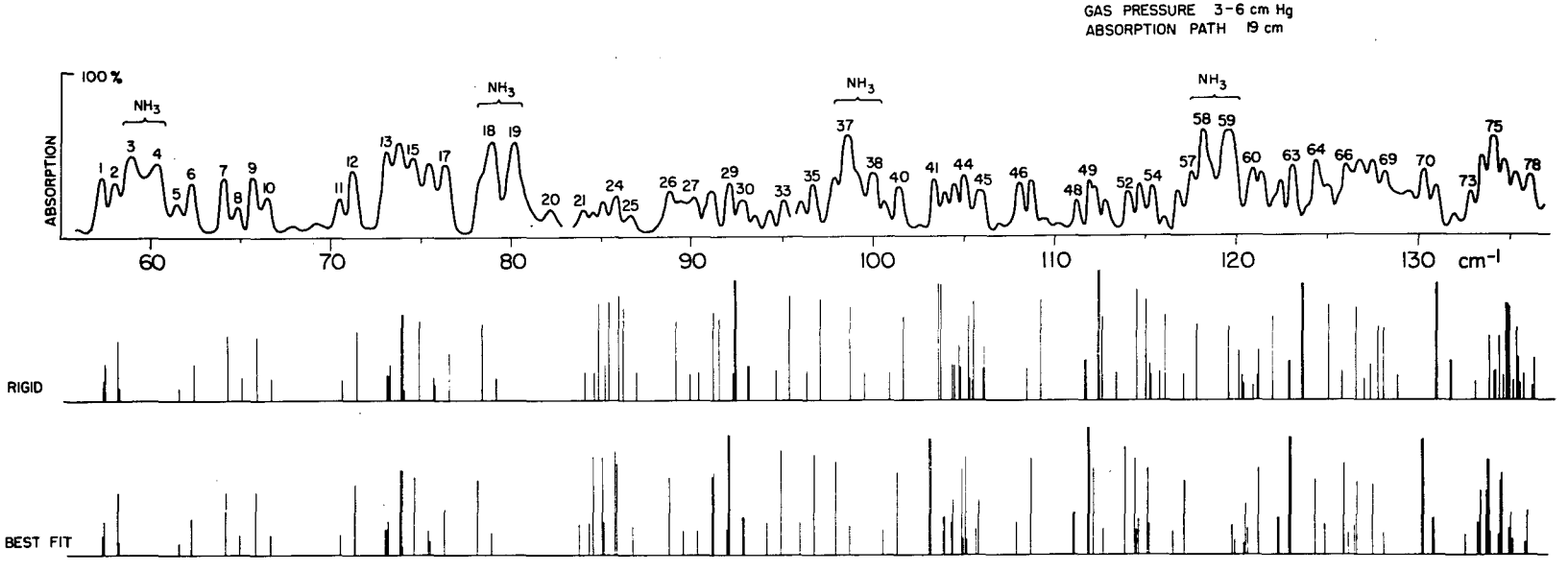

FIG. 17. Observed spectrum, rigid rotator spectrum, and best fit spectrum of NH_2D.

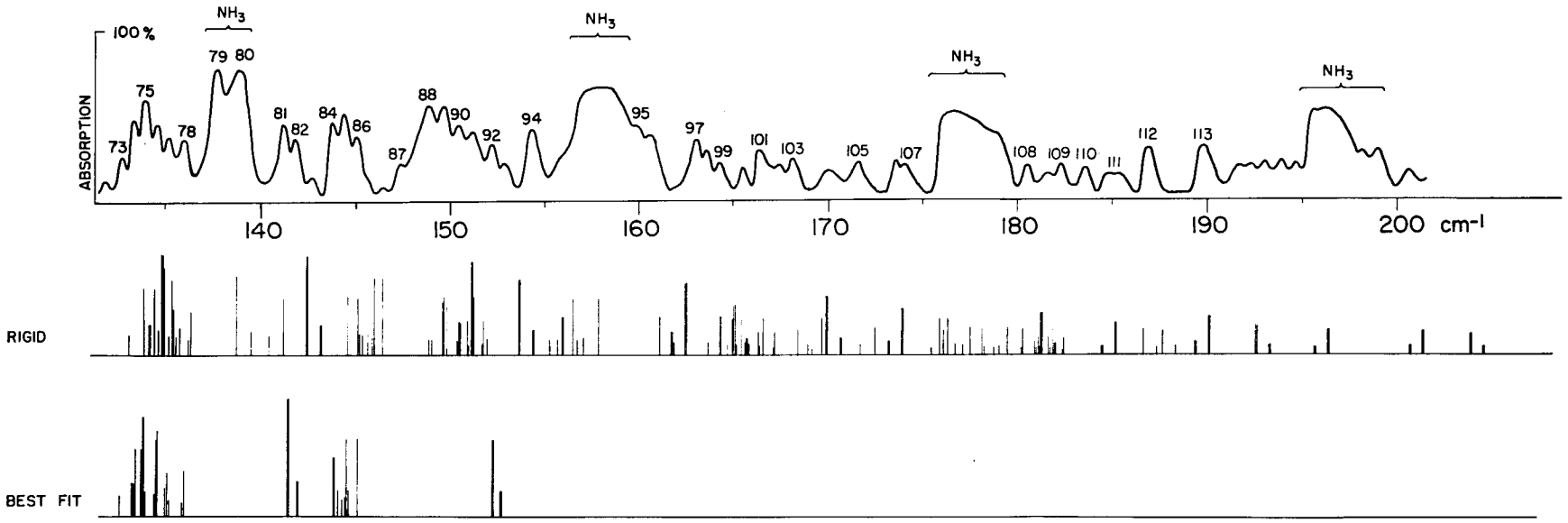

FIG. 18. Observed spectrum, rigid rotator spectrum, and best fit spectrum of NH_2D.

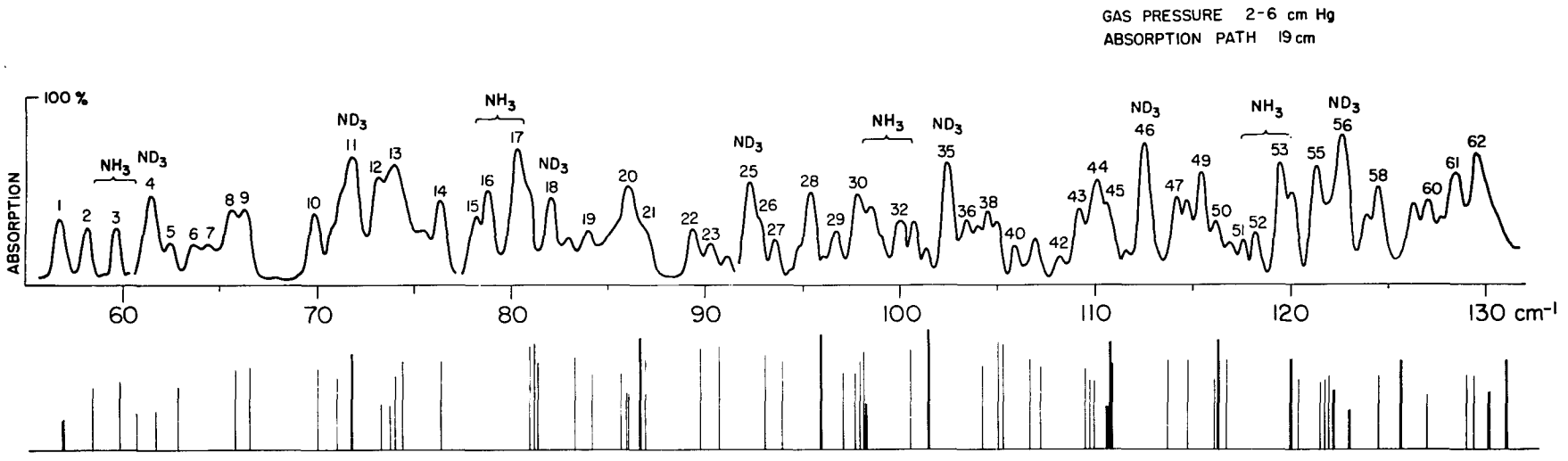

FIG. 19. Observed spectrum and rigid rotator spectrum of NHD_2 neglecting the inversion splitting.

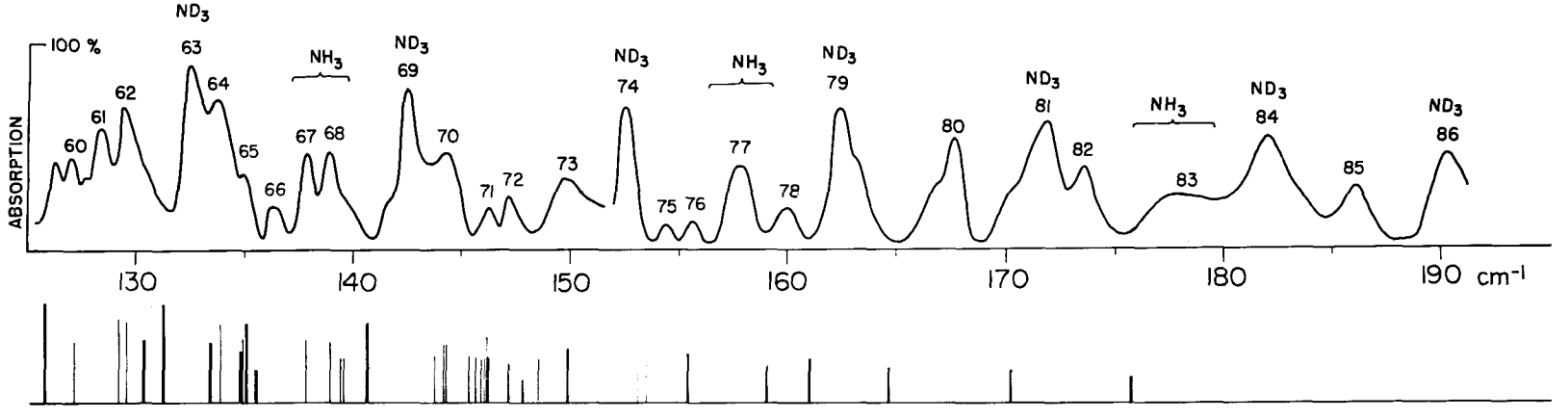

FIG. 20. Observed spectrum and rigid rotator spectrum of NHD_2 neglecting the inversion splitting.

In this case, it was not possible to obtain spectra free from NH_3. Consequently, the assignment of NHD_2 lines is more difficult since there are lines of all four ammonias present with appreciable strength. The spectra are quite complicated showing no obvious regularities. The investion splitting of 0.80 cm^{-1} is evident for NH_2D at the lower frequencies, but the inversion splitting for NHD_2 could not be resolved.

Theory and Analysis:

Review of NH_3 Theory.

Spectroscopic studies of NH_3 have shown that the molecule is pyramidal in shape and an oblate rotator with $a = b > c$. The term values for an oblate rotator can be expressed as

$$F(J,K) = bJ(J+1) + (c-b)K^2 - D_J J^2(J+1)^2 - D_{JK}J(J+1)K^2 - D_K K^4 \qquad (4.2)$$

where the first two terms are the energy for a rigid rotator, while the last three terms take into consideration the centrifugal distortion of the molecule.

However, ammonia is of particular interest since it exhibits the inversion doubling of all the vibrational levels. The property that the nitrogen atom has two equivalent positions of equilibrium, one on each side of the H_3 plane has been studied by Dennison and Uhlenbeck[19] by considering

---

(19) D. M. Dennison and G. E. Uhlenbeck, Phys. Rev. 41, 313 (1932).

the quantum mechanical behavior of a particle in a double-minimum potential well. The result is that each vibrational level is split into a doublet, the splitting being a function of the shape of the potential well. Physically, the nitrogen atom has a finite possibility of tunneling through the H_3 plane or from another viewpoint, the H_3 plane and the nitrogen atom both move to turn the molecule inside out.

The upper inversion level of each pair has associated with it a wave function which is antisymmetric with respect to inversion. Inversion is accomplished formally by reflection of the molecule in the a, b plane. Dennison and Uhlenbeck chose a potential function of the form shown in Figure 21, p. 103. Then, for the ground state each rotation level is split by

$$\Delta_0 = \nu_2 \left(\frac{2\alpha}{\pi^{1/2}}\right) e^{\left[-\alpha^2 - 2(x_0 - \alpha)(\alpha^2 - 1)^{1/2}\right]} \qquad (4.3)$$

with $x_0 = \left(\frac{4\pi^2 \mu \nu_2}{h}\right)^{\frac{1}{2}} q$ and the barrier height $V = \frac{\alpha^2 h \nu_2}{2}$. Here ν_2 is the A_1 fundamental or bending frequency, q is the height of the pyramid, μ is the reduced mass.

The inversion splitting is not a constant for ammonia, but depends on the centrifugal distortion as shown by Sheng, Barker and Dennison.[20] The following simple consideration will show this. For the lowest K levels, the molecule can be thought of as rotating nearly around the a axis. In this

---

(20) H. Y. Sheng, E. F. Barker and D. M. Dennison, Phys. Rev. 60, 786 (1941).

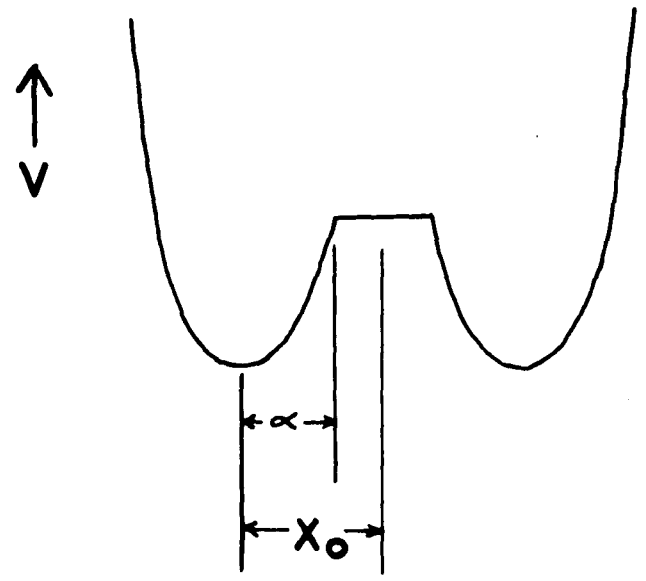

FIG. 21. Dennison and Uhlenbeck potential function for NH_3.

case, the centrifugal forces act to hinder the inversion, that is, the potential barrier for the nitrogen atom is raised. This raising of the barrier reduces the splitting of the rotation-inversion levels. On the other hand, rotation about the c axis tends to flatten the pyramid, lowering the potential barrier, and thus causing the rotation-inversion levels to spread apart for the highest K levels. The inversion frequency can be expressed as

$$\nu_{\text{inv.}} = \Delta_0 - a[J(J+1)-K^2] + \mathcal{B} K^2 \qquad (4.4)$$

where a and $\mathcal{B}$ are positive constants.

With this added effect considered, the term values for the rotation-inversion levels are given by

$$F^a(J,K) = bJ(J+1)+(c-b)K^2-D_J J^2(J+1)^2-D_{JK}J(J+1)K^2 - D_K K^4 + \left\{ \frac{\Delta_0 - a[J(J+1)-K^2]+\mathcal{B}K^2}{2} \right\}$$

$$F^s(J,K) = bJ(J+1)+(c-b)K^2-D_J J^2(J+1)^2-D_{JK}J(J+1)K^2 - D_K K^4 - \left\{ \frac{\Delta_0 - a[J(J+1)-K^2] + \mathcal{B}K^2}{2} \right\}. \qquad (4.5)$$

Here the a and s denote the antisymmetric and symmetric inversion levels. The frequencies of the $\Delta J = 1$, $\Delta K = 0$, and $a \leftrightarrow s$ transitions are given by

$$\nu_{s\to a} = 2B J' - D_J J'^3 - D_{JK} J' K'^2 + \Delta_0 - a[J'^2 - K'^2] + \mathcal{B} K^2$$

$$\nu_{a\to s} = 2B J' - D_J J'^3 - D_{JK} J' K'^2 - \Delta_0 + a[J'^2 - K'^2] - \mathcal{B} K^2. \qquad (4.6)$$

The rotation-inversion lines occur in pairs. The difference in frequency between a pair of these lines is

$$\nu_{s\to a} - \nu_{a\to s} = 2\Delta_o - 2\alpha[J'^2 - K'^2] + 2\beta K'^2. \qquad (4.7)$$

Asymmetric Rotator Theory:

Except for the inversion effect, the pure rotational spectra of NH_2D and NHD_2 can be studied using the usual asymmetric rotator theory. When one of the hydrogen atoms in NH_3 is replaced by a deuterium atom, the molecule becomes very asymmetric ($\kappa_{NH_3} = 1 \to \kappa_{NH_2D} = -0.315$). The center of mass is shifted, and the principal axes are tipped with respect to the geometric symmetry axis as shown in Figure 22, p. 106.

The rotational energy can be expressed in the King, Hainer, and Cross[21] formulation as

$$W(J,\tau) = \tfrac{1}{2}(a+c)J(J+1) + \tfrac{1}{2}(a-c)E^J_\tau(\kappa) \qquad (4.8)$$

For the partially deuterated ammonias, there are components of the dipole moment along two of the three principal axes, so that there are two sets of selection rules allowed besides the usual $\Delta J = 0, \pm 1$ selection rules. One is for the dipole moment along the axis of greatest moment of inertia, a c-type transition, $\begin{matrix} ++ \leftrightarrow +- \\ -+ \leftrightarrow -- \end{matrix}$. The other is for the dipole

---

(21) G. W. King, R. M. Hainer and P. C. Cross, J. Chem. Phys. 11, 27 (1943).

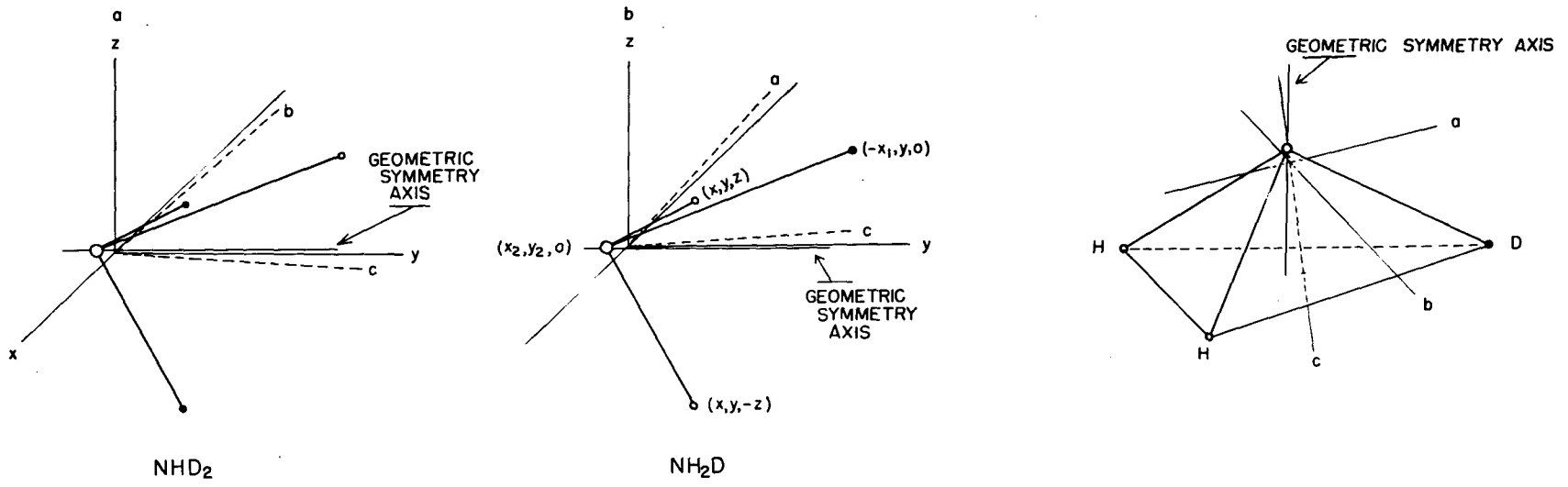

FIG. 22. Molecular geometry of NH_2D and NHD_2.

moment along the axis of least moment of inertia, an a-type transition, $\begin{matrix}++ \leftrightarrow -+ \\ +- \leftrightarrow --\end{matrix}$ for NH_2D, or for the dipole moment along the axis of intermediate moment of inertia, a b-type transition $\begin{matrix}++ \leftrightarrow -- \\ +- \leftrightarrow -+\end{matrix}$ for NHD_2. However, the angle between the geometric symmetry axis and the c principal axis is only about 10°, so that the a-type and b-type transitions will be weak compared to the c-type transitions. Therefore, a-type and b-type transitions can be neglected, at least at the beginning of the analysis. Weiss and Strandberg did not observe any a-type or b-type transitions.

The partially deuterated ammonias also exhibit the inversion effect, although the splitting of the levels decreases from NH_3 to ND_3. Weiss and Strandberg have applied the simple theory of Dennison and Uhlenbeck to the inversion effect for NH_2D and NHD_2 with good agreement at least for the ground state. For NH_2D, $\Delta_o = 0.40\ cm^{-1}$ and for NHD_2, $\Delta_o = 0.17\ cm^{-1}$. For these molecules inversion is accomplished by reflection of the molecules in the a,b plane.

Weiss and Strandberg have shown that an inversion transition must take place during a rotational transition. Therefore, besides the usual asymmetric rotator selection rules, there is the rule $s \leftrightarrow a$.

Because NH_2D and NHD_2 have pairs of identical particles with spins $\frac{1}{2}$ and 1 which obey Fermi-Dirac and Bose-Einstein statistics, respectively, the inversion levels of NH_2D have

weight factors of 3 and 1 while the inversion levels of NHD_2 have weight factors of 2 and 1. For NH_2D, the lower inversion state of K_{-1} even and the upper inversion state and K_{-1} odd has weight factor 1, while the lower inversion state and K_{-1} odd and upper inversion state and K_{-1} even has weight factor 3. For NHD_2, for lower inversion level and C_2^b even or for upper inversion level and C_2^b odd, the weight factor is 2, while the other inversion levels have weight factor 1. Because of these weight factors, the inversion-rotation pairs have relative intensities of 3 to 1 or 2 to 1. However, the stronger component is not always on the same side of the doublet.

In Figure 23, p. 109, are shown the J = 3 and J = 4 levels of NH_2D (not drawn to scale) showing the classification of the levels by K_{-1}, K_1, τ, C_2^a, C_2^c, inversion symmetry, and weight factor. The allowed c-type transitions are also shown.

The relative intensities of the c-type transitions are computed using the tables of line strengths for the asymmetric rotator as given by Cross, Hainer and King.[22]

The microwave pure rotational spectra of NH_2D and NHD_2 have provided considerable information about these molecules. The pertinent results are listed in Table VIII, p. 115. These include values for $\frac{a-c}{2}$ and $\varkappa$, and effective values for the N-H distance r and the H-N-H angle θ. According to Weiss and

---

(22) P. C. Cross, R. M. Hainer and G. W. King, J. Chem. Phys. 12, 210 (1944).

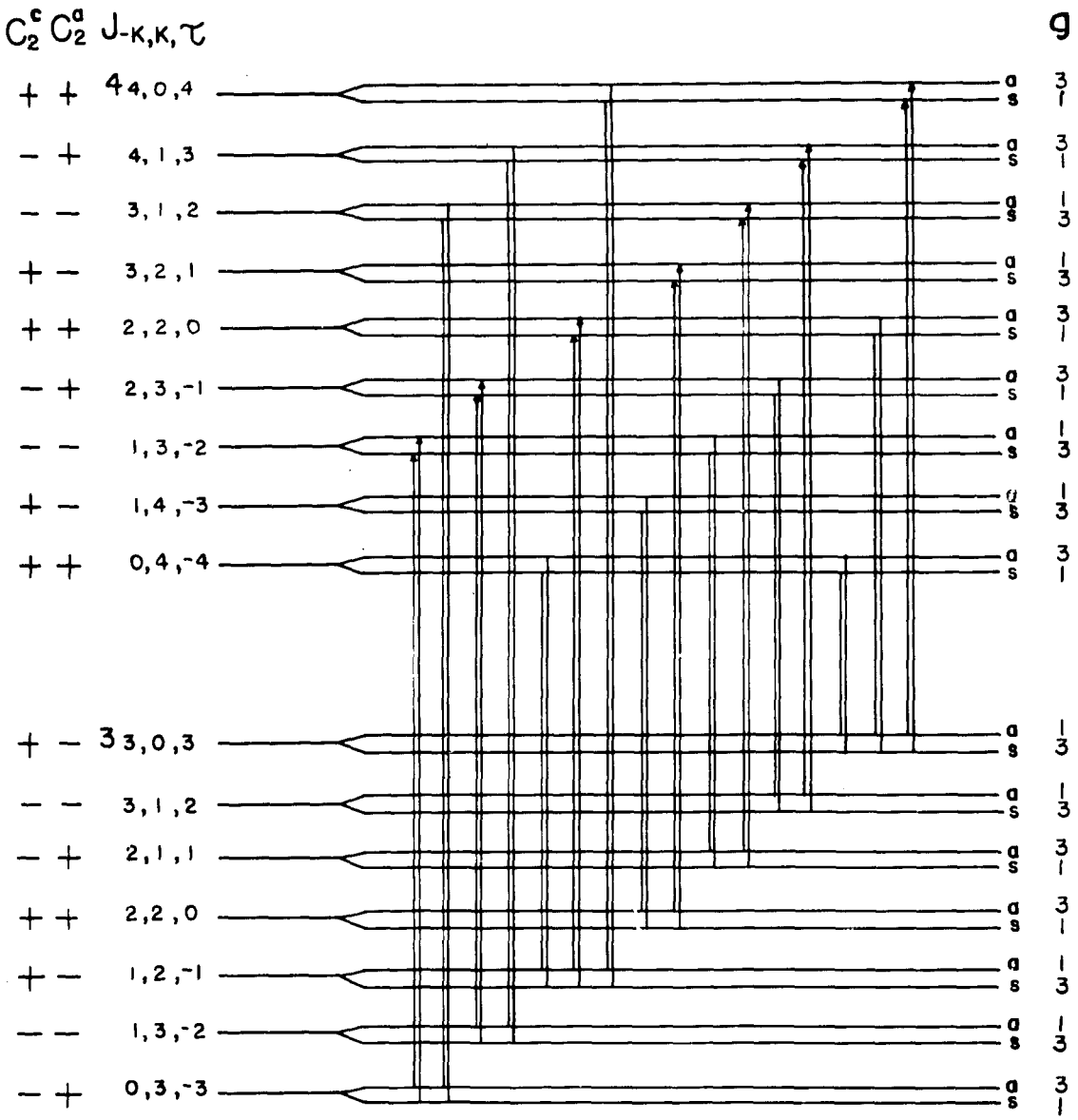

FIG. 23. Energy level diagram for NH_2D. Strongest transitions indicated by arrows. Not drawn to scale.

Strandberg, the principal moments of inertia I_1, I_2, and I_{zz} are given by the following relations

$$\frac{I_{zz}}{mr^2} = \frac{\beta(2+\alpha)}{2+\alpha+\beta} + \frac{2\sin^2\frac{1}{2}\theta}{(2+\alpha+\beta)^2}\left[3\alpha(\alpha+2) - \beta(\beta+2) + 2\alpha\beta\right]$$

$$\frac{I_{xx}+I_{yy}}{2mr^2} = \frac{I_{zz}}{2mr^2} + 2\sin^2\tfrac{1}{2}\theta \qquad (4.9)$$

$$\frac{I_{xx}-I_{yy}}{2mr^2} = \frac{\beta(2+\alpha)}{2(2+\alpha+\beta)} - \frac{\sin^2\frac{1}{2}\theta}{3(2+\alpha+\beta)^2}\left[9\alpha(\alpha+2)+5\beta(\beta+2)+2\alpha\beta(11+2\alpha+2\beta)\right]$$

$$\frac{I_{xy}^2}{mr^2} = \frac{(1-\alpha)^2(2\beta)^2}{3(2+\alpha+\beta)^2}\left[\sin^2\tfrac{1}{2}\theta - \tfrac{4}{3}\sin^4\tfrac{1}{2}\theta\right]$$

$$I_1 = \tfrac{1}{2}(I_{xx}+I_{yy}) + \sqrt{\left[\tfrac{1}{2}(I_{xx}-I_{yy})\right]^2 + I_{xy}^2}$$

$$I_2 = \tfrac{1}{2}(I_{xx}+I_{yy}) - \sqrt{\left[\tfrac{1}{2}(I_{xx}-I_{yy})\right]^2 + I_{xy}^2}$$

$$\phi = \tan^{-1}\left[\frac{-(I_{xx}-I_2)}{I_{xy}}\right]$$

where α = mass ratio of the unique atom in the base of the pyramid to the mass of one of the two equal atoms, β = mass ratio of the apex atom to one of the two equal atoms, r = distance from apex to corner of pyramid, θ = corner to apex to corner angle, ϕ = angle between the geometric symmetry axis and the c principal axis, and m = mass of the hydrogen or deuterium atom for NH_2D and NHD_2 respectively. The origins of both coordinate systems shown are at the center of mass

of the molecule.

The angle ϕ is positive for NH_2D and negative for NHD_2. This is shown in the two models in Figure 22, p. 106. The a and b axes switch roles from NH_2D to NHD_2 while the c axis remains the same. For NH_2D, $I_{zz} = I_b$, $I_1 = I_c$, $I_2 = I_a$, and for NHD_2 $I_{zz} = I_a$, $I_1 = I_c$, $I_2 = I_b$. It was necessary to solve for the products of inertia from basic principles to determine their proper signs to be used to obtain ϕ.

From just a knowledge of a-c and $\varkappa$ Weiss and Strandberg used these equations to obtain values for r and θ. Equations (4.9) can be rewritten as

$$\frac{I_{zz}}{r^2} = A + B \sin^2 \tfrac{1}{2}\theta$$

$$\frac{I_{xx} + I_{yy}}{r^2} = \frac{I_{zz}}{r^2} + C \sin^2 \tfrac{1}{2}\theta \qquad (4.10)$$

$$\frac{I_{xx} - I_{yy}}{r^2} = A + D \sin^2 \tfrac{1}{2}\theta$$

$$\frac{I_{xy}^2}{r^2} = E[\sin^2 \tfrac{1}{2}\theta - \tfrac{4}{3} \sin^4 \tfrac{1}{2}\theta] .$$

For NH_2D	For NHD_2
A = 5.1972	A = 6.1512
B = -1.4779	B = -3.8578
C = 6.6951	C = 13.3796
D = -12.3816	D = -12.5466
E = -1.3417	E = 0.60222

From a-c and $\varkappa = \frac{2b-a-c}{a-c}$ two complicated expressions can be obtained which contain only r and θ as unknowns. They are of the form

$$a-c = \left(\frac{1}{I_2} - \frac{1}{I_1}\right) 27.986 = f_1(r,\theta)$$
$$\varkappa(a-c) = 2b-a-c = \left[\frac{2}{I_{zz}} - \left(\frac{1}{I_2} + \frac{1}{I_1}\right)\right] 27.986 = f_2(r,\theta) . \qquad (4.11)$$

Evidently, it is tedious to compute values for r and θ which satisfy both equations.

Application of Theory:

Using equations (4.9), the principal moments of inertia were calculated. From these, the reciprocals of inertia were obtained. However, the values of $\frac{a-c}{2}$ and $\varkappa$ calculated from these reciprocals of inertia did not agree exactly with the values given directly by Weiss and Strandberg. The moments of inertia were recomputed using extreme values for r and θ which would be allowed within the limits of error stated by Weiss and Strandberg. Even these did not give an $\frac{a-c}{2}$ and $\varkappa$ which agreed with the experimentally determined $\frac{a-c}{2}$ and $\varkappa$. For example for NH_2D using r = 1.012, 1.008 and 1.004 A and θ = 107.5°, 107.3° and 107.1° it was found that $\frac{a-c}{2}$ = 2.396, 2.421 and 2.453 cm^{-1} while $\varkappa$ = -0.269, -0.283 and -0.300. The experimental value for $\frac{a-c}{2}$ is 2.478 $\pm$ 0.005 cm^{-1} and for $\varkappa$ is -0.315 $\pm$ 0.002.

However, one of these sets of reciprocals of inertia was used to compute the rigid rotator energy levels, neglecting inversion. The allowed c-type transitions were determined and the intensities calculated for $\varkappa$ = -0.315 and $\varkappa$ = -0.138.

Then each rotational line was equally split into two components 2 Δ_o apart taking into account the nuclear weight factor to determine the relative intensity of each rotation-inversion component. The agreement was fairly good for the low J lines ($J < 6$). Although the centrifugal distortion was significant for higher J lines, many of these could also be tentatively assigned.

For NH_2D, the pairs of lines split by 0.80 cm^{-1} and having an intensity ratio of 3 to 1 are clearly evident for low J transitions in the region from 60 to 80 cm^{-1} in Figures 17, p. 97 and 18, p. 98. However, the spectrum becomes more complex as J increases. For NHD_2, the inversion splitting is 0.34 cm^{-1} which could not be resolved with the spectrograph.

It was now possible to improve the fit for the low J lines by making use of the expression for the frequencies of the rigid rotator

$$\nu = (a+c)J' + \left(\frac{a-c}{2}\right)\left[E_{\tau'}^{J'}(\varkappa) - E_{\tau''}^{J''}(\varkappa)\right]. \quad (4.12)$$

The term (a+c) was adjusted to give the best fit for the $3 \rightarrow 4$ transitions already identified using the microwave values for a-c and $\varkappa$. These were assumed to be only slightly shifted by centrifugal distortion of the molecule, perhaps 0.0 to 0.2 cm^{-1}. This seemed reasonable since, for example, the $3 \rightarrow 4$ transitions of NH_3 and ND_3 are shifted only 0.1 to 0.2 cm^{-1} at most, toward lower frequencies.

The value for a+c which best fit the data for NH_2D is a+c = 14.40 cm^{-1}. From this and the microwave values for a-c and κ , it is found that a = 9.68_0, b = 6.41_9, and c = 4.72_0 cm^{-1}. With these values, the effective dimensions r and θ can be determined from equations (4.10) in a more straight forward manner than that used by Weiss and Strandberg. The results are r = 1.01_4 A and $\theta = 107^{\circ}8'$.

For NHD_2, a+c = 11.21 cm^{-1}. Then a = 7.44_6, b = 5.35_0, and c = 3.76_4 cm^{-1}. The effective dimensions are r = 1.01_4 A and $\theta = 107^{\circ}13'$. For NH_3 and ND_3, near infrared data give r = 1.014 A and $\theta = 106.78^{\circ}$. These results are listed in Table VIII, p. 115. The difference between θ_{NH_2D} and θ_{NHD_2} is not significant. Very accurate measurements would show that the effective dimensions are different for the two molecules in the ground state, because the amplitudes of the zero point vibrations are slightly different in each molecule.

The angle ϕ between the geometric symmetry axis and the c principal axis for NH_2D is $7^{\circ}13'$ while for NHD_3 $\phi = -12^{\circ}57'$.

Centrifugal distortion corrections and results:

With a good fit of the rigid rotator spectrum to the experimental spectrum for both molecules for low J values, the entire rigid rotator spectrum through J = 12 was recomputed. In the second column of Table IX, p. 116, are listed the rigid rotator levels. In Figures 17, p. 97 and

TABLE VIII.

MOLECULAR CONSTANTS OF NH_2D AND NHD_2.

Microwave Data

NH_2D	NHD_2
$\frac{a-c}{2} = \begin{cases} 74{,}350 \pm 150 \text{ Mc/sec} \\ 2.478 \pm 0.005 \text{ cm}^{-1} \end{cases}$	$\frac{a-c}{2} = \begin{cases} 55{,}200 \pm 100 \text{ Mc/sec} \\ 1.841 \pm 0.003 \text{ cm}^{-1} \end{cases}$
$\kappa = -0.315 \pm 0.002$	$\kappa = -0.1385 \pm 0.002$
$r = 1.008 \pm 0.004$ A	$r = 1.016 \pm 0.008$ A
$\theta = 107.3^\circ \pm 0.2^\circ$	$\theta = 107^\circ \pm 2^\circ$

Far infrared data (using microwave values of a-c and κ).

NH_2D	NHD_2
$a = 9.68_0 \text{ cm}^{-1}$	$a = 7.446 \text{ cm}^{-1}$
$b = 6.41_9$	$b = 5.35_0$
$c = 4.72_0$	$c = 3.76_4$
$I_a = 2.89$, gm cm^2	$I_a = 3.75_8$ gm cm^2
$I_b = 4.35_9$	$I_b = 5.23_1$
$I_c = 5.92_9$	$I_c = 7.43_5$
$r = 1.01_4$ A	$r = 1.01_4$ A
$\theta = 107^\circ 8'$	$\theta = 107^\circ 13'$

TABLE IX.

RIGID ROTATOR ROTATIONAL ENERGY LEVELS, CALCULATED INVERSION SPLITTING ν_i, BEST FIT ROTATION-INVERSION LEVELS AND NUCLEAR WEIGHT FACTOR.

J_τ	Rigid rotator rotational levels (cm^{-1})	Calculated inversion splitting (cm^{-1})	Best fit rotation-inversion levels (cm^{-1})	Nuclear weight factor
0_0	0.00	0.40	0.00	1
1_1	16.09	0.40	16.3	1
			15.9	3
1_0	14.40	0.40	14.6	1
			14.2	3
1_{-1}	11.14	0.40	11.3	3
			10.9	1
2_2	50.36	0.39	50.5	3
			50.1	1
2_1	49.85	0.39	50.0	3
			49.6	1
2_0	40.08	0.39	40.3	1
			39.9	3
2_{-1}	34.98	0.40	35.2	1
			34.8	3
2_{-2}	32.91	0.40	33.1	3
			32.7	1
3_3	104.21	0.38	104.3	1
			103.9	3
3_2	104.11	0.38	104.2	1
			103.8	3
3_1	85.59	0.38	85.7	3
			85.3	1
3_0	83.30	0.39	83.4	3
			83.0	1
3_{-1}	75.66	0.39	75.9	3
			75.5	3
3_{-2}	65.57	0.40	65.8	1
			65.4	3
3_{-3}	64.53	0.40	64.7	3
			64.3	1

TABLE IX.. (Cont'd.)

4_4	177.58	0.36	177.6	3
			177.2	1
4_3	177.56	0.36	177.6	3
			176.2	1
4_2	150.12	0.37	150.1	1
			149.7	3
4_1	149.45	0.37	149.5	1
			149.1	3
4_0	133.30	0.37	133.5	3
			133.1	1
4_{-1}	127.43	0.38	127.6	3
			127.2	1
4_{-2}	122.26	0.38	122.3	1
			121.9	3
4_{-3}	105.94	0.41	106.1	1
			105.7	3
4_{-4}	105.50	0.41	105.6	3
			105.2	1
5_5	270.34	0.34	269.9	1
			269.5	3
5_4	270.34	0.34	269.9	1
			269.5	3
5_3	234.52	0.35	234.2	3
			233.8	1
5_2	234.38	0.35	234.1	3
			233.7	1
5_1	208.49	0.35	208.4	1
			208.2	3
5_0	206.12	0.36	205.0	1
			205.6	3
5_{-1}	193.18	0.35	193.1	3
			192.7	1
5_{-2}	182.00	0.38	181.9	3
			181.5	1
5_{-3}	179.03	0.37	179.0	1
			178.6	3
5_{-4}	155.93	0.41	156.0	1
			155.6	3
5_{-5}	155.76	0.41	155.9	3
			155.5	1
6_6	382.48	0.31	381.5	3
			381.1	1
6_5	382.48	0.31	381.5	3
			381.1	1
6_4	338.52	0.32	337.7	1
			337.3	3

6_3	338.50	0.32	337.7	1
			337.2	3
6_2	303.46	0.33	302.9	3
			302.5	1
6_1	302.79	0.33	302.3	3
			301.9	1
6_0	279.72	0.32	279.3	1
			278.9	3
6_{-1}	273.86	0.35	273.5	1
			273.1	3
6_{-2}	264.54	0.33	264.4	3
			264.2	1
6_{-3}	246.66	0.37	246.7	3
			246.3	1
6_{-4}	245.22	0.37	245.0	1
			244.6	3
6_{-5}	215.43	0.42	215.4	1
			215.0	3
6_{-6}	215.37	0.42	215.4	3
			215.0	1
7_7	513.97	0.27	511.9	1
			511.7	3
7_6	513.97	0.27	511.9	1
			511.7	3
7_5	461.94	0.29	460.2	3
			460.0	1
7_4	461.94	0.29	460.2	3
			460.0	1
7_3	418.46	0.30	417.2	1
			416.8	3
7_2	418.31	0.30	417.2	1
			416.8	3
7_1	384.93	0.30	383.9	3
			383.5	1
7_0	382.76	0.31	381.8	3
			381.4	1
7_{-1}	363.65	0.30	362.7	1
			362.3	3
7_{-2}	352.37	0.34	351.9	1
			351.5	3
7_{-3}	346.49	0.32	345.9	3
			345.5	1
7_{-4}	321.16	0.37	320.8	3
			320.4	1
7_{-5}	320.54	0.37	319.9	1
			319.5	3
7_{-6}	284.40	0.42	284.2	1
			283.8	3
7_{-7}	284.38	0.42	284.2	3
			283.8	1

8_8	664.83	0.23		
8_7	664.83	0.23		
8_6	604.74	0.25	601.8	1
			601.6	3
8_5	604.74	0.25	601.8	1
			601.6	3
8_4	553.08	0.27	550.7	3
			550.5	1
8_3	553.06	0.27	550.7	3
			550.5	1
8_2	510.47	0.27	508.4	1
			508.2	3
8_1	509.87	0.28	507.9	1
			507.6	3
8_0	479.46	0.27	477.5	3
			477.3	1
8_{-1}	474.09	0.29	472.8	3
			472.6	1
8_{-2}	459.61	0.27	458.2	1
			458.0	3
8_{-3}	441.27	0.32		
8_{-4}	438.07	0.31	437.0	3
			436.6	1
8_{-5}	405.28	0.37	404.5	3
			404.1	1
8_{-6}	405.04	0.37	404.4	1
			404.0	3
8_{-7}	362.82	0.43	362.4	1
			362.0	3
8_{-8}	362.82	0.43	362.4	3
			362.0	1
9_9	835.05	0.19		
9_8	835.05	0.19		
9_7	766.91	0.21		
9_6	766.91	0.21		
9_5	707.15	0.23		
9_4	707.14	0.23	703.1	1
			702.9	3
9_3	656.07	0.24	652.6	3
			652.4	1
9_2	655.93	0.24	652.7	3
			652.3	1

TABLE IX. (Cont'd.)

9_1	615.01	0.24	612.3 612.1	1 3
9_0	613.15	0.25		
9_{-1}	587.14	0.23	584.7 584.3	3 1
9_{-2}	576.48	0.28		
9_{-3}	566.66	0.25	564.7 564.5	1 3
9_{-4}	540.23	0.32		
9_{-5}	538.70	0.31	537.4 537.0	3 1
9_{-6}	498.94	0.38	498.0 497.6	3 1
9_{-7}	498.85	0.37	497.9 497.5	1 3
9_{-8}	450.69	0.44		
9_{-9}	450.69	0.44		
10_{10}	1024.63	0.14		
10_9	1024.63	0.14		
10_8	948.43	0.16		
10_7	948.43	0.16		
10_6	880.60	0.18		
10_5	880.60	0.18		
10_4	821.31	0.20		
10_3	821.28	0.20		
10_2	771.17	0.24		
10_1	770.67	0.21		
10_0	732.68	0.20	728.6 728.4	1 3
10_{-1}	728.03	0.23		
10_{-2}	707.45	0.19		

TABLE IX. (Cont'd.)

10_{-3}	689.56	0.26		
10_{-4}	683.70	0.23	681.4 681.2	1 3
10_{-5}	648.97	0.31		
10_{-6}	648.31	0.31		
10_{-7}	602.06	0.38		
10_{-8}	602.03	0.38		
10_{-9}	547.99	0.45		
10_{-10}	547.99	0.45		
11_{11}	1233.56	0.08		
11_{10}	1233.56	0.08		
11_{9}	1149.32	0.11		
11_{8}	1149.32	0.11		
11_{7}	1073.42	0.13		
11_{6}	1073.42	0.13		
11_{5}	1005.99	0.15		
11_{4}	1005.98	0.15		
11_{3}	947.38	0.17		
11_{2}	947.26	0.17		
11_{1}	898.78	0.17		
11_{0}	897.26	0.18		
11_{-1}	863.82	0.15		
11_{-2}	854.24	0.20		
11_{-3}	839.42	0.16		
11_{-4}	812.94	0.24		
11_{-5}	809.87	0.23		

TABLE IX. (Cont'd.)

11_{-6}	767.32	0.31
11_{-7}	767.06	0.31
11_{-8}	714.63	0.38
11_{-9}	714.62	0.38
11_{-10}	654.74	0.47
11_{-11}	654.74	0.47
12_{12}	1461.86	0.02
12_{11}	1461.86	0.02
12_{10}	1369.57	0.05
12_{9}	1369.57	0.05
12_{8}	1285.60	0.08
12_{7}	1285.60	0.08
12_{6}	1210.07	0.10
12_{5}	1210.07	0.10
12_{4}	1143.20	0.12
12_{3}	1143.18	0.12
12_{2}	1085.58	0.13
12_{1}	1085.10	0.13
12_{0}	1039.49	0.12
12_{-1}	1035.64	0.15
12_{-2}	1008.14	0.10
12_{-3}	991.43	0.18
12_{-4}	981.89	0.14
12_{-5}	946.29	0.23
12_{-6}	944.85	0.22
12_{-7}	895.18	0.31
12_{-8}	895.08	0.31
12_{-9}	836.64	0.39
12_{-10}	836.64	0.39
12_{-11}	770.92	0.48
12_{-12}	770.92	0.48

18, p. 98, the rigid rotator spectrum of NH_2D is compared with the observed spectrum including the inversion splitting of 0.80 cm^{-1}. The rigid rotator lines are obtained by subtracting the appropriate rigid levels given in Table IX, p. 116 and then splitting these lines equally into two components 0.8 cm^{-1} apart. In Figures 19, p. 99, and 20, p. 100, the rigid rotator spectrum of NHD_2 is compared with the observed spectrum ignoring the inversion splitting of 0.34 cm^{-1}. Any difference between the position of a rigid rotator line and the corresponding experimental line could be attributed to centrifugal distortion. There are, however, two types of centrifugal distortion to consider, the effect on the rotation frequency or the mean frequency of the rotation-inversion pair, and the effect on the splitting of the rotation-inversion pair.

To study the first type of distortion, attention was focused on the mean of the rotation-inversion pairs. In some cases, the spectrum is so complicated, that it is difficult to pick out the rotation-inversion pair with certainty. It was observed that the shift in frequency $\Delta\nu$ of an experimental rotation line from the rigid rotation line increased from low τ to high τ for each value of J. This appears reasonable from the following simple considerations: Since $\kappa = -0.315$, this rotator is in the region of the prolate limiting case with the a axis the closest to being the unique axis. Classically, low τ transitions correspond to low K

transitions or to rotation about the c axis. Since the pyramid is quite flat, this rotation leads primarily to bond stretching with little bending of the apex angle. For high K transitions, (high τ transitions) corresponding to rotation nearly about the a axis, the forces primarily tend to close the apex bond angle with some bond stretching. Since, in general, bond angles are more easily deformed than bond lengths, it is reasonable to expect that there will be more distortion for high τ transitions than for low τ transitions. For these highest τ transitions, a plot of $\Delta\nu$ against J'^3 proved to be a straight line, a result observed for the pure rotational spectra of several asymmetric molecules including H_2O, D_2O, H_2S, and H_2Se.

An attempt has been made to use the centrifugal distortion formula of Lawrance and Strandberg[23] to correct the rigid rotator line positions of NH_2D. This formula was used by Weiss and Strandberg to account for the distortion of $\Delta J = 0$ transitions for both NH_2D and NHD_2. However, only five of the six constants are obtained. The sixth constant S should be obtainable from the far infrared data, since $\Delta J = 1$ transitions are observed. An attempt to determine S to predict the observed distortion, however, was not successful. In a private communication, Strandberg suggests that since the Weiss and Strandberg distortion constants were obtained from a set of transitions with $K_{-1} = J$, the five

constants could not be determined precisely and uniquely. Therefore, the far infrared spectrum would be useful, since there is a wider variety of data. The constants as determined from the far infrared data probably would not differ very much from the constants of Weiss and Strandberg.

However, attempts to determine six new constants from several sets of six equations to account for the observed distortion were not fruitful. Some of the constants determined were of a different order of magnitude or different sign from the constants of Weiss and Strandberg.

The distorted rotational levels were determined empirically as in the case of H_2Se. The lowest levels were adjusted using the fact that the highest τ levels are distorted by an amount proportional to $J^2(J+1)^2$. Then mean values of $3 \rightarrow 4$ transition pairs were added to the proper $J = 3$ levels to determine the $J = 4$ transitions. It is possible to build up a set of levels in this way. However, there are no useful combination relations to aid in this procedure, because only $\Delta\tau = 1$ transitions have relative intensities large enough to be seen in the experimental spectrum. Other transitions with $\Delta\tau = 3$ and $\Delta\tau = 5$ are weaker in intensity by factors of five or more. The rotational energy levels have been split equally into two components, called rotation-inversion levels, separated by the inversion frequency. The amount of splitting is determined by a method outlined in the following paragraphs.

The second effect of centrifugal distortion, that of causing the rotation-inversion doublets to spread apart or move together, has been studied in the case of NH_3 by Sheng, Barker and Dennison. The inversion frequency is expressed as

$$\nu_{inv.} = \Delta_o - a[J(J+1) - K^2] + b K^2. \qquad (4.13)$$

The term in brackets is just the matrix elements of $\underline{P}^2 - \underline{P}_z^2 = \underline{P}_x^2 + \underline{P}_y^2$ where $\underline{P}$ is the total angular momentum and $\underline{P}_z$ is the body-fixed component of the angular momentum along the geometric symmetry axis. The representation used is one in which $\underline{P}_z$ and $\underline{P}$ commute and are, therefore, diagonal in all the quantum numbers. In this choice of representation $\underline{P}_x$ and $\underline{P}_y$ have both diagonal and off-diagonal elements.

Formally, it is possible to consider that the energy of an asymmetric rotator can be expressed in terms of average angular momenta $\underline{P}_a$, $\underline{P}_b$ and $\underline{P}_c$ along the three principle axes. Then the energy is expressed in terms of the average squared momenta $\langle P_a^2 \rangle$, $\langle P_b^2 \rangle$ and $\langle P_c^2 \rangle$ as

$$W = a \langle P_a^2 \rangle + b \langle P_b^2 \rangle + c \langle P_c^2 \rangle . \qquad (4.14)$$

Bragg and Golden [24] have found that these average squared momenta are given by

[24] J. K. Bragg and S. Golden, Phys. Rev. 75, 735 (1949).

$$P_b^2 = \frac{dE(\varkappa)}{d\varkappa}$$

$$P_a^2 = [J(J+1)+E(\varkappa) - (1+\varkappa) \langle P_b^2 \rangle] /_2 \qquad (4.15)$$

$$P_c^2 = J(J+1) - \langle P_a^2 \rangle - \langle P_b^2 \rangle .$$

Substitution of these equations into equation (4.14) gives the energy of an asymmetric rotator in the King, Hainer and Cross formulation. As the molecule becomes symmetric, these average squared momenta go over into the usual expressions $(J,K,M \mid P_x^2 \mid J,K,M)$, $(J,K,M \mid P_y^2 \mid J,K,M)$, and $(J,K,M \mid P_z^2 \mid J,K,M)$ for the symmetric rotator.

According to Weiss and Strandberg, the form of equation (4.13) is still valid for the asymmetric ammonias. For $K^2 = (J,K,M \mid P_z^2 \mid J,K,M)$, the square of the angular momentum along the geometric symmetry axis of the symmetric rotator, it is possible to substitute $\langle P_c^2 \rangle$ since $\underline{P}_c$ almost points along the symmetry axis. Now, for the partially deuterated ammonias,

$$\nu_i = \Delta_o + \alpha' [J(J+1) - \langle P_c^2 \rangle] + \beta' \langle P_c^2 \rangle . \qquad (4.16)$$

Weiss and Strandberg have used this expression in their study of the inversion splitting of NH_2D and NHD_2. They have found that for NH_2D

$$\nu_i = 0.406 - 0.00256[J(J+1) - \langle P_c^2 \rangle] + 0.000787 \langle P_c^2 \rangle . \qquad (4.17)$$

In this equation, their unit of Mc/sec has been converted to cm^{-1}. For the present investigation, $\langle P_c^2 \rangle$ has been computed for NH_2D and used in equation (4.17) to obtain ν_i. The

amount of splitting of each rotation-inversion pair is just $\nu_i(J'_\tau) + \nu_i(J''_\tau)$ which is not constant. In fact, the splitting in most cases decreases as J increases. For example, the observed splitting for the $7_0 - 6_{-1}$ transition is 0.68 cm^{-1}; the calculated value is 0.66 cm^{-1}. The observed splitting for the $8_6 - 7_5$ transition is 0.55 cm^{-1} while the calculated splitting is 0.54 cm^{-1}. While the agreement is not always this good, equation (4.17) does predict the splitting satisfactorily.

In Table IX, p. 116, are listed the rigid rotator rotational energy levels, the calculated inversion splitting of the levels and the best fit rotation-inversion energy levels for NH_2D with their weight factors. However, values for the best fit rotation-inversion levels have been rounded off to one decimal place since the method of determining the best fit levels was so crude. The average of each pair of best fit inversion-rotation levels gives the best fit rotational levels.

The frequencies of the observed lines and the best fit lines are listed in Table X, p. 129, together with the relative intensities. In the column labled "Transition," each transition appears twice since each rotation line is split into two components, one of which originates from the lower or symmetric inversion level and the other originates from the upper or antisymmetric inversion level. The inversion symmetry of the initial level of each transition is denoted

TABLE X.

OBSERVED AND BEST FIT TRANSITIONS WITH RELATIVE INTENSITIES FOR NH_2D.

Line No.	$\nu_{obs.}$ (cm^{-1})	$\nu_{calc.}$ best fit (cm^{-1})	Transition $J'_\tau - J''_\tau$	Relative Intensity
1	57.23	57.2	$4_0 - 3_{-1}$ a	117
			$4_{-2} - 3_{-3}$ a	200
2	57.97	58.0	$4_0 - 3_{-1}$ s	350
		58.0	$4_{-2} - 3_{-3}$ s	67
NH_3 3	58.91			
NH_3 4	60.44			
5	61.40	61.4	$4_{-1} - 3_{-2}$ a	67
6	62.22	62.2	$4_{-1} - 3_{-2}$ s	200
7	64.01	64.0	$4_2 - 3_1$ a	360
8	64.77	64.8	$4_2 - 3_1$ s	120
9	65.62	65.7	$4_1 - 3_0$ a	358
10	66.38	66.5	$4_1 - 3_0$ s	119
11	70.43	70.4	$5_{-1} - 4_{-2}$ a	133
12	71.14	71.2	$5_{-1} - 4_{-2}$ s	398
13	73.00	72.9	$4_4 - 3_3$ a	162
		73.0	$4_3 - 3_2$ a	161
		73.0	$5_{-3} - 4_{-4}$ a	203
14	73.70	73.7	$4_4 - 3_3$ s	486
		73.8	$4_3 - 3_2$ s	483
		73.8	$5_{-3} - 4_{-4}$ s	68
15	74.50	74.5	$5_1 - 4_0$ a	451
16	75.41	75.3	$5_1 - 4_0$ s	150
		75.4	$5_{-2} - 4_{-3}$ a	90

TABLE X. (Continued)

	17	76.30	76.2	$5_{-2} - 4_{-3}$	s	270
NH_3	18	79.81	78.0	$5_0 - 4_{-1}$	a	430
			78.8	$5_0 - 4_{-1}$	s	143
NH_3	19	80.15				
	20	82.00				
	21	83.78	83.7	$5_3 - 4_2$	a	184
	22	84.34	84.2	$5_2 - 4_1$	a	183
			84.5	$5_3 - 4_2$	s	551
	23	85.01	85.0	$5_2 - 4_1$	s	550
			85.0	$6_{-2} - 5_{-3}$	a	194
	24	85.75	85.8	$6_{-2} - 5_{-3}$	s	583
			85.9	$6_0 - 5_{-1}$	a	512
	25	86.62	86.7	$6_0 - 5_{-1}$	s	171
	26	88.85	88.7	$6_{-4} - 5_{-5}$	a	447
			89.5	$6_{-4} - 5_{-5}$	s	149
	27	90.13	90.3	$6_{-3} - 5_{-4}$	a	148
	28	91.12	91.1	$6_{-3} - 5_{-4}$	s	445
			91.2	$6_{-1} - 5_{-2}$	a	469
	29	92.05	92.0	$6_{-1} - 5_{-2}$	s	156
			92.0	$5_4 - 4_3$	a	673
			92.0	$5_5 - 4_4$	a	673
	30	92.75	92.8	$5_4 - 4_3$	s	224
			92.8	$5_5 - 4_4$	s	224
	31	93.41				
	32	94.16	94.1	$6_2 - 5_1$	a	193
	33	94.90	94.9	$6_2 - 5_1$	s	580
	34	95.94	95.9	$6_1 - 5_0$	a	187

TABLE X. (Continued)

	35	96.56	96.7	$6_1 - 5_0$	s	562
	36	97.72	97.9	$7_{-1} - 6_{-2}$	a	520
NH_3	37	98.38	98.7	$7_{-1} - 6_{-2}$	s	173
NH_3	38	99.70				
	39	100.49	100.5	$7_{-3} - 6_{-4}$	a	155
	40	101.27	101.3	$7_{-3} - 6_{-4}$	s	466
	41	103.20	103.1	$6_4 - 5_3$	a	657
			103.2	$6_3 - 5_2$	a	657
	42	103.88	103.9	$6_4 - 5_3$	s	219
				$6_3 - 5_2$	s	219
	43	104.39	104.3	$7_{-5} - 6_{-6}$	a	310
			104.3	$7_1 - 6_0$	a	185
	44	104.90	104.9	$7_{-2} - 6_{-3}$	a	464
			105.0	$7_{-4} - 6_{-5}$	a	101
			105.1	$7_{-5} - 6_{-6}$	s	103
			105.1	$7_1 - 6_0$	s	555
	45	105.71	105.7	$7_{-2} - 6_{-3}$	s	155
			105.8	$7_{-4} - 6_{-5}$	s	303
	46	107.95	107.9	$7_0 - 6_{-1}$	a	183
	47	108.63	108.7	$7_0 - 6_{-1}$	s	550
	48	111.17	111.1	$6_6 - 5_5$	a	240
			111.1	$6_5 - 5_4$	a	240
	49	111.84	111.9	$6_6 - 5_5$	s	720
			111.9	$6_5 - 5_4$	s	720
	50	112.08	112.1	$8_{-2} - 7_{-3}$	a	478
	51	112.76	112.7	$8_{-2} - 7_{-3}$	s	159
	52	113.93	113.9	$7_3 - 6_2$	a	606

TABLE X. (Continued)

	53	114.59	114.5	$7_2 - 6_1$	a	550
			114.6	$8_0 - 7_{-1}$	a	163
			114.7	$7_3 - 6_2$	s	202
	54	115.21	115.2	$8_0 - 7_{-1}$	s	489
			115.3	$7_2 - 6_1$	s	183
	55	115.93				
	56	116.67	116.6	$8_{-4} - 7_{-5}$	a	141
	57	117.39	117.4	$8_{-4} - 7_{-5}$	s	423
NH_3	58	118.14				
NH_3	59	119.53	119.8	$8_{-6} - 7_{-7}$	a	278
			120.0	$8_{-5} - 7_{-6}$	a	93
	60	120.81	120.6	$8_{-6} - 7_{-7}$	s	93
			120.6	$8_{-5} - 7_{-6}$	s	280
			120.7	$8_{-1} - 7_{-2}$	a	162
	61	121.25	121.3	$8_{-1} - 7_{-2}$	s	487
	62	122.30	122.4	$7_5 - 6_4$	a	214
				$7_4 - 6_3$	a	214
	63	122.92	122.9	$7_5 - 6_4$	s	641
			122.9	$7_4 - 6_3$	s	641
	64	124.32	124.3	$8_2 - 7_1$	a	523
	65	124.87	124.9	$8_2 - 7_1$	s	174
	66	125.86	125.9	$8_1 - 7_0$	a	518
			126.2	$9_{-1} - 8_{-2}$	a	135
	67	126.78	126.5	$8_1 - 7_0$	s	173
			126.6	$9_{-1} - 8_{-2}$	s	404
	68	127.42				
	69	128.04	127.5	$9_{-3} - 8_{-4}$	a	400
			128.1	$9_{-3} - 8_{-4}$	s	133

TABLE X. (Continued)

	70	130.21	130.2	$7_7 - 6_6$	a	646
			130.2	$7_6 - 6_5$	a	646
	71	130.79	130.8	$7_7 - 6_6$	s	215
			130.8	$7_6 - 6_5$	s	215
	72	131.80				
	73	132.65	132.6	$9_{-5} - 8_{-6}$	a	118
	74	133.38	133.3	$8_3 - 7_2$	a	178
			133.3	$8_4 - 7_3$	a	178
			133.4	$9_{-5} - 8_{-6}$	s	354
	75	133.89	133.8	$9_{-4} - 8_{-5}$	a	354
			133.9	$8_3 - 7_2$	s	535
			133.9	$8_4 - 7_3$	s	535
			133.9	$9_{-2} - 8_{-3}$	a	133
			134.4	$9_{-4} - 8_{-5}$	s	118
	76	134.58	134.5	$9_{-2} - 8_{-3}$	s	400
			134.6	$9_1 - 8_0$	a	458
	77	135.15	135.0	$9_1 - 8_0$	s	153
			135.1	$9_{-7} - 8_{-8}$	a	237
			135.2	$9_{-6} - 8_{-7}$	a	79
	78	135.99	135.9	$9_{-7} - 8_{-8}$	s	79
			136.0	$9_{-6} - 8_{-7}$	s	237
NH_3	79	137.76				
NH_3	80	139.21				
	81	141.25	141.4	$8_6 - 7_5$	a	524
			141.4	$8_5 - 7_4$	a	524
	82	141.80	141.8	$8_6 - 7_5$	s	175
			141.8	$8_5 - 7_4$	s	175
	83	142.68				

TABLE X. (Continued)

84	143.79	143.8	$10_{-4} - 9_{-5}$	a	310
		143.8	$10_{0} - 9_{-1}$	a	299
		144.0	$9_{3} - 8_{2}$	a	138
85	144.39	144.2	$10_{0} - 9_{-1}$	s	99
		144.4	$10_{-4} - 9_{-5}$	s	103
		144.4	$9_{3} - 8_{2}$	s	415
		144.6	$9_{2} - 8_{1}$	a	139
86	144.98	145.0	$9_{2} - 8_{1}$	s	417
87	147.30				
88	148.87				
89	149.58				
90	150.42				
91	151.15				
92	152.23	152.2	$9_{4} - 8_{3}$	a	404
		152.2	$9_{5} - 8_{4}$	a	404
93	152.73	152.6	$9_{4} - 8_{3}$	s	135
		152.6	$9_{5} - 8_{4}$	s	135
94	154.40				
95	159.98				
96	160.60				
97	163.08				
98	163.74				
99	164.40				
100	165.58				
101	166.57				
102	167.49				
103	168.08				

TABLE X. (Continued)

104	169.45
105	171.43
106	173.54
107	173.92
108	180.38
109	182.17
110	183.69
111	184.86
112	186.85
113	189.88

by the a or s at the right side of the "Transition" column. In Figures 17, p. 97 and 18, p. 98, the best fit spectrum is compared with the observed spectrum of NH_2D.

The splitting of any pair of rotation-inversion lines can be found by subtracting their frequencies. This is compared with the calculated splitting $\nu_i(J'_\tau) + \nu_j(J''_\tau)$ for some of the more obvious inversion-rotation pairs in Table XI, p. 137.

The NHD_2 spectrum is additionally complicated because the sample always showed traces of NH_3 and NH_2D besides the lines of NHD_2 and ND_3. No attempt has been made to determine the centrifugal distortion empirically. The rigid rotator levels, ignoring inversion, are listed in Table XII, p. 138. In Table XIII, p. 141, are listed the rigid rotator lines along with the observed lines, tentative transitions and relative intensities. The fit is reasonable at the low frequency end of the spectrum. Several groups of rigid rotator transitions have been bracketed together indicating only that they probably fall in the general area of similar groups of lines in the observed spectrum.

In Figures 19, p. 99 and 20, p. 100, the rigid rotator spectrum is compared with the observed spectrum.

TABLE XI.

OBSERVED AND CALCULATED INVERSION SPLITTING FOR SOME OF THE ROTATION-INVERSION DOUBLETS.

$J'_\tau - J''_\tau$	Observed inversion splitting $\nu_i(J'_\tau) + \nu_i(J''_\tau)$	Calculated inversion splitting $\nu_i(J'_\tau) + \nu_i(J''_\tau)$
$4_0 - 3_{-1}$	0.74	0.76
$4_{-2} - 3_{-3}$	0.74	0.78
$4_{-1} - 3_{-2}$	0.82	0.78
$4_2 - 3_1$	0.76	0.75
$4_1 - 3_0$	0.76	0.76
$5_{-1} - 4_{-2}$	0.72	0.73
$5_5 - 4_3$	0.70	0.70
$6_2 - 5_1$	0.74	0.68
$6_1 - 5_0$	0.61	0.69
$7_{-3} - 6_{-4}$	0.78	0.69
$6_4 - 5_3$	0.68	0.67
$7_0 - 6_{-1}$	0.68	0.66
$6_6 - 5_5$	0.67	0.65
$8_{-2} - 7_{-3}$	0.66	0.59
$7_5 - 6_4$	0.62	0.61
$8_2 - 7_1$	0.55	0.57
$7_7 - 6_6$	0.58	0.58
$8_6 - 7_5$	0.55	0.54
$9_5 - 8_4$	0.50	0.50

TABLE XII.

RIGID ROTATOR ENERGY LEVELS FOR NHD_2.

J_τ	Rigid rotator energy levels (cm^{-1})	J_τ	Rigid rotator energy levels (cm^{-1})
0_0	0.00	5_5	209.56
1_1	12.79	5_4	209.55
1_0	11.21	5_3	185.09
1_{-1}	9.12	5_2	184.79
		5_1	168.30
2_2	39.51	5_0	164.91
2_1	38.89	5_{-1}	157.97
2_0	32.62	5_{-2}	146.41
2_{-1}	27.86	5_{-3}	145.28
2_{-2}	26.73	5_{-4}	124.89
		5_{-5}	124.85
3_3	81.18		
3_2	81.01	6_6	296.13
3_1	68.89	6_5	296.13
3_0	66.25	6_4	265.95
3_{-1}	61.84	6_3	265.87
3_{-2}	52.49	6_2	242.61
3_{-3}	52.03	6_1	241.28
		6_0	227.87
4_4	137.90	6_{-1}	220.31
4_3	137.86	6_{-2}	216.17
4_2	119.41	6_{-3}	198.56
4_1	118.36	6_{-4}	198.04
4_0	108.58	6_{-5}	172.47
4_{-1}	102.20	6_{-6}	172.45
4_{-2}	99.69		
4_{-3}	84.88	7_7	397.59
4_{-4}	84.73	7_6	397.59
		7_5	361.80

TABLE XII. (Cont'd.)

7_4	361.79	9_7	598.26
7_3	332.32	9_6	598.26
7_2	331.91	9_5	557.32
7_1	311.05	9_4	557.29
7_0	307.15	9_3	522.91
7_{-1}	297.46	9_2	522.39
7_{-2}	284.16	9_1	497.15
7_{-3}	282.14	9_0	492.93
7_{-4}	258.43	9_{-1}	480.24
7_{-5}	258.29	9_{-2}	465.62
7_{-6}	227.58	9_{-3}	462.48
7_{-7}	227.57	9_{-4}	435.85
		9_{-5}	435.54
8_8	513.95	9_{-6}	400.90
8_7	513.95	9_{-7}	400.89
8_6	472.58	9_{-8}	360.39
8_5	472.58	9_{-9}	360.39
8_4	437.30		
8_3	437.19	10_{10}	791.34
8_2	409.18	10_9	791.34
8_1	407.65	10_8	738.83
8_0	390.48	10_7	738.83
8_{-1}	382.07	10_6	692.28
8_{-2}	376.04	10_5	692.26
8_{-3}	356.10	10_4	651.99
8_{-4}	355.27	10_3	651.85
8_{-5}	325.89	10_2	619.13
8_{-6}	325.85	10_1	617.48
8_{-7}	290.22	10_0	596.40
8_{-8}	290.22	10_{-1}	587.43
		10_{-2}	579.24
9_9	645.20	10_{-3}	557.38
9_8	645.20	10_{-4}	556.00

TABLE XII. (Cont'd.)

10_{-5}	523.23	12_{9}	1064.67
10_{-6}	523.13	12_{8}	1006.95
10_{-7}	483.45	12_{7}	1006.95
10_{-8}	483.43	12_{6}	955.29
10_{-9}	438.09	12_{5}	955.29
10_{-10}	438.09	12_{4}	910.05
		12_{3}	909.90
11_{11}	952.37	12_{2}	872.50
11_{10}	952.37	12_{1}	870.79
11_{9}	894.31	12_{0}	845.64
11_{8}	894.31	12_{-1}	836.33
11_{7}	842.17	12_{-2}	825.73
11_{6}	842.16	12_{-3}	802.32
11_{5}	796.15	12_{-4}	800.22
11_{4}	796.12	12_{-5}	764.36
11_{3}	756.88	12_{-6}	764.17
11_{2}	756.35	12_{-7}	720.64
11_{1}	726.62	12_{-8}	720.64
11_{0}	722.23	12_{-9}	671.12
11_{-1}	706.31	12_{-10}	671.12
11_{-2}	690.70	12_{-11}	616.07
11_{-3}	686.21	12_{-12}	616.07
11_{-4}	657.03		
11_{-5}	656.49		
11_{-6}	618.17		
11_{-7}	618.14		
11_{-8}	573.52		
11_{-9}	573.52		
11_{-10}	523.31		
11_{-11}	523.31		
12_{12}	1128.30		
12_{11}	1128.30		
12_{10}	1064.67		

TABLE XIII.

OBSERVED AND RIGID ROTATOR LINES WITH TENTATIVE TRANSITIONS FOR NHD_2.

Line No.	$\nu_{obs.}$ (cm^{-1})	$\nu_{calc.}$ best fit (cm^{-1})	Transition $J'_\tau - J''_\tau$	Relative Intensity
1	56.68	56.72	$4_4 - 3_3$	334
		56.85	$4_3 - 3_2$	332
2	58.11	58.28	$5_{-1} - 4_{-2}$	308
3	59.58	59.72	$5_1 - 4_0$	338
		60.55	$5_{-3} - 4_{-4}$	194
4	61.55	61.53	$5_{-2} - 4_{-3}$	196
5	62.45	62.71	$5_0 - 4_{-1}$	317
6	64.10			
7	64.80			
8	65.61	65.68	$5_3 - 4_2$	405
9	66.31	66.43	$5_2 - 4_1$	420
10	69.78	69.90	$6_0 - 5_{-1}$	413
		70.89	$6_{-2} - 5_{-3}$	366
11	71.80	71.66	$5_5 - 4_4$	494
		71.69	$5_4 - 4_3$	492
12	73.13	73.19	$6_{-4} - 5_{-5}$	232
		73.67	$6_{-3} - 5_{-4}$	230
13	73.91	73.90	$6_{-1} - 5_{-2}$	370
		74.31	$6_2 - 5_1$	457
14	76.29	76.37	$6_1 - 5_0$	454
15	78.10			
16	78.68			

TABLE XIII. (Cont'd.)

17	80.68	80.36	$6_4 - 5_3$	532
		81.08	$6_3 - 5_2$	532
		81.29	$7_{-1} - 6_{-2}$	453
18	82.06			
	82.83	83.18	$7_1 - 6_0$	478
19	83.90	84.10	$7_{-3} - 6_{-4}$	398
20	85.90	85.60	$7_{-2} - 6_{-3}$	394
		85.84	$7_{-5} - 6_{-6}$	254
		85.96	$7_{-4} - 6_{-5}$	247
		86.57	$6_6 - 5_5$	595
		86.58	$6_5 - 5_4$	595
21	86.47	86.84	$7_0 - 6_{-1}$	477
22	89.39	89.71	$7_3 - 6_2$	535
23	90.23	90.63	$7_2 - 6_1$	530
24	91.02			
25	92.15			
26	92.61	93.02	$8_0 - 7_{-1}$	480
27	93.45	93.90	$8_{-2} - 7_{-3}$	456
28	95.35	95.85	$7_5 - 6_4$	586
		95.92	$7_4 - 6_3$	586
29	96.67	96.98	$8_{-4} - 7_{-5}$	398
30	97.68	97.67	$8_{-3} - 7_{-4}$	390
		97.91	$8_{-1} - 7_{-2}$	458
		98.13	$8_2 - 7_1$	502
		98.28	$8_{-6} - 7_{-7}$	247
		98.31	$8_{-5} - 7_{-6}$	247
31	98.41			
32	99.98	100.50	$8_1 - 7_0$	510

TABLE XIII. (Cont'd.)

33	100.62	101.46	$7_7 - 6_6$	625
		101.46	$7_6 - 6_5$	625
34	101.30			
35	102.30			
36	103.29			
37	103.88	104.20	$9_{-1} - 8_{-2}$	427
38	104.36	104.98	$8_4 - 7_3$	540
39	104.85	105.28	$8_3 - 7_2$	538
40	105.80	106.67	$9_1 - 8_0$	468
41	106.80	107.21	$9_{-3} - 8_{-4}$	426
42	108.18			
43	109.11	109.52	$9_{-2} - 8_{-3}$	416
		109.69	$9_{-5} - 8_{-6}$	358
44	110.11	109.96	$9_{-4} - 8_{-5}$	355
		110.67	$9_{-7} - 8_{-8}$	227
45	110.48	110.68	$9_{-6} - 8_{-7}$	227
		110.78	$8_6 - 7_5$	565
		110.79	$8_5 - 7_4$	557
46	112.45	113.73	$9_3 - 8_2$	465
47	114.08	114.74	$9_2 - 8_1$	463
48	114.55	116.16	$10_0 - 9_{-1}$	362
49	115.30	116.36	$8_7 - 7_6$	562
		116.36	$8_8 - 7_7$	562
50	115.99	116.76	$10_{-2} - 9_{-3}$	462
51	117.47			
52	117.79			

TABLE XIII. (Cont'd.)

53	119.30	120.02	$9_5 - 8_4$	470
		120.10	$9_4 - 8_3$	470
54	119.91	120.46	$10_{-4} - 9_{-5}$	365
55	121.17	121.53	$10_{-3} - 9_{-4}$	347
		121.81	$10_{-1} - 9_{-2}$	462
		121.98	$10_2 - 9_1$	370
56	122.48	122.24	$10_{-6} - 9_{-7}$	302
		122.33	$10_{-5} - 9_{-6}$	305
		123.04	$10_{-8} - 9_{-9}$	198
		123.06	$10_{-7} - 9_{-8}$	198
57	123.76	124.55	$10_1 - 9_0$	375
58	124.54	125.68	$9_6 - 8_5$	467
		125.68	$9_7 - 8_6$	467
59	126.16	127.07	$11_{-1} - 10_{-2}$	280
60	126.83	129.08	$10_4 - 9_3$	374
		129.46	$10_3 - 9_2$	375
61	128.33	130.21	$11_{-3} - 10_{-4}$	290
		130.22	$11_1 - 10_0$	288
62	129.43	131.25	$9_8 - 8_7$	452
		131.25	$9_9 - 8_8$	453
63	132.53	133.32	$11_{-2} - 10_{-3}$	288
		133.36	$11_{-5} - 10_{-6}$	282
		133.80	$11_{-4} - 10_{-5}$	352
64	133.86	134.71	$11_{-7} - 10_{-8}$	240
		134.72	$11_{-6} - 10_{-7}$	240
		134.80	$11_0 - 10_{-1}$	292
65	134.93	134.96	$10_6 - 9_5$	367
		135.01	$10_5 - 9_4$	367
		135.43	$11_{-9} - 10_{-10}$	151
		135.43	$11_{-8} - 10_{-9}$	151

TABLE XIII. (Cont'd.)

66	136.35	137.75	$11_3 - 10_2$	286
		137.87	$11_2 - 10_1$	284
67	137.84	139.33	$12_0 - 11_{-1}$	206
		139.52	$12_{-2} - 11_{-3}$	203
68	138.95	140.57	$10_8 - 9_7$	348
		140.57	$10_7 - 9_6$	348
69	142.51	143.73	$12_{-4} - 11_{-5}$	209
		144.16	$11_5 - 10_4$	274
		144.27	$11_4 - 10_3$	274
70	144.20	145.29	$12_{-3} - 11_{-4}$	213
		145.63	$12_{-1} - 11_{-2}$	206
		145.88	$12_2 - 11_1$	205
		146.03	$12_{-6} - 11_{-7}$	209
		146.14	$10_9 - 9_8$	316
		146.14	$10_{10} - 9_9$	316
		146.19	$12_{-5} - 11_{-6}$	209
71	146.31			
72	147.23			
73	149.30			
74	152.53			
75	154.54			
76	155.80			
77	157.75			
78	160.19			
79	163.12			
80	167.58			
81	171.65			
82	173.61			
83	178.02			

CHAPTER V.

SUMMARY

Pure rotational spectra of DBr, HI, DI, H_2Se, HD_2D and NHD_2 have been measured in the spectral region from 50 to 250 cm^{-1}.

For DBr, HI and DI, the following molecular constants have been determined.

Molecule	Reciprocal of Inertia B_o	Centrifugal Distortion Constant D_o
DBr	4.247_3 cm^{-1}	0.000090 cm^{-1}
HI	6.427	0.00020_4
DI	3.255_2	0.000056

For H_2Se, the reciprocals of inertia, effective moments of inertia, asymmetry parameter κ , inertial defect Δ , H-Se distance r, and apex angle 2α are

$a = 8.16_5$ cm^{-1} $\quad I_a = 3.43_0 \times 10^{-40}$ gm cm^2

$b = 7.71_2$ $\quad I_b = 3.62_8 \times 10^{-40}$

$c = 3.91_5$ $\quad I_c = 7.14_8 \times 10^{-40}$

$\kappa = 0.787$ $\quad \Delta = 0.09_0 \times 10^{-40}$ gm cm^2

$r(H\text{-}Se) = 1.47$ A $\quad 2\alpha = 91.0^\circ$

For NH_2D and NHD_2, the reciprocals of inertia, effective moments of inertia, (N-H) distance r, and H-N-H angle θ are respectively

NH_2D

$a = 9.68_0\ cm^{-1}$ $\quad I_a = 2.89_1 \times 10^{-40}\ gm\ cm^2$

$b = 6.41_9$ $\quad I_b = 4.35_9 \times 10^{-40}$

$c = 4.72_0$ $\quad I_c = 5.92_9 \times 10^{-40}$

$r = 1.01_4$ A $\quad \theta = 107^\circ 8'$

NHD_2

$a = 7.44_6\ cm^{-1}$ $\quad I_a = 3.75_8 \times 10^{-40}\ gm\ cm^2$

$b = 5.35_0$ $\quad I_b = 5.23_1 \times 10^{-40}$

$c = 3.76_4$ $\quad I_c = 7.43_5 \times 10^{-40}$

$r = 1.01_4$ A $\quad \theta = 107^\circ 13'$

APPENDIX

The random distribution of hydrogen and deuterium atoms in groups of three can be calculated as follows: Suppose there are available M red balls and N black balls mixed together in a box. Let M and N be very large numbers. Then one can ask what is the chance in drawing the balls out in groups of three, of getting three red, two red and one black, one red and two black, or three black.

Letting the M red balls be hydrogen atoms (H) and the N black balls be deuterium atoms (D), on the first draw, the chance or probability of getting an H is $\frac{M}{M+N}$, just the fraction of the H atoms available. On the second draw, the probability is almost $\frac{M}{M+N}$ again, since M and N are large numbers. On the third draw, again the probability in almost $\frac{M}{M+N}$. The chance of getting a D atom on the first draw is $\frac{N}{M+N}$; likewise on the second and third draws. The probability of getting three H atoms on the first three draws is just the product of the probability for each drawing. For three H atoms, the probability is

$$P_{HHH} = \frac{M}{(M+N)} \frac{M}{(M+N)} \frac{M}{(M+N)} = \frac{M^3}{(M+N)^3}$$

For three D atoms, the probability is

$$P_{DDD} = \frac{N}{(M+N)} \frac{N}{(M+N)} \frac{N}{(M+N)} = \frac{N^3}{(M+N)^3}$$

For two H atoms and one D atom, the probability would be

$$P_{HHD} = \frac{M}{(M+N)}\frac{M}{(M+N)}\frac{N}{(M+N)} + \frac{M}{(M+N)}\frac{N}{(M+N)}\frac{M}{(M+N)} + \frac{N}{(M+N)}\frac{M}{(M+N)} \times \frac{M}{(M+N)} = \frac{3MMN}{(M+N)^3}$$

because there are three different ways of picking two H atoms and one D atom in three drawings. Similarly, for one H atom and two D atoms, the probability is

$$P_{HDD} = \frac{3MNN}{(M+N)^3}$$

If now, p is the fraction of the H atoms available, and q is the fraction of the D atoms available, then

$$P_{HHH} = p^3 \qquad P_{HHD} = 3p^2q \qquad P_{HDD} = 3pq^2 \qquad P_{DDD} = q^3$$

Since the concentration will be proportional to the probability, it is possible to consider p^3 as the fractional portion of the H_3 formed, $3p^2q$ as the fractional portion of H_2D, etc. Since the total probability of getting H_3, H_2D, HD_2, or D_3 is 1, it is evident that

$$1 = p^3 + 3p^2q + 3pq^2 + q^3$$

Using this equation, the results below are obtained. The various final fractions of NH_3, NH_2D, NHD_2 and ND_3 are listed for several initial mixtures of H_2O and D_2O.

H_2O p	D_2O q	NH_3 p^3	NH_2D $3p^2q$	NHD_2 $3pq^2$	ND_3 q^3
0.9	0.1	0.729	0.243	0.027	0.001
0.8	0.2	0.512	0.348	0.096	0.008
0.7	0.3	0.343	0.441	0.189	0.027
0.6	0.4	0.216	0.432	0.288	0.064
0.5	0.5	0.125	0.375	0.375	0.125

BIBLIOGRAPHY

Badger, R. M., and C. H. Cartwright, Phys. Rev. 33, 692 (1929).

Barnes, R. B., Phys. Rev. 39, 562 (1932).

Benedict, W. S., Phys. Rev. 75, 1317 A (1949).

Berlad, A. L., "Infrared Spectrum of Trideutero-Ammonia" (Ph. D. Dissertation, The Ohio State University, 1950).

Boyd, D. R. J., and H. W. Thompson, Spetrochimica Acta 5, 308 (1952).

Bragg, J. K., and S. Golden, Phys. Rev. 75, 735 (1949).

Burgess, J. S., "Infrared Spectra of Methane and Deutero-Ammonia," (Ph. D. Dissertation, The Ohio State University, 1949).

Burnside, P. B., "An Analysis of the Far Infrared Absorption Spectrum of Hydrogen Sulfide," (M. Sc. Thesis, The Ohio State University, 1954).

Burrus, C. A., and W. Gordy, Phys. Rev. 92, 1437 (1953).

Burrus, C. A., W. Gordy, B. Benjamin, and R. Livingston, Phys. Rev. 97, 1661 (1955).

Cameron, D. M., W. C. Sears, and H. H. Nielsen, J. Chem. Phys. 7, 994 (1939).

Czerny, M., Z. Physik 34, 227 (1925); 44, 235 (1927).

Dadieu, A., and W. Engler, Wiener Anzeiger 128, 13 (1935).

Darling, B. T., and D. M. Dennison, Phys. Rev. 57, 128 (1940).

Davis, P. W., "The Far Infrared Spectra of Several Pyramidal Tri-halides," (Ph. D. Dissertation, The Ohio State University, 1954).

Dennison, D. M., Rev. Mod. Phys. 3, 280 (1931).

Dennison, D. M., and G. E. Uhlenbeck, Phys. Rev 41, 313 (1932).

Foley, H. M., and H. M. Randall, Phys. Rev. 59, 171 (1941).

Fuson, N., H. M. Randall, and D. M. Dennison, Phys. Rev. 56, 982 (1939).

Gordy, W., and C. A. Burrus, Phys. Rev. 93, 419 (1954).

Gordy, W., W. V. Smith, and R. F. Trambarulo, "Microwave Spectroscopy," (John Wiley & Sons, Inc., New York, 1953).

Hainer, R. M., and G. W. King, J. Chem. Phys. 15, 89 (1947).

Hadni, A., Comp. Rend. 237, 317 (1953).

Hansler, R. L., "Recent Studies in the Spectral Region from 40 to 140 Microns," (Ph. D. Dissertation, The Ohio State University, 1952).

Hansler, R. L., and R. A. Oetjen, J. Chem. Phys. 21, 1340 (1953).

Herzberg, G., "Molecular Spectra and Molecular Structure I. Spectra of Diatomic Molecules," (D. Van Nostrand Company, Inc., New York, 1950).

Herzberg, G., "Molecular Spectra and Molecular Structure II. Infrared and Raman Spectra of Polyatomic Molecules," (D. Van Nostrand Company, Inc., New York 1951).

Keller, F. L., and A. H. Nielsen, J. Chem. Phys. 22, 294 (1954).

King, G. W., J. Chem. Phys. 15, 85 (1947).

King, G. W., R. M. Hainer, and P. C. Cross, Phys. Rev. 71, 433 (1947).

King, G. W., R. M. Hainer, and P. C. Cross, J. Chem. Phys. 11, 27 (1943).

Kirshenbaum, I., "Physical Properties and Analysis of Heavy Water," (McGraw-Hill, New York, 1951), p. 55.

Kivelson, D., and E. B. Wilson, J. Chem. Phys. 20, 1575 (1952).

Kyhl, R. L., M. I. T. Physics Department Thesis (1947).

Lawrance, R. B., and M. W. P. Strandberg, Phys. Rev. 83, 363 (1951).

Lyons, H., M. Kessler, L. J. Rueger, and R. G. Nuckolls, Phys. Rev. 81, 297, 630 (1951).

McCubbin, T. K., J. Chem. Phys. 20, 668 (1952).

McCubbin, T. K., and W. W. Sinton, J. Opt. Soc. Am. 40, 537 (1950).

Mellor, J. W., "A Comprehensive Treatise on Inorganic and Theoretical Chemistry," Vol. 10, (Longmans, Green and Co., New York, 1928).

Migotte, M. V., and E. F. Barker, Phys. Rev. 50, 418 (1936).

Mills, I. M., H. W. Thompson, and R. L. Williams, Proc. Roy. Soc. A, 217, 29 (1953).

Mischke, W., Z. Physik 106, 67 (1931).

Nielsen, H. H., Rev. Mod. Phys. 23, 90 (1951).

Oetjen, R. A., W. H. Haynie, W. M. Ward, R. L. Hansler, H. E. Schauwecker, and E. E. Bell, J. Opt. Soc. Am. 42, 559 (1952).

Palik, E. D., J. Chem. Phys. 23, 217 (1955).

Pauling, L. C., "The Nature of the Chemical Bond and the Structure of Molecules and Crystals," (Cornell University Press, Ithaca, N. Y., 1939).

Pickworth, J., and H. W. Thompson, Proc. Roy. Soc. A 217, 37 (1953).

Randall, H. M., D. M. Dennison, N. Ginsburg, and L. R. Weber, Phys. Rev. 52, 160 (1937).

Ray, B. S., Z. Physik 78, 74 (1932).

Rosenblum, B., and A. H. Nethercot, Jr., Phys. Rev. 97, 84 (1955).

Sheng, H. Y., E. F. Barker, and D. M. Dennison, Phys. Rev. 60, 786 (1941).

Stedman, D. F., J. Chem. Phys. 20, 718 (1952).

Stroup, R. E., "A Study of the Rotational Spectra of Some of the Tri-hydrides of the Fifth Group of Elements of the Periodic Table," (Ph. D. Dissertation, The Ohio State University, 1953).

Stroup, R. E., R. A. Oetjen, and E. E. Bell, J. Chem. Phys. 21, 2072 (1953).

Stroup, R. E., R. A. Oetjen, and E. E. Bell, J. Opt. Soc. Am. 43, 1096 (1953).

Taussky, "Contributions to the Solutions of Systems of Linear Equations and the Determination of Eigenvalues," (National Bureau of Standards, Applied Mathematics Series, U. S. Government Printing Office, Washington 25, D. C., 1954).

Thompson, H. W., R. L. Williams, and H. J. Calloman, Spectrochimica Acta 5, 313 (1952).

Talley, R. M., H. M. Kaylor, and A. H. Nielsen, Phys. Rev. 77, 529 (1950).

Wang, S. C., Phys. Rev. 34, 243 (1929).

Weiss, M. T., and M. W. P. Strandberg, Phys. Rev. 83, 567 (1951).

Wright, N., and H. M. Randall, Phys. Rev. 44, 391 (1933).

AUTOBIOGRAPHY

I, Edward Daniel Palik, was born in Elyria, Ohio, September 21, 1928. I received my secondary school education in the public schools of Elyria, Ohio. My undergraduate training was obtained at The Ohio State University, from which I received the degree Bachelor of Science in 1950. I received the degree Master of Science from The Ohio State University in 1952. While in the Graduate School I have held the following positions: Graduate Assistant 1951-1952, Research Assistant for The Ohio State University Research Foundation 1952-1953, Research Fellow 1953-1954, and DuPont Fellow 1954-1955.